UNIVERSITÀ
DEGLI STUDI
DI PADOVA

Head Office: University of Padova

Department of Agronomy, Food, Natural resources, Animals and Environment - DAFNAE
Department of Land, Environment, Agriculture and Forestry - TeSAF

Ph.D. COURSE IN CROP SCIENCE
XXX CYCLE

ROLE OF *FUSARIUM GRAMINEARUM* CERATO-PLATANIN AND HYDROPHOBIN PROTEINS IN FUNGAL GROWTH AND PLANT INFECTION

Coordinator: Ch.mo Prof. Sergio Casella
Supervisor: Ch.mo Prof. Luca Sella
Co-Supervisor: Ch.mo Prof. Francesco Favaron

Ph.D. student: Alessandra Quarantin

Declaration

I hereby declare that this submission is my own work and that, to the best of my knowledge and belief, it contains no materials previously published or written by another person nor material which to a substantial extent has been accepted for the award of any other degree or diploma of the University or other institute of higher learning, except where due acknowledgment has been made in the text.

A copy of the thesis will be available at
http://paduaresearch.cab.unipd.it/dottorato/

Index

Summary **1**

Preface **3**

Chapter I **5**
Involvement of the *Fusarium graminearum* cerato-platanin proteins in fungal growth and plant infection

Abstract **7**

1.1. Introduction **9**

1.2. Materials and methods **13**
1.2.1. Sequences analysis and primer design *13*
1.2.2. Fungal strains and culture conditions *13*
1.2.3. Construction of the gene replacement vectors and fungal transformation-mediated gene disruption *14*
1.2.4. Southern blot analysis *17*
1.2.5. Plant growth and infection *17*
1.2.6. Inoculation of wheat flower leaves *18*
1.2.7. RNA extraction and Reverse Transcription (RT) *18*
1.2.8. Expression of the FgCPP encoding genes in vitro and during wheat spikes infection *18*
1.2.9. Treatment of F. graminearum *strains with chitinase and glucanase* *19*

1.3. Results **21**
1.3.1. In silico analysis of cerato-platanin box genes in the F. graminearum *genome* *21*
1.3.2. Features of the putative FgCPP1 and FgCPP2 *22*
1.3.3. The fgcpp1 *gene is the most expressed during early stages of wheat spike infection and during in vitro growth on different carbon sources* *24*
1.3.4. Targeted gene disruption shows that the FgCPPs do not contribute to fungal virulence *25*
1.3.5. In vitro characterization of the $\Delta\Delta$fgcpp$_{1,2}$ *knock-out mutant* *29*

1.4. Discussion **33**

Acknowledgments **35**

References **37**

Supplementary figure captions **43**

Chapter II **51**
The *Fusarium graminearum* cerato-platanin proteins interact with carboxymethyl cellulose reducing its viscosity and favor cellulase activity

Abstract **53**

2.1. Introduction **55**

2.2. Materials and methods **59**
2.2.1. Sequences analysis and primers design *59*
2.2.2. Cloning and expression of the FgCPPs in P. pastoris *59*
2.2.3. SDS-PAGE analysis and preparation of the F. graminearum *recombinant CPPs* *60*
2.2.4. Effect of FgCPPs on polysaccharide substrates *61*
2.2.5. Effect of FgCPPs on filter paper *62*
2.2.6. Cellulase activity produced by F. graminearum *WT and* ΔΔfgcpp$_{1,2}$ *mutant in CMC containing medium* *62*
2.2.7. Binding assay of FgCPPs with CMC and chitin *63*
2.2.8. Plants growth and detection of hydrogen peroxide and necrotic symptoms *63*

2.3. Results **65**
2.3.1. Features of the FgCPPs *65*
2.3.2. Heterologous expression of the FgCPPs *67*
2.3.3. The FgCPPs reduce the CMC viscosity *68*
2.3.4. The FgCPPs are trapped by CMC and not by chitin *69*
2.3.5. The FgCPPs favour the cellulase activity *70*
2.3.6. The FgCPPs weaken filter paper cellulose *72*
2.3.7. The ΔΔfgcpp$_{1,2}$ *mutant produces higher cellulase activity than WT in CMC containing medium* *73*
2.3.8. FgCPPs do not elicit defense responses in A. thaliana *leaves* *74*

2.4. Discussion **75**

References **79**

Supplementary figure captions **85**

Chapter III **87**
***Fusarium graminearum* hydrophobins are involved in water-air interface penetration, maturation of perithecia and plant infection**

Abstract **89**

3.1. Introduction **91**

3.2. Material and methods **95**
3.2.1. Sequences analysis and primer design *95*
3.2.2. Fungal strains and growth analysis *95*
3.2.3. Transcriptomic analysis *96*
3.2.4. Single and triple knock-out mutants production *96*
3.2.5. Penetration of fungal hyphae through the air-liquid barrier *98*
3.2.6. Stress response assays *98*
3.2.7. Calcofluor White assay *98*
3.2.8. Inhibition of fungal growth by β-1,3-glucanase treatment *99*
3.2.9. Tebuconazole inhibition assay *99*
3.2.10. Perithecia viability assay *99*
3.2.11. Pathogenicity assays on wheat plants *100*
3.2.12. Fluorescence microscopy *100*

3.3 Results **103**
3.3.1. Sequence analysis and phylogenetic relationships of the F. graminearum *hydrophobins* *103*
3.3.2. Expression of the F. graminearum *hydrophobins during fungal growth and wheat infection* *106*
3.3.3. Production of single and triple disruption mutants of F. graminearum *hydrophobin genes* *106*

3.3.4. The deletion of FgHyd2 reduces mycelia growth *107*
3.3.5. Mutants without FgHyd2 recover their growth under osmotic and oxidative stress *107*
3.3.6. The deletion of FgHyd2 and FgHyd3 affects hyphal ability to penetrate the water-air interface *109*
3.3.7. FgHyd2 and FgHyd3 are involved in adhesion of conidia to wheat spikes during the early stages of the infection process *109*
3.3.8. Deletion of the F. graminearum *hydrophobins do not cause chitin defects at the cell wall level* *111*
3.3.9. F. graminearum *triple hydrophobin mutants are more sensitive to β-1,3-glucanase treatment* *113*
3.3.10. F. graminearum *hydrophobin mutants exhibit higher susceptibility to tebuconazole fungicide* *113*
3.3.11. The deletion of F. graminearum *hydrophobins affects perithecia maturation* *114*

3.4. Discussion **117**

Acknowledgments **119**

References **121**

Supplementary figure captions **125**

Conclusions **141**

References **143**

Summary

Cerato-platanins (CPPs) and hydrophobins (HPs) are small secreted non-catalytic cysteine-rich proteins typical of filamentous fungi. CPPs are possibly localized in the fungal cell walls, they are similar to plant expansins having carbohydrate binding/loosening properties with a non-enzymatic mechanism and can have phytotoxic activity. HPs, after being secreted as monomers from the hyphal apexes, cover the fungal surfaces with a hydrophobic layer and may be involved in several processes such as formation of fungal aerial structures, attachment to hydrophobic surfaces, interaction with the environment and protection against the host defense system by masking the fungal cell wall. The genome of *Fusarium graminearum*, the causal agent of *Fusarium* head blight disease (FHB) of wheat and other cereal grains, contains two genes putatively encoding for proteins with a CP domain, named *fgcpp1* and *fgcpp2*, and five genes encoding for HPs, named FgHyd1-5. In order to verify their contribution during plant infection and fungal growth, single and multiple gene knock-out mutants were produced and characterized. Besides, the two *F. graminearum* CPPs (FgCPPs) were heterologously expressed to investigate their activity.

The FgCPPs seem to be dispensable for fungal virulence but protect fungal cell wall polysaccharides from enzymatic degradation. The FgCPPs show a strong ability to reduce, mainly by a non-enzymatic mechanism, the viscosity of carboxymethyl cellulose (CMC), with higher affinity for substrates with medium/high viscosity and favour fungal cellulase activity. The observation that the double knock-out mutant Δ*Δfgcpp*$_{1,2}$ grown on CMC produced more cellulase activity than the wild type suggests that the higher enzymatic activity produced by the mutant could compensate during infection for the absence of the FgCPPs activity on plant cellulose.

The *F. graminearum* Hyd2 and Hyd3 are responsible of the hydrophobicity of aerial hyphae and are involved in adhesion of conidia to the host surface during the early stages of the infection process, as shown by the reduced virulence of the Δ*hyd2* and Δ*hyd3* on *Triticum aestivum* observed by spray inoculation. Interestingly, triple Δ*hyd1,2,3,* Δ*hyd2,3,4* and Δ*hyd2,3,5* mutants produced a reduced number of mature perithecia and showed defects at the cell wall level, being significantly more

inhibited than the wild type by β-1,3-glucanase and more susceptible to tebuconazole, an ergosterol biosynthesis inhibitor fungicide.

Based on our results, FgCPPs and FgHyds could be used as targets of new molecules in innovative disease management strategies aimed at increasing fungal susceptibility to plant defense proteins or at reducing fungal ability to adhere to host plant tissues. Furthermore, the ability of FgCPPs to loosen CMC and favor cellulase activity could make these proteins suitable for future potential applications in biofuel production using cellulose rich tissues as substrate.

Preface

Fusarium graminerarum is a devastating Ascomycete pathogen of cereals worldwide, attacking crops such as wheat, maize and barley, that are of paramount importance for food and animal feed. Besides, this fungus is also responsible for root and collar rot of soybean seedlings, a dicotyledonous species (Pioli et al., 2004; Sella et al., 2014). On cereal crops, *F. graminearum* is the primary responsible of the *Fusarium* head blight (FHB) disease (Goswami and Kistler, 2004) and causes losses of billions of dollars annually by reducing the yield and contaminating the harvest with heat-stable mycotoxins, such as trichothecenes, which are cytotoxins harmful to human and animal health (McMullen et al., 1997). In particular, wheat is one of the main cultivated species and it is therefore important to develop innovative disease-protection strategies in addition to conventional ones based on introgression of resistance characters and distribution of fungicides, which is to date the most commonly control method used, although not always effective (Nicholson et al., 2003).

Molecules involved in the plant infection process differ structurally and functionally in relation to the attacking strategy of the pathogen. The knowledge of the infection mechanisms of pathogens and the identification of secreted fungal virulence factors is an essential requirement to identify new control methods potentially usable to protect plants. For example, improving the plant defensive mechanism with inhibitors of secreted fungal virulence factors would render the pathogen less virulent. Therefore, the identification of *F. graminearum* genes involved in the pathogenetic process would be essential to develop innovative plant protection strategies, such as the obtain of resistant varieties of cereals, the synthesis of new fungicide molecules able to block the infection process, or the use of fungal non-pathogenic mutants as antagonists of pathogens in biological control programs. However, at present, only few virulence factors of *F. graminearum* are known (the trichothecene mycotoxin deoxynivalenol and a lipase) (Bai et al., 2002; Voigt et al., 2005). The infection process of *F. graminearum* has been well-studied (Schäfer, 1994; Boenisch and Schäfer, 2011); during wheat infection, the fungus expresses and secretes cerato-platanins (CPPs) and hydrophobins (HPs) (Brown et al., 2012; this thesis), small non-catalytic cysteine-rich proteins that could play a broad spectrum

of functions in fungal growth and pathogenicity. In order to clarify their role, single and multiple *F. graminearum* knock-out mutants of the corresponding encoding genes have been produced and characterized in vitro and in vivo. Besides, the *F. graminearum* CPPs have been heterologously expressed in the *Pichia pastoris* yeast to investigate their biological activity.

Chapter I

Involvement of the *Fusarium graminearum* cerato-platanin proteins in fungal growth and plant infection

Abstract

The genome of *Fusarium graminearum*, a necrotrophic fungal pathogen causing *Fusarium* head blight (FHB) disease of wheat, barley and other cereal grains, contains five genes putatively encoding for proteins with a cerato-platanin domain. Cerato-platanins are small secreted cysteine-rich proteins possibly localized in the fungal cell walls and also contributing to the virulence. Two of these *F. graminearum* proteins (*fgcpp1* and *fgcpp2*) belong to the class of SnodProt proteins which exhibit phytotoxic activity in the fungal pathogens *Botrytis cinerea* and *Magnaporthe oryzae*. In order to verify their contribution during plant infection and fungal growth, single and double gene knock-out mutants were produced and no reduction in symptoms severity was observed compared to the wild type strain on both soybean and wheat spikes. Histological analysis performed by fluorescence microscopy on wheat spikelets infected with mutants constitutively expressing the dsRed confirmed that FgCPPs do not contribute to fungal virulence. In particular, the formation of compound appressoria on wheat paleas was unchanged. Looking for other functions of these proteins, the double mutant was characterized by in vitro experiments. The mutant was inhibited by salt and H_2O_2 stress similarly to wild type. Though no growth difference was observed on glucose, the mutant grew better than wild type on carboxymethyl cellulose. Additionally, the mutant's mycelium was more affected by treatments with chitinase and β-1,3-glucanase, thus indicating that FgCPPs could protect fungal cell wall polysaccharides from enzymatic degradation.

1.1. Introduction

Cerato-platanin (CP) is a phytotoxic cysteine-rich protein produced by *Ceratocystis platani*, the causal agent of canker stain disease of the European plane tree *Platanus acerifolia* (Pazzagli et al., 1999). CP is the founder member of the cerato-platanin proteins (CPPs) family (Pfam domain PF07249), which include a large enigmatic group of proteins produced only by pathogenic and non-pathogenic filamentous fungi (Chen et al., 2013). CPPs are small noncatalytic and moderately hydrophobic proteins (120-140 amino acids) containing a cerato-platanin domain and four conserved cysteine residues that have been experimentally proven to form two disulfide bridges (Pazzagli et al., 2014). Recent data show that Ascomycete genomes usually contain one or two CPPs encoding genes and information available to date on CPPs comes almost exclusively from these fungi (Chen et al., 2013; Gaderer et al., 2014). All the CPPs characterized so far in Ascomycetes (Pazzagli et al., 2014) have a primary structure similar to the CP of *C. platani*. These CPPs contain a signal peptide that targets them to the secretory pathway and are abundantly secreted into fungal culture media, but several studies have shown that these proteins can bind to N-acetylglucosamine oligomers and chitin (de Oliveira et al., 2011) and are likely also localized in the fungal cell walls (Gaderer et al., 2014; Pazzagli et al., 2014). Differently from what initially hypothesized (Sbrana et al., 2007), CPPs are not hydrophobin-like proteins since they have different biochemical and structural properties (Gaderer et al., 2014; Pazzagli et al., 2014).

Regarding Basidiomycetes, their genome may possess up to twelve cerato-platanin genes often showing highly different sequences, but only those from *Moniliophthora perniciosa*, *Heterobasidion annosum* and *H. irregulare* have been studied to date (de O Barsottini et al., 2013; Baccelli et al., 2015; Chen et al., 2015).

At present, the main function of CPPs is not clear. Several studies revealed that CPPs could play at least two roles in fungi; the first is associated with fungal growth and development, probably due to their presence in the cell wall, and the second is associated with CPPs secretion during fungal-plant interactions (Baccelli, 2015). In fact, CPPs are structurally related to plant expansins, which mediate

cell wall loosening and are involved in growth and other various processes (Sampedro and Cosgrove, 2005): like expansins, CPPs weaken cellulosic materials with a non-hydrolytical mechanism (Baccelli et al., 2014) but, differently from expansins, they do not bind to cellulose (Baccelli et al., 2014; Pazzagli et al., 2014). Therefore, CPPs could be involved in hyphal elongation (Baccelli, 2015) but they might play also a function during plant infection by loosening plant cell wall and favoring the advancement of the fungal hyphae in the plant tissue or by exploiting their necrosis-inducing ability (Pazzagli et al., 2014). A role of CPPs as virulence factors has been demonstrated with CPPs-disrupted mutants of the hemibiotrophic pathogen *Magnaporthe oryzae* during its necrotrophic stage on rice (Jeong et al., 2007), and of the necrotrophic pathogen *Botrytis cinerea* on tobacco and tomato leaves (Frías et al., 2011).

Fusarium graminearum Schwabe [teleomorph *Gibberella zeae* (Schwein) Petch] is a ubiquitous hemibiotrophic fungal plant pathogen (Brown et al., 2010) belonging to the Ascomycetes phylum and is the causal agent of the *Fusarium* head blight (FHB) disease, which affects monocot cereal species such as wheat, barley and corn (Goswami and Kistler, 2004). This fungus is also responsible for root and collar rot of soybean seedlings, a dicotyledonous species (Pioli et al., 2004). *F. graminearum* causes significant economic losses by reducing kernel weight and by contaminating seeds with mycotoxins belonging to the group of trichothecenes (Goswami and Kistler, 2004). Among trichothecenes, deoxynivalenol (DON) is the major cause of contamination of wheat (McMullen et al., 1997; Goswami and Kistler, 2005) and its secretion in infected tissues facilitates the infection process of *F. graminearum*: this mycotoxin is in fact important for the aggressiveness of the fungus in durum and mostly in soft wheat (Langevin et al., 2004) as it blocks the defensive responses of the host, favoring the spread of the fungus in the rachis and thus in the entire spike (Bai et al., 2002), and it elicits cell death (Desmond et al., 2008). During the infection process *F. graminearum* enters the host through natural openings or through epidermal cells by secreting cell wall degrading enzymes (Wanyoike et al., 2002). By combining several bioinformatic approaches, *F. graminearum* has been proposed to be able to secrete 574 proteins (Brown et al., 2012); several annotated proteins include

enzymes and toxic proteins possibly contributing to virulence (Brown et al., 2012). In particular, two putatively secreted proteins (FGSG_10212 and FGSG_11205; Lu and Edwards, 2016) are structurally related to CPPs and particularly to the phytotoxin SnodProt1, secreted by the pathogenic fungus *Stagonospora nodorum* during infection of wheat leaves (Hane et al., 2007). A previous proteomic study had showed that the FGSG_10212 and FGSG_11205 proteins are secreted in planta during wheat spike infection (Paper et al., 2007); furthermore, a transcriptomic analysis confirmed that the corresponding genes are expressed in the early stages of wheat spike infection (Lysøe et al., 2011). Since the function of these two *F. graminearum* CPPs (FgCPPs) is not yet known, the aim of the present study is to characterize their biological function by producing single (Δ*fgcpp*$_1$) and double (ΔΔ*fgcpp*$_{1,2}$) knock-out mutants of the corresponding genes by targeted homologous recombination.

1.2. Materials and methods

1.2.1. Sequences analysis and primer design

An in-silico analysis of the *F. graminearum* genome (Cuomo et al., 2007; MIPS database, http://mips.helmholtz-muenchen.de/genre/proj/fusarium/) revealed the presence of two putative cerato-platanin encoding genes related to SnodProt (MIPS database entries: FGSG_10212 and FGSG_11205, here named FgCPP1 and FgCPP2) and other three additional genes encoding proteins with a cerato-platanin domain (MIPS database entries: FGSG_03971, FGSG_04471 and FGSG_17103).

Prediction of signal peptides (SP) and cerato-platanin (CP) conserved domains were performed by SMART analysis tool (http://smart.embl-heidelberg.de/) and Motif Scan (MyHits, SIB, Switzerland; http://myhits.isb-sib.ch/cgi-bin/motif_scan), respectively.

Alignments of amino acid (aa) sequences of the fungal CPPs, including the putative *F. graminearum* cerato-platanins, were obtained by Clustal X 2.1 software. Analysis of conserved regions was performed using GeneDoc v.2.3.0 program.

A multiple sequence alignment generated with CLUSTALW was used as input for determining phylogenetic relationships by the Neighbour Joining model using MEGA 5 software.

The hydropathy score of the FgCPP1 and FgCPP2 was calculated with ProtScale software (http://expasy.org/tools/) by using the Kyle and Doolittle aa scale. All the primers used were designed by using PRIMER3 (http://primer3.ut.ee/) and PerlPrimer v.1.1.17 softwares (Table S1.1).

1.2.2. Fungal strains and culture conditions

The *F. graminearum* wild type (WT:8/1) and the mutant strains were cultured at 25 °C on potato dextrose agar (PDA, Difco). The hydrophobicity of the colony surface was evaluated as reported by Li et al. (2006). Conidia were obtained by culturing *F. graminearum* strains in carboxymethyl cellulose (CMC; Sigma-Aldrich) as reported in Sella et al. (2016).

For dry weight experiments and expression analysis of the FgCPPs, mycelia of WT and mutant strains were grown in flasks containing 20 mL of Szécsi medium (0.09% w/v $NH_4H_2PO_4$, 0.2% w/v $(NH_4)_2HPO_4$, 0.01% w/v $MgSO_4 \cdot 7 H_2O$, 0.05% w/v KCl) supplemented with 1% (w/v) D-(+)-glucose (Sigma-Aldrich) or 1% (w/v) carboxymethyl cellulose (CMC) with high viscosity and 10^5 conidia mL^{-1}. Flasks were incubated at 25 °C on an orbital shaker at 150 rpm. The mycelium was recovered after 3 and 5 days for RNA extraction; for dry weight experiments, after 4 days of culture, the mycelium was filtered through a Wilson-sieve (40 µm), washed twice with deionized water, oven dried at 80 °C for 3 days and weighed.

For growth assays in the presence of NaCl and H_2O_2, mycelial plugs from the edge of a 3-day-old colony grown on complete medium (CM) were placed in the middle of the assay plates. One liter of CM contained 10 mL of solution A [$Ca(NO_3)_2 \cdot 4 H_2O$ at 100 g L^{-1}], 10 mL of solution B [KH_2PO_4 at 20 g L^{-1}, $MgSO_4 \cdot 7H_2O$ at 25 g L^{-1}, and NaCl at 10 g L^{-1}, sterilized by filtration], 10 g of glucose, 1 mL of suspension D [H_3BO_3 at 60 g L^{-1}, $CuSO_4 \cdot 5H_2O$ at 390 mg L^{-1}, KI at 13 mg L^{-1}, $MnSO_4 \cdot H_2O$ at 60 mg L^{-1}, $(NH_4)_6Mo_7O_{24} \cdot 4H_2O$ at 51 mg L^{-1}, $ZnSO_4 \cdot 7H_2O$ at 5.48 g L^{-1}, and $FeCl_3 \cdot 6 H_2O$ at 932 mg L^{-1}], 1 g of yeast extract, 0.5 g of enzymatically hydrolyzed casein, and 0.5 g of acid-hydrolyzed casein. The growth assay plates were supplemented with NaCl or H_2O_2 to obtain a final concentration of 1 M or 10, 15 and 20 mM, respectively. The plates were incubated at 28 °C for 3 days in the dark. The diameter of the colonies was measured using a technical ruler. The analyses were performed with three replicates.

1.2.3. Construction of the gene replacement vectors and fungal transformation-mediated gene disruption

To generate the construct for disrupting the *fgcpp1* gene, its flanking homologous regions, necessary for targeted homologous recombination, were amplified by PCR using *F. graminearum* WT genomic DNA as template. Specific oligonucleotides were designed to amplify the upstream (primers UP10212for/rev) and downstream (primers DOWN10212for/rev) flanking regions (Table S1.1 and

Fig. S1.1A) of about 900 bp. The amplification was performed by using the REDTaq ReadyMix PCR Reaction Mix (Sigma-Aldrich) in a 50 μL volume. PCR conditions were as follows: 94 °C for 3 min, followed by 35 cycles of 94 °C for 30 s, 55 °C for 30 s and 72 °C for 1 min. The amplicons obtained were purified and used in a second PCR to fuse the homologous flanking regions with the hygromycin resistance gene (hygromycin B phosphotransferase, *Hyg*), used as selection marker. The fusion PCR reaction was performed with the REDTaq ReadyMix PCR Reaction Mix in a 50 μL volume using 100 ng of the purified flanking regions containing tails homologous to the 5' and 3' *Hyg* gene (Fig. S1.1A) and 300 ng of the *Hyg* gene cut with *Sma*I (Fermentas) from pAN7-1 vector (Voigt et al., 2005). The fusion PCR conditions were as follows: 94 °C for 3 min, followed by 20 cycles of 94 °C for 30 s, 60 °C for 1 min and 72 °C for 4 min. The fusion PCR product was then used as template in a nested PCR reaction with the primers NEST10212for/rev (Table S1.1 and Fig. S1.1A). Nested PCR conditions were as follows: 94 °C for 3 min, followed by 35 cycles of 94 °C for 30 s, 54 °C for 30 s and 72 °C for 4 min. The amplicon obtained was cut from agarose gel, purified and then cloned into the pGEM-T easy vector (Promega) following the manufacturer's instruction. An *Escherichia coli* positively transformed colony was grown in high salt lysogeny broth culture and the plasmid DNA was extracted with the "GenElute HP Plasmid Midiprep" kit (Sigma-Aldrich) following manufacturer's instructions. The construct of 3460 bp was then amplified from pGEM-T vector by PCR and 10 μg were used to transform protoplasts of the WT strain.

To obtain the double knock-out mutant, the flanking homologous regions of the *fgcpp2* gene were amplified by PCR using *F. graminearum* WT genomic DNA as template and specific oligonucleotides (primers UP11205for and UPGEN11205rev; DOWNGEN11205for and DOWN11205rev) (Table S1.1 and Fig. S1.1B). The amplification was performed as above reported. The amplicons obtained were purified and used in a second PCR to fuse the homologous flanking regions with the geneticin (*GEN*) resistance gene, used as selection marker. The fusion PCR reaction was performed as above reported using 100 ng of the purified flanking regions containing tails homologous to the 5' and 3' region of the *GEN* gene (Fig. S1.1B) and 900 ng of the *GEN* gene cut

with *Bgl*II and *Hind*III (Promega) from the pII99 plasmid (Jansen et al., 2005). The fusion PCR product was then used as template in a PCR reaction for the production of two Split-marker constructs using the primer pairs NESTGEN11205for/SPLITUPGENrev and SPLITDOWNGENfor/NESTGEN11205rev, respectively (Table S1.1 and Fig. S1.1B). The PCR conditions were as follows: 94 °C for 3 min, followed by 35 cycles of 94 °C for 1 min, 55 °C for 30 s and 72 °C for 3 min. Purification and cloning of the amplicons and plasmid DNA extraction were performed as above reported. Approximately 10 μg of the SPLIT UP construct (~3 Kb) and 10 μg of the SPLIT DOWN construct (~2.8 Kb) were excised from the pGEM-T vector (Promega) with *Apa*I and *Sac*I enzymes (Fermentas) and the linearized constructs were used to transform protoplasts of the Δ*fgcpp*$_1$ mutant (strain 1.14).

The generation of dsRed-fluorescent strains for mycelium localization in wheat tissue was obtained by transforming with the vector p99II:dsRed carrying the dsRed gene under the control of the constitutive glycerol-3-phosphate dehydrogenase promoter (gpdA) of *Aspergillus nidulans* (Van Nguyen et al., 2012). Infection structures produced by the dsRed strains were investigated by fluorescence microscopy using Axio Imager Z1 microscope equipped with a Zeiss ApoTome. A UV (ultra violet) lamp HAL 100 served as UV light source. DsRed was excited in the range of 538 to 562 nm and detected in the 570 to 640 nm range. Images were taken with Zeiss AxioCam MRm CCD camera. Image processing, including overlay of different fluorescence channels and generation of maximum intensity projections (MIP) of z-stacks were done with Zeiss AxioVision software.

Protoplast preparation and fungal transformation were performed according to Van Nguyen et al. (2012). Hygromycin and geneticin resistant colonies were collected and transferred to 30-mm CM plates supplemented with 400 μg mL^{-1} of hygromycin B (Duchefa Biochemie) or geneticin (Invitrogen Life Technologies). Resistant mutants were single-conidiated and preliminarily screened by PCR using the primer pairs INT10212for/rev (Ta 51 °C), INT11205for/rev (Ta 51 °C), HygPRB2for/rev (Ta 55 °C) and GenPRBf/r (Ta 55 °C) (Table S1.1 and Fig. S1.1A-B). The PCR

conditions were as follows: 94 °C for 3 min, followed by 35 cycles of 94 °C for 30 s, 51 or 55 °C for 30 s and 72 °C for 40 s. Transformants were then confirmed by Southern blot hybridization.

1.2.4. Southern blot analysis

Genomic DNAs from *F. graminearum* WT and mutant strains were extracted as reported by Henrion et al. (1994) from 200 to 400 mg of mycelium; 3 μg of genomic DNA samples were digested with the restriction enzymes specified in Fig. S1.1A-B, separated on a 1% (w/v) agarose gel and blotted onto an Hybond NX membrane (Amersham Biosciences). Digoxygenin (DIG; Roche)-labeled specific probes were generated with primers specific for *fgcpp1, fgcpp2, Hyg* or *GEN* genes (Table S1.1 and Fig. S1.1A-B) by using genomic or plasmid DNA as template, and were used for overnight hybridization at 65 °C. The PCR reaction, performed in a 100 μL volume using DIG-11-dUTP (Roche), consisted of 3 min at 94 °C, followed by 35 cycles of 94 °C for 30 s, 51 or 55 °C for 1 min and 72 °C for 2 min. Southern Blot hybridization and detection of the DIG-labeled probes were performed according to manufacturer's instruction. Membranes were exposed to X-ray film (X-Omat AR; Kodak) for approximately 3 h.

1.2.5. Plant growth and infection

Wheat plants (*Triticum aestivum* cv. Bobwhite) were grown and inoculated at anthesis with approximately 2000 conidia as reported in Sella et al. (2014). Four independent infection experiments were performed by inoculating at least 10 plants with each strain. After inoculation, the spikes were covered for 3 days with a plastic bag to maintain a moist environment. Disease symptoms were assessed up to 21 days post inoculation (dpi) by counting the number of visually diseased spikelets and by relating them to the total number of spikelets of the respective head, resulting in a percentage of symptomatic spikelets. Data were statistically analyzed by applying the Student's t-test.

The pathogenicity tests in soybean (*Glycine max* cv. Demetra, Syngenta) were performed according to the "Rolled Towel" protocol reported in Sella et al. (2014) using 20,000 conidia, previously pre-

germinated for 16 h, per seed. As control the conidial suspension was replaced with water. After 6 days of incubation in the dark at 25 °C, the virulence of the *F. graminearum* strains was determined by measuring the Disease Severity Index (DSI), defined as the ratio between the length of the lesion and the total length of the seedling × 100. Infection experiments were repeated at least four times.

1.2.6. Inoculation of wheat flower leaves

For the bioassay with detached floret tissues, spikelets of wheat plants were taken at anthesis to isolate paleas. Organs were detached from the floret with a razor blade and placed after washing with sterile H_2O in Petri dishes (92 × 16 mm) on 1.6% (w/v) granulated agar (BD Difco). One Petri dish contained 8 biological replicates of one floret organ and represented one independent experiment. The adaxial side of palea was inoculated with 5 µL sterile water containing 100 conidia of WT, Δ*fgcpp*$_1$ and ΔΔ*fgcpp*$_{1,2}$ mutants constitutively expressing dsRed. After inoculation, the Petri dishes were sealed with Parafilm and incubated in a growth chamber at 18 °C for 6 days.

1.2.7. RNA extraction and Reverse Transcription (RT)

RNA was extracted from 100 to 200 mg of frozen wheat spikes infected with WT and mutant strains and collected at 0, 1, 2 and 3 dpi, or from 100 to 200 mg of frozen mycelium grown in Szécsi medium for 3 and 5 days. RNA extraction, DNase treatment and RT were performed as reported in Sella et al. (2016).

1.2.8. Expression of the FgCPP encoding genes in vitro and during wheat spikes infection

The amplification of the FgCPPs and *β-tubulin* (MIPS database entry FGSG_06611) encoding genes was performed by qPCR (Rotor-Gene Q 2plex, QIAGEN) using specific primers (Table S1.1) and RNA extracted as above reported from infected spikelets or mycelium. The 20 µL reaction mixture contained 10 µL of 2X Rotor-Gene SYBR Green PCR MasterMix (QIAGEN), 0.4 µM of each specific primer and 3 µL of cDNA as template. The qPCR was performed by repeating 40 times the

following cycle: 20 s at 95 °C; 20 s at 52 °C; 30 s at 72 °C. Reactions were performed in triplicates. Relative expression results were calculated using the Rotor-Gene v. 2.0.3.2 software (QIAGEN) which uses the threshold cycle and the amplification efficiency of each amplicon to calculate the comparative concentration of each gene by setting the relative expression of the *β-tubulin* reference gene to 1. PCR reactions performed using RNA as template excluded contamination with genomic DNA.

The qPCR amplification of the *FGSG_03971* and *FGSG_04471* genes was performed with specific primers (Table S1.1) using RNA extracted as above reported from infected spikelets or mycelium and repeating for 35 times the following cycle (20 s at 95 °C; 20 s at 55 °C; 30 s at 72 °C). Two independent qPCR experiments starting from different cDNA preparations were performed.

1.2.9. Treatment of F. graminearum *strains with chitinase and glucanase*

Microtiter plate wells were filled with 200 µL of potato dextrose broth (PDB; Difco Laboratories) 2X at pH 6.85 supplemented with 0.15 and 0.3 U of chitinase from *Streptomyces griseus* (Sigma-Aldrich) resuspended in 50 mM potassium phosphate pH 6.0 or with 0.15 and 0.3 U of β-1,3-glucanase from *Trichoderma longibrachiatum* (Sigma-Aldrich) resuspended in 20 mM sodium citrate pH 5.0. Controls were performed by adding the respective buffer solutions instead of the enzyme solutions. After addition of macroconidia of *F. graminearum* WT and Δ*fgcpp*$_{1,2}$ mutant (strains 1.1 and 1.4) to obtain a final concentration of 2×10^5 spores mL^{-1}, 68 µg mL^{-1} of resazurin dye (Sigma-Aldrich) were added to each well to measure fungal growth. Resazurin is reduced to pink color in presence of actively growing cells and was previously used to evaluate *F. graminearum* growth inhibition (Sella et al., 2014). The microtiter plate wells were incubated in the dark at 25 °C and the absorbance was read at 578 nm at different time points. The percentage of fungal growth was calculated as 100 minus the percentage of the ratio between net absorbance values of each sample and net absorbance of the medium with the resazurin dye but without the fungus. Each experiment was replicated three times and inhibition was calculated when the control samples reached about 50% of growth.

To determine reducing sugars released from mycelia of WT and ΔΔ*fgcpp*$_{1,2}$ mutant (strains 1.1 and 1.4) by β-1,3-glucanase treatment, 2×10^4 conidia mL^{-1} were grown in flasks containing 15 mL of Szécsi medium supplemented with 1% (w/v) D-(+)-glucose. After 4 days of incubation at 25 °C and 150 rpm, mycelia were washed twice with deionized water and then treated for 24 h at 30 °C with 0.15 U of β-1,3-glucanase solution prepared as above reported. Mycelia incubated only with 20 mM sodium citrate buffer pH 5.0 were used as control. One hundred μL of samples supernatant were assayed as reported by Nelson et al. (1944) by using D-(+)-glucose as standard.

1.3. Results

1.3.1. In silico analysis of cerato-platanin box genes in the F. graminearum *genome*

The putative aa sequences of FgCPP1 and FgCPP2 were aligned with other CPPs of different Ascomycetes fungal species and with three additional putative *F. graminearum* CPPs (FGSG_04471; FGSG_17103; FGSG_03971) identified in the fungal genome (Fig. S1.2). The alignment showed that the putative FgCPP1 and FgCPP2 share a 61% protein identity. The FgCPPs showed the highest identity percentage with the CPPs of *M. oryzae* (51%) and *S. nodorum* (46%) and the lowest identity percentage (about 8%) with the other three putative *F. graminearum* CPPs (Fig. S1.2). FgCPP1 and FgCPP2, as well as the CPPs of *S. nodorum*, *C. platani*, *B. cinerea* and *M. oryzae*, show the typical conserved 4-cysteine residues and have a predicted molecular weight of about 13 kDa. Differently, the FGSG_04471 shows the same conserved cysteines with five additional ones, the FGSG_03971 possesses three conserved and six additional cysteines, while the FGSG_17103 contains only one conserved cysteine (Fig. 1.1 and Fig. S1.2). All the proteins analyzed contain a secretion signal peptide, except the FGSG_17103 (Fig. 1.1). The FGSG_03971, FGSG_04471 and FGSG_17103 proteins contain a putative cerato-platanin domain, although with predicted e-values of only 0.00077, 0.0011 and $6.5e^{-7}$, respectively. Besides, these proteins do not have the typical length of 120-140 aa characterizing the CPPs family (Fig. 1.1 and Fig. S1.2) and do not contain the two-peptide motives of 10 residues (PepA and PepB) putatively responsible of the necrosis-inducing activity (Frías et al., 2014), which are present in all the other proteins analyzed (Fig. S1.2).

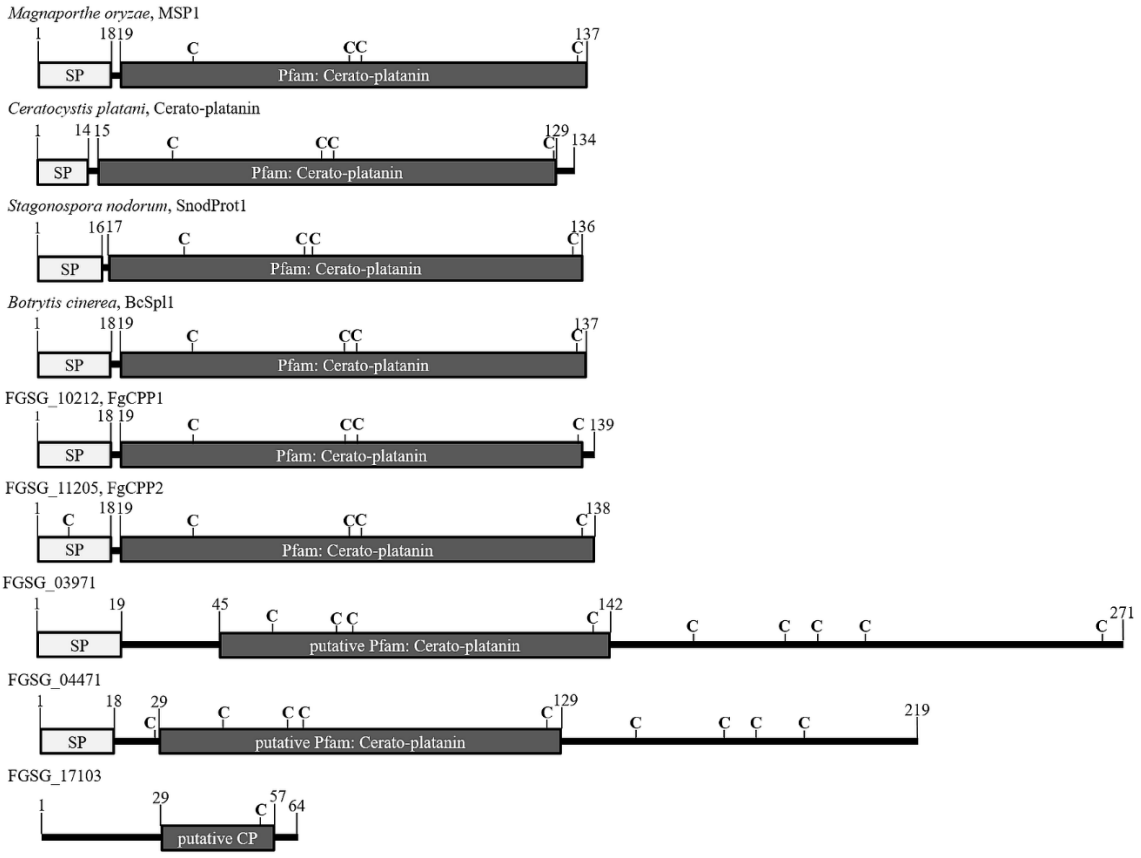

Fig. 1.1. Domain structure of several putative cerato-platanin proteins of different fungi. Prediction of signal peptides (SP) and cerato-platanin (CP) conserved domains were performed by SMART analysis tool (http://smart.embl-heidelberg.de/) and Motif Scan (MyHits, SIB, Switzerland; http://myhits.isb-sib.ch/cgi-bin/motif_scan), respectively. All the cysteine residues are indicated by a "C". The numbers stand for amino acid positions and show the start and the end of predicted domains. The fungal proteins used are*: Fusarium graminearum* FGSG_10212 (FgCPP1, XP_011319159.1); *F. graminearum* FGSG_11205 (FgCPP2, XP_011325136.1); *F. graminearum* FGSG_03971 (XP_011321691.1); *F. graminearum* FGSG_04471 (XP_011321126.1); *F. graminearum* FGSG_17103 (CEF76364.1); *Stagonospora nodorum* SnodProt1 (SP1, AAC26870.1); *Ceratocystis platani* Cerato-platanin (Cerato-pla, CAC84090.2); *Magnaporthe oryzae* SnodProt1 (MSP1, XP_003710181.1); *Botrytis cinerea* SnodProt-like1 (BcSpl1, XP_001559499.1). The corresponding accession numbers were obtained from the NCBI database (http://www.ncbi.nlm.nih.gov/).

1.3.2. Features of the putative FgCPP1 and FgCPP2

The putative FgCPP1 and FgCPP2 mature proteins have relatively low hydropathy index and similar hydropathy plots, with a succession of small positive peaks of hydrophobic aa (Fig. S1.3). The aa sequences of the CPPs of different ascomycetes fungal species, including FgCPP1 and FgCPP2, were used to build a Neighbour joining tree. Phylogenetic tree reveals that the two putative FgCPPs belong to two sister-clades of sequences (Fig. 1.2). The FgCPP2 clusters with EPL1 of *T. atroviride* and SM1

of *T. virens* with a high level of similarity, whereas the FgCPP1 clusters with the CPP of *M. oryzae* and *N. crassa* although with a lower bootstrap value (Fig. 1.2).

The 5'-upstream region of the *fgcpp1* and *fgcpp2* genes was analyzed in order to identify the TATA box consensus sequence TATAA. A canonical TATA box was detected only in the *fgcpp1* promoter region, 153 bp upstream of the ATG start codon (data not shown).

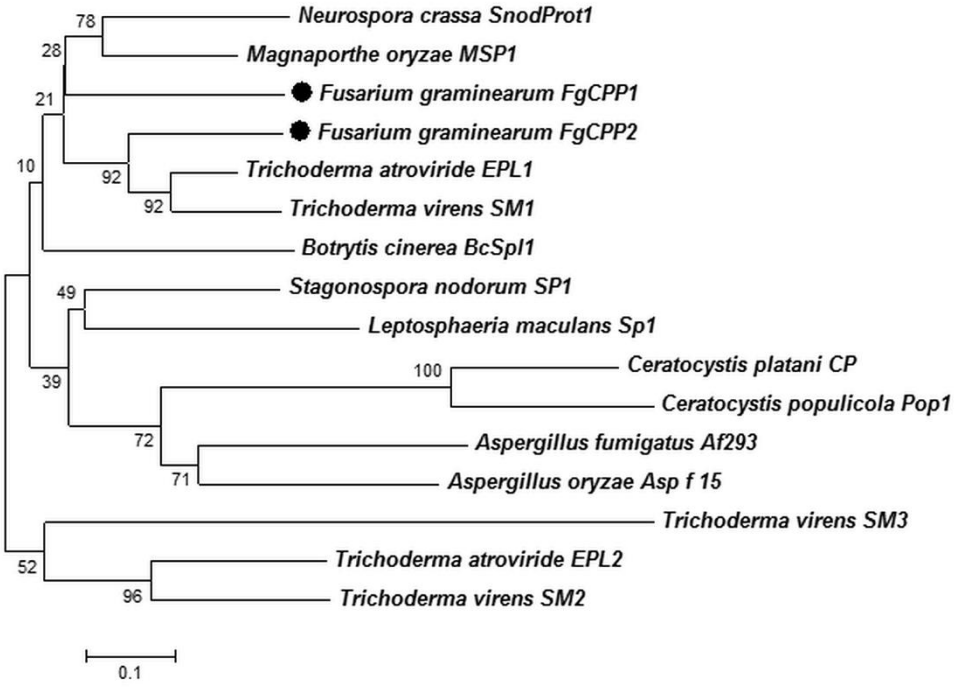

Fig. 1.2. Phylogenetic tree of the FgCPP1, FgCPP2 and the CPPs from different Ascomycetes fungal species. The Neighbour Joining model was built using MEGA 5 software. Two main clades can be distinguished. Robustness of the generated tree was determined using 1000 bootstrap replicates. Bootstrap values are provided at the beginning of each branch and are given as a percentage. The fungal proteins used are: *Fusarium graminearum* FgCPP1 (XP_011319159.1); *F. graminearum* FgCPP2 (XP_011325136.1); *Neurospora crassa* SnodProt1 (CAC28585.2); *Ceratocystis platani* CP (CAC84090.2); *Magnaporthe oryzae* MSP1 (XP_003710181.1); *Botrytis cinerea* BcSpl1 (XP_001559499.1); *Trichoderma atroviride* EPL1 (ABE73692.1); *T. atroviride* EPL2 (EHK46032.1); *T. virens* SM1 (EHK25601); *T. virens* SM2 (EHK20677); *T. virens* SM3 (EHK25819); *C. populicola* Pop1 (ABM63506.1); *Stagonospora nodorum* SP1 (AAC26870.1); *Leptosphaeria maculans* SP1 (AAM33130.1); *Aspergillus fumigatus* Af293 (EAL93557.1); *A. oryzae* Asp f 15 (KDE77497.1). The corresponding accession numbers were obtained from the NCBI database (http://www.ncbi.nlm.nih.gov/).

1.3.3. The fgcpp1 *gene is the most expressed during early stages of wheat spike infection and during in vitro growth on different carbon sources*

Expression analysis of *fgcpp1* and *fgcpp2* genes was conducted by qPCR using RNA extracted from wheat spikelets harvested at different hours post infection (0, 24, 48 and 72 hpi) and the *F. graminearum β-tubulin* gene (*FGSG_06611*) as reference. The *fgcpp1* gene was already transcribed at 24 hpi, and its expression was further induced at 48 and 72 hpi (~1.8-fold compared to the expression level of *β-tubulin*, set to 1). Differently, the *fgcpp2* gene was poorly expressed at every time point (Fig. 1.3).

A relative low level of expression of the *fgcpp2* gene was also observed when the fungus was grown in liquid media containing glucose or CMC as sole carbon source, whilst the *fgcpp1* gene was much more expressed, particularly on glucose after 5 days of growth (~9-fold compared to the expression level of the *β-tubulin* gene) (Table 1.1).

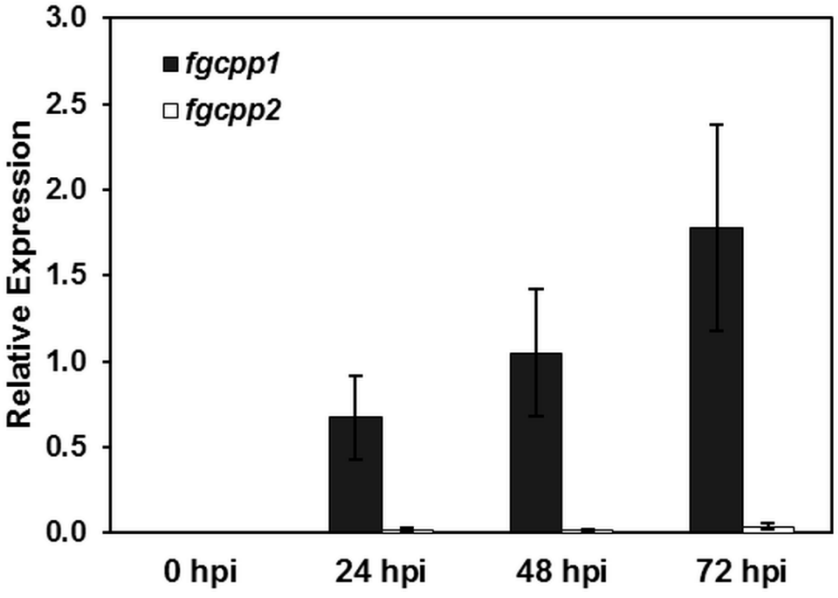

Fig. 1.3. Relative expression level of *fgcpp1* and *fgcpp2* genes during wheat spike infection. Expression analysis was performed by qPCR with Rotor-Gene Q (QIAGEN) at 0, 24, 48 and 72 h post infection (hpi). Each transcript was normalized with the *Fusarium graminearum β-tubulin* gene as reference (set to 1) and the relative expression was calculated using the Rotor-Gene v. 2.0.3.2 software. Data represent the mean ± standard error (indicated by bars) of four independent qPCR experiments.

Table 1.1. Relative expression level of the *fgcpp1* and *fgcpp2* genes after 3 and 5 days of growth in Szécsi medium supplemented with glucose or carboxymethyl cellulose (CMC) as the sole carbon source. qPCR was performed with Rotor-Gene Q 2plex (QIAGEN). Each transcript was normalized with the *Fusarium graminearum β-tubulin* gene as reference (set to 1) and the relative expression was analyzed using the Rotor-Gene v. 2.0.3.2 software. Data represent the mean of at least two independent experiments ± standard error.

WT	In vitro (glucose)		In vitro (CMC)	
	3 days	5 days	3 days	5 days
fgcpp1	1.730 ± 0.100	9.380 ± 2.320	0.234 ± 0.019	0.283 ± 0.043
fgcpp2	0.028 ± 0.005	0.182 ± 0.030	0.011 ± 0.001	0.028 ± 0.003

1.3.4. Targeted gene disruption shows that the FgCPPs do not contribute to fungal virulence

F. graminearum WT protoplasts were initially transformed with a construct containing the *Hyg* resistance gene in order to replace the *fgcpp1* gene. Forty-seven hygromycin-resistant regenerated colonies were checked by PCR for the presence/absence of the 252 bp internal fragment of the *fgcpp1* gene. Six putative Δ*fgcpp*$_1$ mutant strains selected by PCR (strains 1.8, 1.14, 1.16, 1.19, 1.44 and 1.47; Fig. S1.4A and data not shown) were further analyzed by high-stringency Southern blot using the *fgcpp1* and *Hyg* specific probes. Hybridization results showed the disruption of the gene of interest in all the six mutant strains analyzed, since only the WT strain showed the hybridization signal at the expected position of about 5 kb (Fig. S1.5A). By using the *Hyg* probe, only 4 of the 6 Δ*fgcpp*$_1$ mutant strains analyzed showed a hybridization band at the expected position of about 6 kb (strains 1.8, 1.14, 1.16 and 1.44) and at least one ectopic integration of the construct in their genome. The 1.14, 1.16 and 1.44 single mutant strains, showing a lower number of ectopic integrations (Fig. S1.5B), were selected to inoculate soybean in order to evaluate their virulence. At 6 dpi, the DSI of all the mutant strains showed no reduction compared with the WT strain (Fig. 1.4). Infection experiments on wheat spikes, performed at anthesis with a spore suspension of the WT and the Δ*fgcpp*$_1$ mutant (strain 1.14), showed that the mutant maintained the capability to infect wheat spikes and no significant reduction in the percentage of infected spikelets was observed compared with WT (Fig. 1.5). The expression of

the *fgcpp2* gene was analyzed in the Δ*fgcpp*$_1$ mutant during wheat spikes infection at 3 dpi and during in vitro growth; its expression still remained at basal level as observed in the WT strain (Table 1.2). Protoplasts of the Δ*fgcpp*$_1$ mutant were therefore transformed with a construct containing the *GEN* resistance gene in order to replace also the *fgcpp2* gene. Five geneticin-resistant regenerated colonies were checked by PCR for the presence/absence of the 262 bp internal fragment of the *fgcpp2* gene (Fig. S1.4B). Two putative disruption ΔΔ*fgcpp*$_{1,2}$ mutant strains selected by PCR (strains 1.1 and 1.4) were further analyzed by high-stringency Southern blot using the *fgcpp2* and *GEN* specific probes. Hybridization results showed the disruption of the *fgcpp2* gene in both strains since only the WT showed the hybridization signal at the expected position of about 4 kb (Fig. S1.5C, lanes 1-3). By using the *GEN* probe, both mutant strains showed a single hybridization band at the expected position of about 6 kb (Fig. S1.5C, lanes 4-6).

Soybean infections with the ΔΔ*fgcpp*$_{1,2}$ mutant strains showed no reduction in virulence compared with the WT strain (Fig. 1.4). Infections of wheat spikes confirmed that the mutant maintained the capability to infect wheat spikes, with no significant reduction of virulence compared with WT (Fig. 1.5).

Fluorescence microscopy analysis with WT, Δ*fgcpp*$_1$ and ΔΔ*fgcpp*$_{1,2}$ mutants constitutively expressing dsRed, showed no differences in the cellular morphology of infection cushions, lobate appressoria and foot structures originating from runner hyphae on the surface of infected paleas (Fig. 1.6).

To exclude that the full virulence of the ΔΔ*fgcpp*$_{1,2}$ mutant was related to an increased expression of the *FGSG_03971* and *FGSG_04471* genes encoding proteins containing the typical cerato-platanin domain but with low similarity with fungal CPPs, we analyzed their expression level in wheat spikelets at 3 dpi and also after 3 and 5 days of in vitro growth. However, both genes showed a low relative expression similar in WT and ΔΔ*fgcpp*$_{1,2}$ mutant (Table 1.3).

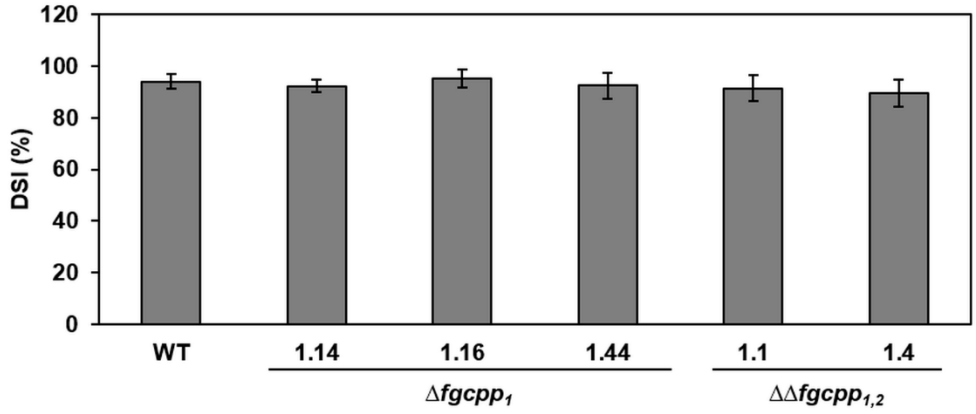

Fig. 1.4. Soybean (*Glycine max* cv. Demetra) infection experiments. Disease symptoms were assessed at 6 days post-inoculation (dpi) and expressed as the ratio of the lesion length and the total seedling length × 100 (Disease Severity Index, DSI). At least 4 independent infection experiments were performed by inoculating 20 soybean seeds with 20,000 conidia/seed of wild type (WT:8/1), Δ*fgcpp1* and ΔΔ*fgcpp1,2* mutant strains. The error bars represent the standard error and data were statistically analyzed by applying the Student's t-test.

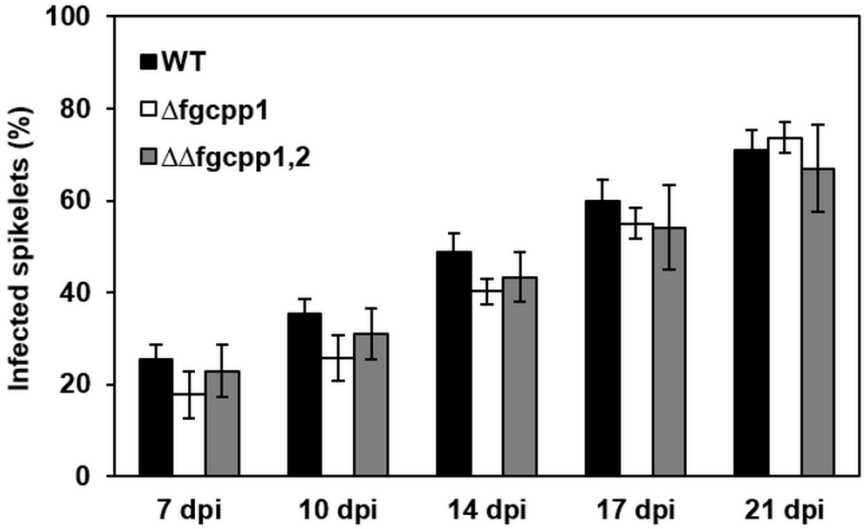

Fig. 1.5. Wheat (*Triticum aestivum* cv. Bobwhite) spikelets infection with *Fusarium graminearum* wild type (WT:8/1), Δ*fgcpp*$_1$ (strain 1.14) and ΔΔ*fgcpp*$_{1,2}$ (strain 1.4) mutants. Disease symptoms were assessed up to 21 dpi by counting the number of visually diseased spikelets. Infected spikelets are expressed as percentage of symptomatic spikelets on total number of spikelets of the respective head. Data represent the mean ± standard error (indicated by bars) of four independent infection experiments performed by inoculating at least 10 plants with 2,000 conidia in each independent experiment. Data were statistically analyzed by applying the Student's t-test.

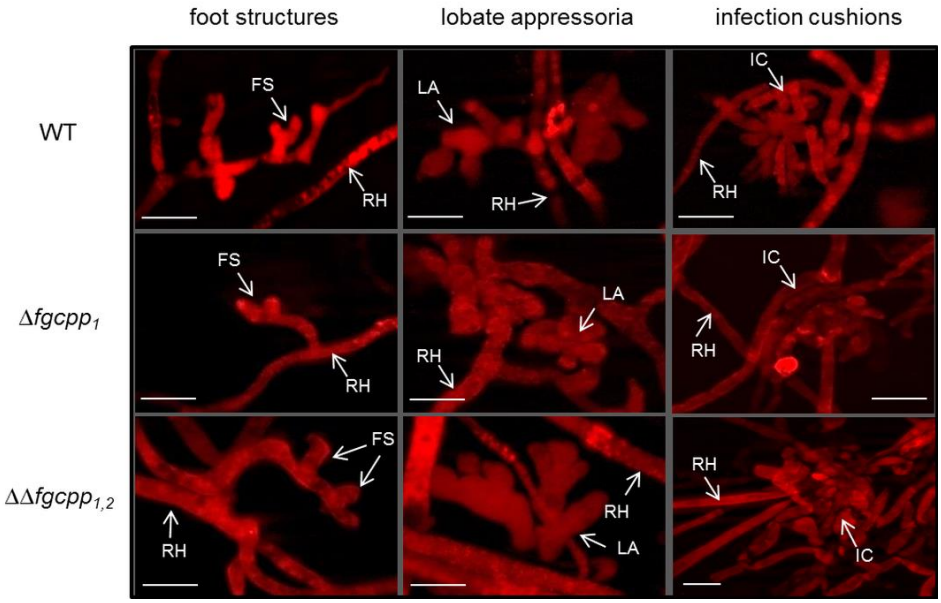

Fig. 1.6. Fluorescence microscopy of compound appressoria of *Fusarium graminearum* wild type (WT:8/1), Δ*fgcpp*$_1$ and ΔΔ*fgcpp*$_{1,2}$ mutants constitutively expressing dsRed. Maximum intensity projection (MIP) images of z-stacks of infected palea at 6 dpi. Cellular morphology of foot structures (FS), lobate appressoria (LA) and infection cushions (IC) originating from runner hyphae (RH) on the surface of paleas. All pictures were taken using the same magnification. All scale bars represent 10 μm.

Table 1.2. Relative expression level of the *fgcpp2* gene in the Δ*fgcpp*$_1$ mutant (strain 1.14) at 3 days after spikelets infection (dpi) and after 3 and 5 days of growth in Szécsi medium supplemented with glucose as the sole carbon source. qPCR was performed with Rotor-Gene Q 2plex (QIAGEN). Each transcript was normalized with the *Fusarium graminearum β-tubulin* gene as reference (set to 1) and the relative expression was analyzed using the Rotor-Gene v. 2.0.3.2 software. Data represent the mean of at least two independent experiments ± standard error.

Δ*fgcpp*$_1$	In planta	In vitro (glucose)	
	3 dpi	3 days	5 days
fgcpp2	0.011 ± 0.005	0.071 ± 0.013	0.135 ± 0.035

Table 1.3. Relative expression level of the *FGSG_03971* and *FGSG_04471* genes in WT and ΔΔ*fgcpp*$_{1,2}$ mutant (strain 1.4) at 3 days after spikelets infection (dpi) and after 3 and 5 days of growth in Szécsi medium supplemented with glucose as the sole carbon source. qPCR was performed with Rotor-Gene Q 2plex (QIAGEN). Each transcript was normalized with the *Fusarium graminearum β-tubulin* gene as reference (set to 1) and the relative expression was analyzed using the Rotor-Gene v. 2.0.3.2 software. Data represent the mean of at least two independent experiments ± standard error.

WT	In planta	In vitro (glucose)	
	3 dpi	3 days	5 days
FGSG_03971	0.047 ± 0.002	0.089 ± 0.001	0.196 ± 0.014
FGSG_04471	0.044 ± 0.000	0.299 ± 0.011	0.146 ± 0.001

ΔΔ*fgcpp*$_{1,2}$	In planta	In vitro (glucose)	
	3 dpi	3 days	5 days
FGSG_03971	0.040 ± 0.002	0.135 ± 0.012	0.150 ± 0.034
FGSG_04471	0.024 ± 0.001	0.241 ± 0.016	0.139 ± 0.007

1.3.5. In vitro characterization of the ΔΔfgcpp$_{1,2}$ *knock-out mutant*

The ΔΔ*fgcpp*$_{1,2}$ mutant strains were tested for phenotypic alterations. When conidia were point inoculated on PDA agar plates, the two double mutant strains formed radial colonies with abundant formation of aerial hyphae and a growth rate similar to WT (data not shown). To confirm that the deletion of both FgCPPs genes did not affect the hydrophobicity of the colony surface, 30 μL of water were placed on the surface of mycelia grown on YPGA solid medium. On colonies of both WT and double mutant strains the water formed a spherical droplet on the surface of the mycelium without extending or being absorbed (data not shown). To evaluate if the two FgCPPs are involved in stress resistance, fungal growth under two different stress conditions was tested. Growth of the double mutant on agar plates supplemented with NaCl or with increasing concentrations of H_2O_2 was similar to that of the WT strain (Fig. 1.7 and Fig. S1.6).

The *F. graminearum* WT and ΔΔ*fgcpp*$_{1,2}$ mutant were also grown for 4 days in liquid culture containing glucose or CMC as the sole carbon source and biomass was determined by measuring the

dry weight. While no difference was observed on glucose (Fig. 1.8A), growth of the double mutant on CMC was significantly higher (by ~50%) compared to the WT strain (Fig. 1.8B).

Since the FgCPPs could bind to the fungal cell wall, the growth of WT and double mutant strains was also tested in the presence of 0.15 and 0.3 U of β-1,3-glucanase or chitinase. While the glucanase doses used did not show any effect (data not shown), 0.3 U of chitinase were able to significantly affect the growth of all the fungal strains. Interestingly, the ΔΔ*fgcpp*$_{1,2}$ strains resulted markedly more inhibited compared to WT (Table 1.4).

To test if the FgCPPs have a protective function against cell wall degrading enzymes, four-day-old mycelia of WT and ΔΔ*fgcpp*$_{1,2}$ mutant were treated with β-1,3-glucanase and reducing sugars were measured. Compared to untreated mycelia, after 24 h the β-1,3-glucanase was able to release ~3.5 µg of glucose equivalents from mycelia of the double mutant strains (Fig. 1.9), whereas no released glucose equivalents were detectable from WT mycelium.

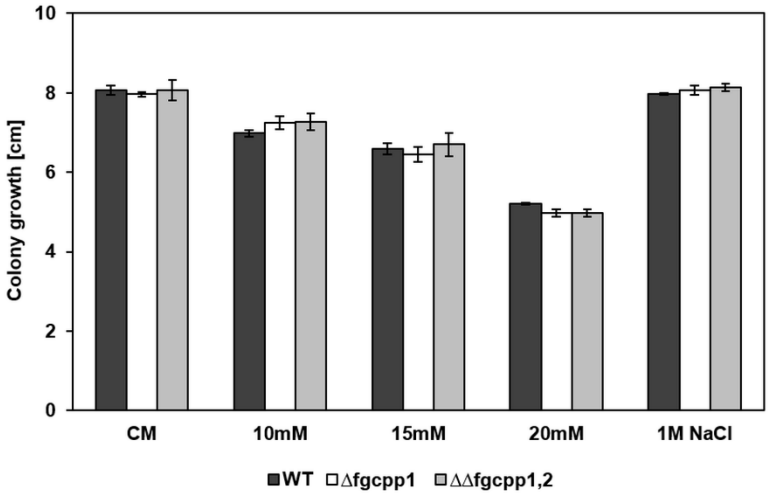

Fig. 1.7. Colony growth of *Fusarium graminearum* wild type (WT:8/1), Δ*fgcpp*$_1$ and ΔΔ*fgcpp*$_{1,2}$ mutants after 3 days of growth on complete medium (CM) and CM containing 10, 15 and 20 mM H_2O_2 or 1 M NaCl. Agar plates were inoculated with mycelial plugs from 3-day-old cultures. The diameter of the colonies was measured using a technical ruler. The analyses were performed with three replicates.

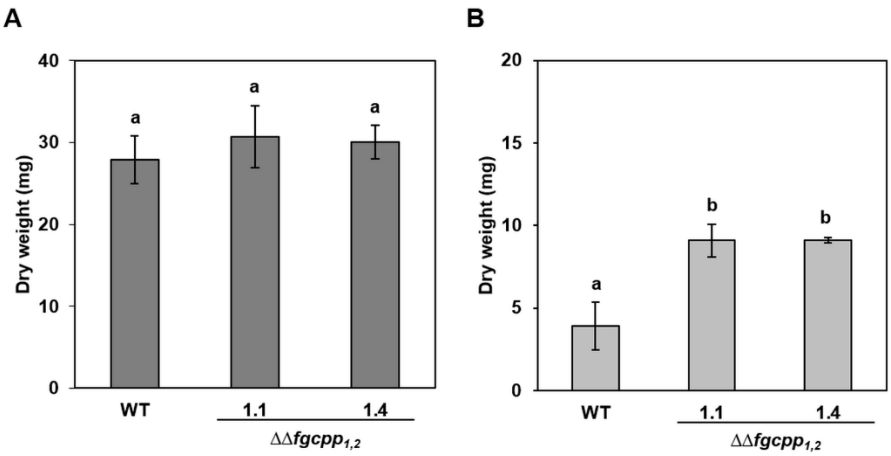

Fig. 1.8. Dry weight of *Fusarium graminearum* wild type (WT:8/1) and Δ*Δfgcpp*$_{1,2}$ mutant strains grown for 4 days in liquid culture containing (A) D-(+)-glucose or (B) carboxymethyl cellulose with high viscosity (CMC) as the sole carbon source. Data are the mean ± standard error (indicated by bars) of two independent experiments. Data were statistically analyzed by applying the Tukey–Kramer's test. Different letters indicate significant differences at $P<0.05$.

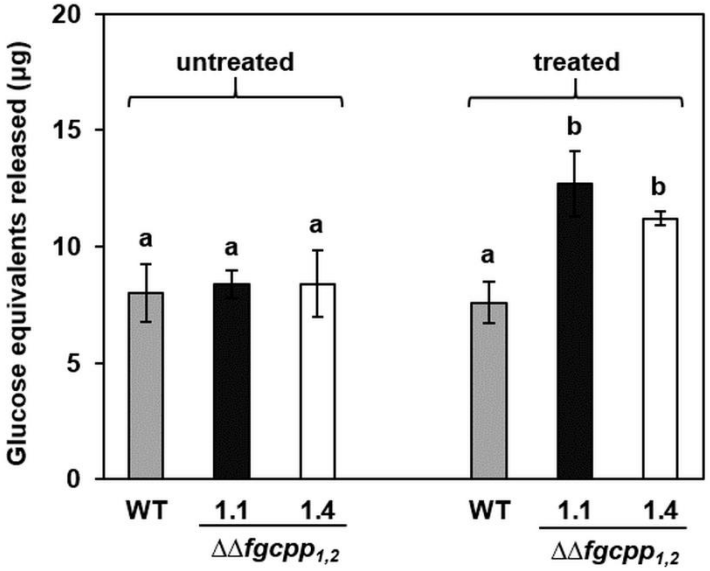

Fig. 1.9. Release of glucans from *Fusarium graminearum* mycelium after treatment with β-1,3-glucanase. Glucans are expressed as µg of reducing end-groups of glucose equivalents. Four-day-old mycelia of *F. graminearum* wild type (WT:8/1) and Δ*Δfgcpp*$_{1,2}$ mutant strains were incubated for 24 h at 30 °C with 2.5 µM β-1,3-glucanase from *Trichoderma longibrachiatum* in 20 mM sodium citrate pH 5.0 or with the same buffer solution as control. One hundred µL of untreated or treated samples were assayed as reported by Nelson et al. (1944) by using D-(+)-glucose as standard. Data represent the mean ± standard error of two independent experiments. Different letters indicate significant differences at $P<0.05$ by applying the Tukey–Kramer's test.

Table 1.4. Growth of *Fusarium graminearum* wild type (WT) and Δ*fgcpp*$_{1,2}$ mutant (strains 1.1 and 1.4) in the presence of 0.3 U of chitinase from *Streptomyces griseus*. Growth was determined by measuring spectrophotometrically the absorbance at 578 nm of the resazurin vital dye as described in Materials and Methods. Data are the mean ± standard error of three independent experiments. Different letters indicate significant differences at $P<0.05$ by applying the Tukey–Kramer's test.

	% Growth		
Strain	Control	Treated	% Inhibition
WT	$48.8^{a} \pm 3.2$	$36.8^{b} \pm 2.8$	24.6
1.1	$54.3^{a} \pm 1.4$	$31.5^{bc} \pm 4.0$	42.1
1.4	$47.5^{a} \pm 1.4$	$24.6^{c} \pm 3.6$	48.2

1.4. Discussion

CPPs belong to a family of small proteins, present only in fungi, that are associated with the fungal cell wall and also secreted extracellularly (Gaderer et al., 2014; Pazzagli et al., 2014). An in-silico analysis of the *F. graminearum* genome allowed us to identify five genes containing a putative cerato-platanin domain. However, only two of them, namely FgCPP1 and FgCPP2, seem to belong to the CPPs family since they are 120-140 aa long and contain the conserved two-peptide motives putatively responsible of the necrosis-inducing activity (Frías et al., 2014).

The putative FgCPP1 and FgCPP2 show a 60% aa identity but belong to two sister-clades of CPP sequences. On different carbon sources and during wheat spike infection the two *fgcpp* genes are differently regulated, with the *fgcpp1* much more expressed than *fgcpp2*. These results could be at least partially explained by the observation that a canonical TATA box consensus sequence is present only in the *fgcpp1* promoter region.

Because of their possible presence at the fungal cell wall and their secretion, their ability to loosen cellulose, also in accordance with their predicted structure highly similar to plant expansins, and their necrosis-inducing activity (Pazzagli et al., 2014), the FgCPPs could facilitate the necrotrophic stage as suggest for other fungi (Frías et al., 2014). In order to shed further light on the involvement of the FgCPPs in fungal virulence, we produced gene disruption mutants of the corresponding encoding genes. Since the *fgcpp1* gene was the most highly transcribed during wheat spike infection and also during in vitro growth, we initially produced a single disruption mutant of this gene. The mutant resulted not impaired in virulence on soybean and wheat spikes, and the expression level of the *fgcpp2* gene remained to the basal levels observed in the WT strain both in vitro and during wheat spikes infection. The low expression of the *fgcpp2* gene seems to suggest that its encoded product might play a marginal role. Nevertheless, we cannot fully exclude that the FgCPP2, although poorly expressed, may be sufficient to at least partially accomplish the CPPs biological functions, thus masking the absence of FgCPP1. Therefore, a double knock-out mutant deleted of both genes was produced, but resulted as virulent as the WT on both wheat spikes and soybean seedlings. *F.*

graminearum forms compound appressoria on wheat flower leaves (Boenisch and Schäfer, 2011). We evaluated these initial fungal infection stages on paleas and noticed that the cellular morphology of infection cushions and lobate appressoria on infected wheat paleas was unaltered in the CPP mutants. Dispensability of the CPPs to fungal virulence was also observed with the CPP of the canola pathogen *Leptosphaeria maculans* (Wilson et al., 2002); in contrast, the CPPs of the grey mold fungus *B. cinerea* (Frías et al., 2011) and the rice pathogen *M. oryzae* (Jeong et al., 2007) were necessary for full virulence during the necrotrophic phase. However, during the infection process *F. graminearum* secretes other factors able to induce necrosis in the host tissue, such as the mycotoxin DON (Bai et al., 2002; Desmond et al., 2008) and several endo-1,4-β-xylanases (Sella et al., 2013; Tundo et al., 2015). Therefore, it is possible that the observed dispensability of the FgCPPs is due to this functional redundancy. At this regard, the relative expression during wheat spikes infection of the two additional *F. graminearum* genes encoding proteins containing the typical cerato-platanin domain but with low similarity with other fungal CPPs seems to exclude a functional compensation effect by these proteins.

Worth of mention is also the unaffected hydrophobicity of the double mutant's colony surface and the abundant formation of aerial hyphae, which depends in many fungal species by the hydrophobic property of the cell surface (Wösten et al., 1999); these observations are in accordance with recent evidences showing that the FgCPPs cannot be considered hydrophobin-like proteins (Gaderer et al., 2014; Pazzagli et al., 2014). Besides, mutant's growth on osmotic media or under oxidative stress conditions was unaltered, which demonstrates that these proteins are not crucially involved in the fungal osmotic cell stress response (Nguyen et al., 2012).

Looking for other functions of these proteins and because of their known ability to loosen cellulose, we verified whether the FgCPPs deletion affects the capacity of *F. graminearum* to grow on CMC. Surprisingly, the mutant's growth was enhanced on this substrate. Whether this result is a side effect of CPPs, which seem to decrease the capacity of the fungus to depolymerize CMC, or depends on the

mutant's alteration in the expression of genes involved in the growth on this substrate, remains to be elucidated.

Since the CPPs are also considered to bind to the fungal cell wall (de Oliveira et al., 2011; Gaderer et al., 2014; Pazzagli et al., 2014), we checked whether the absence of these proteins makes the cell wall of conidia and mycelium of the *F. graminearum* CPPs mutant more susceptible to enzyme degradation. Indeed, in comparison to WT, the growth of the ΔΔ*fgcpp*$_{1,2}$ mutant was delayed in presence of chitinase and, besides, the treatment with β-1,3-glucanase released reducing sugars only from the mycelium of the mutant strains. These results seem to indicate that the FgCPPs protect the fungal cell wall polysaccharides from enzymatic degradation by chitinases and β-1,3-glucanases, which are pathogenesis-related proteins contained in plant tissue before and after infection (van Loon et al., 2006). However, since the virulence of the *F. graminearum* CPPs mutants is not detectably impaired, evidently the level of β-1,3-glucanase and chitinase activities in the host tissues or their effect on the fungal cell wall do not appreciably compromise the infection process.

In conclusion, our results seem to indicate that the FgCPPs play a protective role of fungal cell wall polysaccharides, while they exhibit no detectable influence on fungal virulence. However, a possible role during plant infection cannot be conclusively ruled out because the effect of DON or other effector molecules might compensate for the deletion of the FgCPPs.

Acknowledgments

The article "Involvement of the *Fusarium graminearum* cerato-platanin proteins in fungal growth and plant infection" by Alessandra Quarantin[1], Anika Glasenapp[2], Wilhelm Schäfer[2], Francesco Favaron[1] and Luca Sella[1] has been published in *Plant Physiology and Biochemistry*, 109 (2016): 220-229.

[1]Dipartimento del Territorio e Sistemi Agro-Forestali (TESAF), research group in Plant Pathology, Università degli Studi di Padova, Viale dell'Università 16, 35020, Legnaro, Italy; [2]Biocenter Klein Flottbek, Molecular Phytopathology and Genetics, University of Hamburg, Hamburg (Germany).

References

Baccelli, I., Luti, S., Bernardi, R., Scala, A., Pazzagli, L., 2014. Cerato-platanin shows expansin-like activity on cellulosic materials. Appl. Microbiol. Biotechnol. 98, 175-184.

Baccelli, I., 2015. Cerato-platanin family proteins: one function for multiple biological roles? Front. Plant Sci. 5, 769.

Baccelli, I., Gonthier, P., Bernardi, R., 2015. Gene expression analyses reveal a relationship between conidiation and cerato-platanin in homokaryotic and heterokaryotic strains of the fungal plant pathogen *Heterobasidion irregulare*. Mycol. Prog. 14, 40.

Bai, G.H., Desjardins, A.E., Plattner, R.D., 2002. Deoxynivalenol-nonproducing *Fusarium graminearum* causes initial infection, but does not cause disease spread in wheat spikes. Mycopathol. 153, 91-98.

Boenisch, J.M., Schäfer, W., 2011. *Fusarium graminearum* forms mycotoxin producing infection structures on wheat. BMC Plant Biol. 11, 110.

Brown, N.A., Urban, M., van de Meene, A.M.L., Hammond-Kosack, K.E., 2010. The infection biology of *Fusarium graminearum*: Defining the pathways of spikelet to spikelet colonisation in wheat ears. Fungal Biol. 114, 555-571.

Brown, N.A., Antoniw, J., Hammond-Kosack, K.E., 2012. The predicted secretome of the plant pathogenic fungus *Fusarium graminearum*: A refined comparative analysis. PLoS One. **7**, e33731.

Chen, H., Kovalchuk, A., Keriö, S., Asiegbu, F.O., 2013. Distribution and bioinformatic analysis of the cerato-platanin protein family in Dikarya. Mycol. 105, 1479-1488.

Chen, H.X., Quintana, J., Kovalchuk, A., Ubhayasekera, W., Asiegbu, F.O., 2015. A cerato-platanin-like protein HaCPL2 from *Heterobasidion annosum* sensu stricto induces cell death in *Nicotiana tabacum* and *Pinus sylvestris*. Fungal Genet. Biol. 84, 41-51.

Cuomo, C.A., Güldener, U., Xu, J.R., Trail, F., Turgeon, B.G., Di Pietro, A., Walton, J.D., Ma, L.J., Baker, S.E., Rep, M., et al., 2007. The *Fusarium graminearum* genome reveals a link between localized polymorphism and pathogen specialization. Science. 317, 1400-1402.

de O Barsottini, M.R., de Oliveira, J.F., Adamoski, D., Teixeira, P.J., do Prado, P.F., Tiezzi, H.O., et al., 2013. Functional diversification of cerato-platanins in *Moniliophthora perniciosa* as seen by differential expression and protein function specialization. Mol. Plant-Microbe Interact. 26, 1281-1293.

de Oliveira, A.L., Gallo, M., Pazzagli, L., Benedetti, C.E., Cappugi, G., Scala, A., Pantera, B., Spisni, A., Pertinhez, T.A., Cicero, D.O., 2011. The structure of the elicitor Cerato-platanin (CP), the first member of the CP fungal protein family, reveals a double ψβ-barrel fold and carbohydrate binding. J. Biol. Chem. 286, 17560-17568.

Desmond, O.J., Manners, J.M., Stephens, A.E., Maclean, D.J., Schenk, P.M., Gardiner, D.M., Munn, A., Kazan, K., 2008. The *Fusarium* mycotoxin deoxynivalenol elicits hydrogen peroxide production, programmed cell death and defence responses in wheat. Mol. Plant Pathol. 9, 435-445.

Frías, M., González, C., Brito, N., 2011. BcSpl1, a cerato-platanin family protein, contributes to *Botrytis cinerea* virulence and elicits the hypersensitive response in the host. New Phytol. 192, 483-495.

Frías, M., Brito, N., González, M., González, C., 2014. The phytotoxic activity of the cerato-platanin BcSpl1 resides in a two-peptide motif on the protein surface. Mol. Plant Pathol. 15, 342-351.

Gaderer, R., Bonazza, K., Seidl-Seiboth, V., 2014. Cerato-platanins: a fungal protein family with intriguing properties and application potential. Appl. Microbiol. Biotechnol. 98, 4795-4803.

Goswami, R.S., Kistler, H.C., 2004. Heading for disaster: *Fusarium graminearum* on cereal crops. Mol. Plant Pathol. 5, 515-525.

Goswami, R.S., Kistler, H.C., 2005. Pathogenicity and In Planta Mycotoxin Accumulation Among Members of the *Fusarium graminearum* Species Complex on Wheat and Rice. Phytopathol. 95, 1397-1404.

Hane, J.K., Lowe, R.G.T., Solomon, P.S., Tan, K.C., Schoch, C.L., 2007. Dothideomycete-plant interactions illuminated by genome sequencing and EST analysis of the wheat pathogen *Stagonospora nodorum*. Plant Cell. 19, 3347-3368.

Henrion, B., Chevalier, G., Martin, F., 1994. Typing truffle species by PCR amplification of the ribosomal DNA spacers. Mycol. Res. 98, 37-43.

Jansen, C., von Wettstein, D., Schäfer, W., Kogel, K.H., Felk, A., Maier, F.J., 2005. Infection patterns in barley and wheat spikes inoculated with wild-type and trichodiene synthase gene disrupted *Fusarium graminearum*. Proc. Natl. Acad. Sci. U.S.A. 102, 16892-16897.

Jeong, J.S., Mitchell, T.K., Dean, R.A., 2007. The *Magnaporthe grisea* snodprot1 homolog, MSP1, is required for virulence. FEMS Microbiol. Lett. 273, 157-165.

Langevin, F., Eudes, F., Comeau, A., 2004. Effect of trichothecenes produced by *Fusarium graminearum* during Fusarium head blight development in six cereal species Eur. J. Plant Pathol. 110, 735-746.

Li, S., Myung, K., Guse, D., Donkin, B., Proctor, R.H., Grayburn, W.S., Calvo1, A.M., 2006. FvVE1 regulates filamentous growth, the ratio of microconidia to macroconidia and cell wall formation in *Fusarium verticillioides*. Mol. Microbiol. 62, 1418-1432.

Lu, S., Edwards, M.C., 2016. Genome-Wide Analysis of Small Secreted Cysteine-Rich Proteins Identifies Candidate Effector Proteins Potentially Involved in *Fusarium graminearum*-Wheat Interactions. Phytopathol. 106, 166-176.

Lysøe, E., Seong, K.Y., Kistler, H.C., 2011. The transcriptome of *Fusarium graminearum* during the infection of wheat. Mol. Plant-Microbe Interact. 24, 995-1000.

McMullen, M., Jones, R., Gallemberg, D., 1997. Scab of wheat and barley: a remerging disease of devastating impact. Plant Dis. 81, 1340-1348.

Nelson, N., 1944. A photometric adaptation of the Somoyi method for the determination of glucose. J. Biol. Chem. 153, 275-280.

Nguyen, V.T., Schäfer, W., Bormann, J., 2012. The stress-activated protein kinase FgOS-2 is a key regulator in the life cycle of the cereal pathogen *Fusarium graminearum.* Mol. Plant-Microbe Interact. 25, 1142-1156.

Paper, J.M., Scott-Craig, J.S., Adhikari, N.D., Cuomo, C.A., Walton, J.D., 2007. Comparative proteomics of extracellular proteins in vitro and in planta from the pathogenic fungus *Fusarium graminearum*. Proteomics. 7, 3171-3183.

Pazzagli, L., Cappugi, G., Manao, G., Camici, G., Santini, A., Scala, A., 1999. Purification, Characterization, and Amino Acid Sequence of Cerato-platanin, a New Phytotoxic Protein from *Ceratocystis fimbriata* f. sp. *platani*. J. Biol. Chem. 274, 24959-24964.

Pazzagli, L., Seidl-Seiboth, V., Barsottini, M., Vargas, W.A., Scala, A., Mukherjee, P.K., 2014. Cerato-platanins: elicitors and effectors. Plant Sci. 228, 79-87.

Pioli, R.N., Mozzoni, L., Morandi, E.N., 2004. First report of pathogenic association between *Fusarium graminearum* and soybean. Plant Dis. 88, 220.

Sampedro, J., Cosgrove, D.J., 2005. The expansin superfamily. Genome Biol. 6, 242.

Sbrana, F., Bongini, L., Cappugi, G., Fanelli, D., Guarino, A., Pazzagli, L., Scala, A., Vassalli, M., Zoppi, C., Tiribilli, B., 2007. Atomic force microscopy images suggest aggregation mechanism in cerato-platanin. Eur. Biophys. J. 36, 727-732.

Sella, L., Gazzetti, K., Faoro, F., Odorizzi, S., D'Ovidio, R., Schäfer, W., Favaron, F., 2013. A *Fusarium graminearum* xylanase expressed during wheat infection is a necrotizing factor but is not essential for virulence. Plant Physiol. Biochem. 64, 1-10.

Sella, L., Gazzetti, K., Castiglioni, C., Schäfer, W., Favaron, F., 2014. *Fusarium graminearum* Possesses Virulence Factors Common to Fusarium Head Blight of Wheat and Seedling Rot of Soybean but Differing in Their Impact on Disease Severity. Phytopathol. 104, 1201-1207.

Sella, L., Gazzetti, K., Castiglioni, C., Schäfer, W., D'Ovidio, R., Favaron, F., 2016. The *Fusarium graminearum* Xyr1 transcription factor regulates xylanase expression but is not essential for fungal virulence. Plant Pathol. 65, 713-722.

Tundo, S., Moscetti, I., Faoro, F., Lafond, M., Giardina, T., Favaron, F., Sella, L., D'Ovidio, R., 2015. *Fusarium graminearum* produces different xylanases causing host cell death that is prevented by the xylanase inhibitors XIP-I and TAXI-III in wheat. Plant Sci. 240, 161-169.

van Loon, L.C., Rep, M., Pieterse, C.M.J., 2006. Significance of inducible defense-related proteins in infected plants. Annu. Rev. Phytopathol. 44, 135-162.

Van Nguyen, T., Schäfer, W., Bormann, J., 2012. The stress-activated protein kinase FgOS-2 is a key regulator in the life cycle of the cereal pathogen *Fusarium graminearum*. Mol. Plant-Microbe Interact. 25, 1142-1156.

Voigt, C.A., Schäfer, W., Salomon, S., 2005. A secreted lipase of *Fusarium graminearum* is a virulence factor required for infection of cereals. Plant J. 42, 364-375.

Wanyoike, W.M., Zhensheng, K., Buchenauer, H., 2002. Importance of cell wall degrading enzymes produced by *Fusarium graminearum* during infection of wheat heads. Eur. J. Plant Pathol. 108, 803-810.

Wilson, L.M., Idnurm, A., Howlett, B.J., 2002. Characterization of a gene (sp1) encoding a secreted protein from *Leptosphaeria maculans*, the blackleg pathogen of *Brassica napus*. Mol. Plant Pathol. 3, 487-493.

Wösten, H.A., Richter, M., Willey, J.M., 1999. Structural proteins involved in emergence of microbial aerial hyphae. Fungal Genet. Biol. 27, 153-160.

Supplementary figure captions

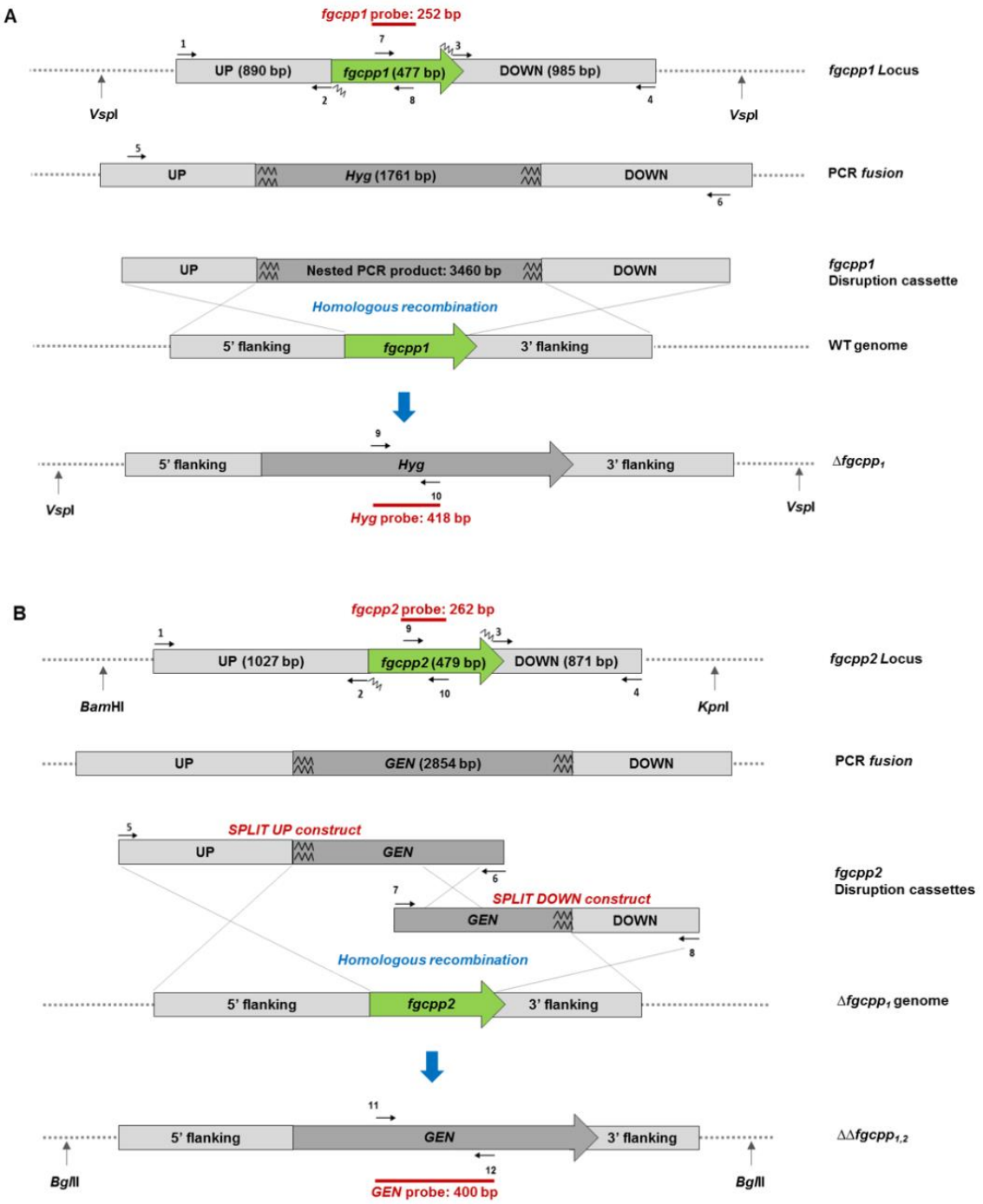

Fig. S1.1. Schematic illustration of the PCR-based construction of the gene replacement vectors. (A) Construction of the vector for *fgcpp1* disruption. Flanking homology regions of the *fgcpp1* gene were amplified by PCR using specific primers; primers 1 (UP10212for) and 2 (UP10212rev) were used for the amplification of the upstream region (UP), primers 3 (DOWN10212for) and 4 (DOWN10212rev) for the downstream region (DOWN). UP and DOWN amplicons were fused with the hygromycin (*Hyg*) resistance gene (1.7 Kb) by the Fusion PCR technique, using as primers the tails (^^^) of primers 2 and 3, complementary to the 5′ and 3′ *Hyg* regions, respectively. The fusion PCR product was used as template in a subsequent Nested PCR reaction, where primers 5 (NEST10212for) and 6 (NEST10212rev) were used to obtain the full construct of 3460 bp.

The *fgcpp1* gene was replaced by homologous recombination via two crossing-over events. Primer pairs 7–8 (INT10212for/rev) and 9–10 (HygPRB2for/rev) were used for PCR screening of mutant colonies and to obtain the *fgcpp1* and *Hyg* probes for Southern blot analysis, respectively. Sites recognized by *Vsp*I (Fermentas), used for DNA digestion, are also indicated. (B) Construction of the vector for obtaining the double knock-out mutant. Flanking homology regions of the *fgcpp2* gene were amplified by PCR using specific primers; primers 1 (UP11205for) and 2 (UPGEN11205rev) were used for the amplification of the upstream region (UP), primers 3 (DOWNGEN11205for) and 4 (DOWN11205rev) for the downstream region (DOWN). UP and DOWN amplicons were fused with the geneticin (*GEN*) resistance gene (2.8 Kb) by the Fusion PCR technique, using as primers the tails (^^^) of primers 2 and 3, complementary to the 5′ and 3′ *GEN* regions, respectively. The fusion PCR product was used as template in subsequent PCR reactions to obtain the SPLIT UP (~3 Kb) and the SPLIT DOWN (~2.8 Kb) constructs. Primers 5 (NESTGEN11205for) and 6 (SPLITUPGENrev) were used for the SPLIT UP construct amplification and primers 7 (SPLITDOWNGENfor) and 8 (NESTGEN11205rev) were used for the SPLIT DOWN construct amplification. The *fgcpp2* gene was replaced by homologous recombination via three crossing-over events. Primer pairs 9–10 (INT11205for/rev) and 11–12 (GenPRBf/r) were used for PCR screening of mutant colonies and to obtain the *fgcpp2* and *GEN* probes for Southern blot analysis, respectively. Sites recognized by *Bam*HI, *Kpn*I (Promega) and *Bgl*II (Promega), used for DNA digestion, are also indicated.

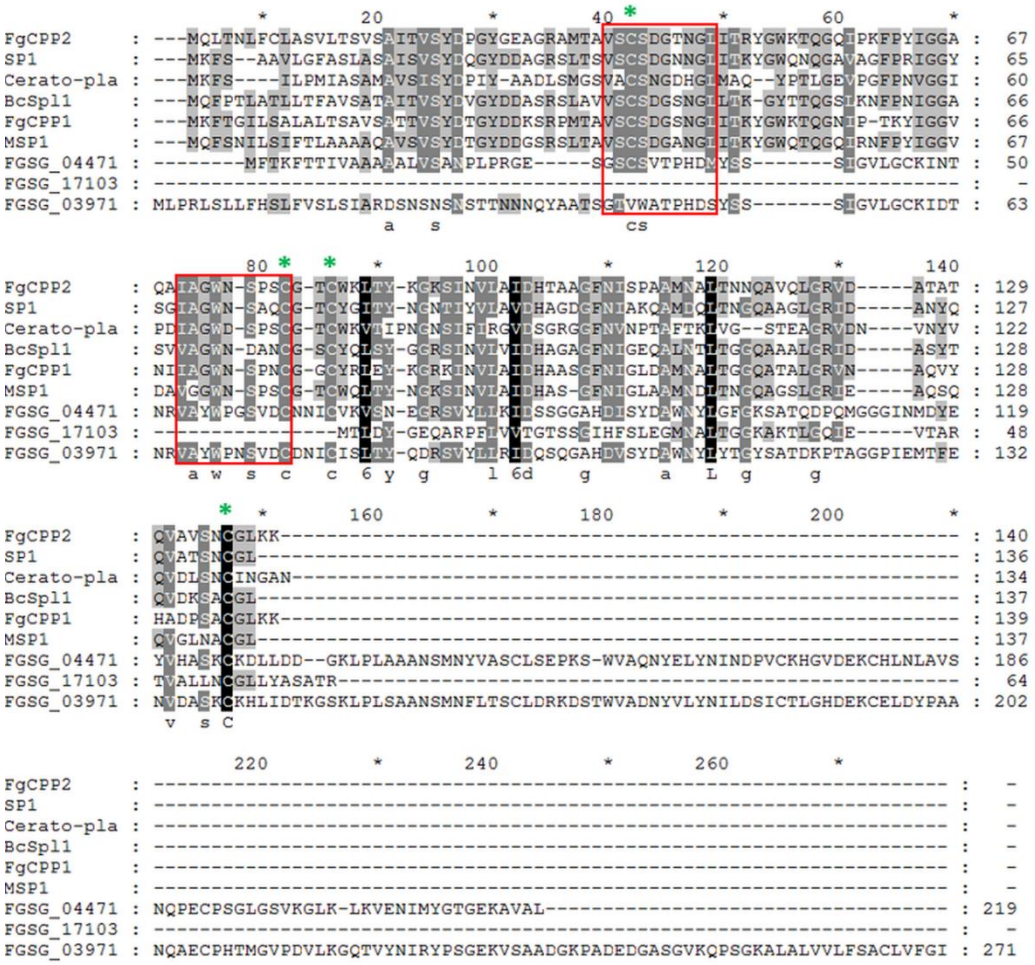

Fig. S1.2. Alignment of amino acid sequences of CPPs from different Ascomycetes fungal species including FgCPP1, FgCPP2 and the other three putative *Fusarium graminearum* CPPs. Sequence alignment was performed using Clustal X 2.1 software and the analysis of conserved regions was performed using GeneDoc

v.2.3.0 program. The four cysteine residues which are conserved in the Cerato-platanin box are marked by green asterisks and the two-peptide motives of 10 residues named PepA and PepB are framed in red. The fungal proteins used are: *F. graminearum* FGSG_10212 (FgCPP1, XP_011319159.1); *F. graminearum* FGSG_11205 (FgCPP2, XP_011325136.1); *F. graminearum* FGSG_03971 (XP_011321691.1); *F. graminearum* FGSG_04471 (XP_011321126.1); *F. graminearum* FGSG_17103 (CEF76364.1); *Stagonospora nodorum* SnodProt1 (SP1, AAC26870.1); *Ceratosystis platani* Cerato-platanin (Cerato-pla, CAC84090.2); *Magnaporthe oryzae* SnodProt1 (MSP1, XP_003710181.1); *Botrytis cinerea* SnodProt-like1 (BcSpl1, XP_001559499.1). The corresponding accession numbers were obtained from the NCBI database (http://www.ncbi.nlm.nih.gov/).

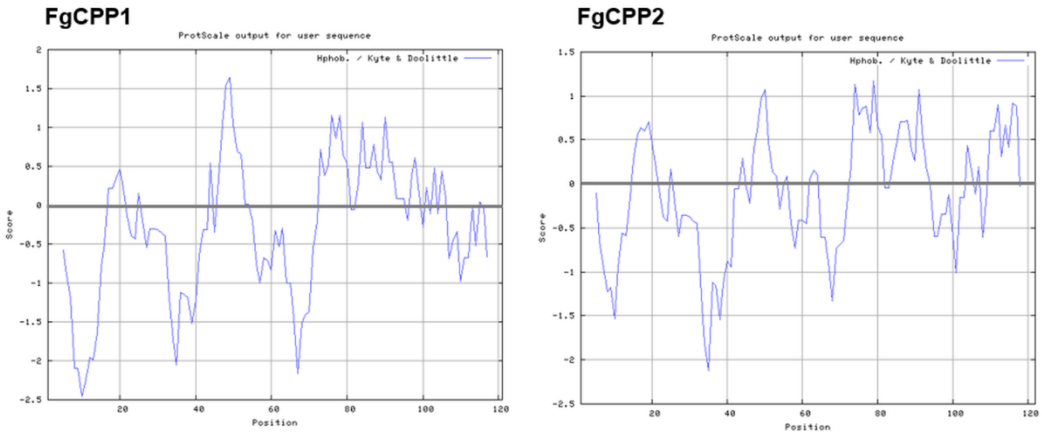

Fig. S1.3. Hydropathy plots of the amino acid (aa) sequences of FgCPP1 and FgCPP2. The x-axis shows the aa sequence position relative to the mature proteins and the y-axis refers to the hydropathy score calculated with ProtScale software (http://expasy.org/tools/) by using the Kyle and Doolittle aa scale. Hydrophobic aa show positive peaks with values above 0 whereas hydrophilic aa show negative peaks.

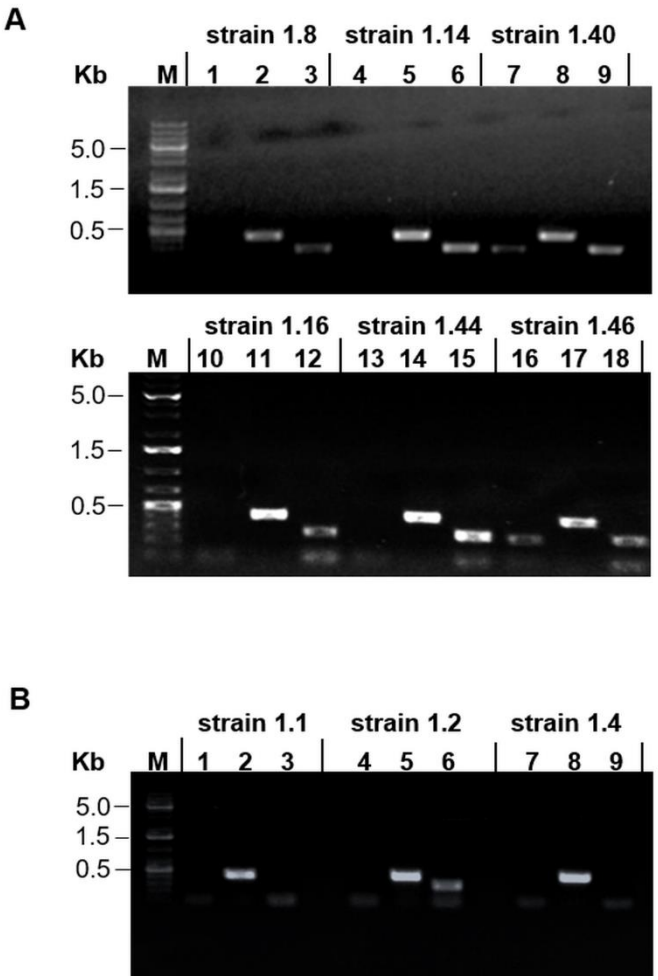

Fig. S1.4. (A) PCR selection of some *fgcpp1* gene disruption mutant strains. For each mutant, *fgcpp1* (252 bp), *Hyg* (418 bp) and *fgcpp2* (262 bp) genes were respectively amplified. M: molecular size markers (GeneRuler™1kb plus DNA ladder, Fermentas); lanes 1-3: strain 1.8; lanes 4-6: strain 1.14; lanes 7-9: strain 1.40; lanes 10-12: strain 1.16; lanes 13-15: strain 1.44; lanes 16-18: strain 1.46. The absence of the *fgcpp1* gene was confirmed in the 1.8, 1.14, 1.16 and 1.44 strains. (B) PCR selection of some mutant strains with double knock-out of the FgCPP encoding genes. For each mutant, *fgcpp1* (252 bp), *GEN* (400 bp) and *fgcpp2* (262 bp) genes were respectively amplified. M: molecular size marker (GeneRuler™1kb plus DNA ladder); lanes 1-3: strain 1.1; lanes 4-6: strain 1.2; lanes 7-9: strain 1.4. The absence of the *fgcpp2* gene was confirmed in the 1.1 and 1.4 strains.

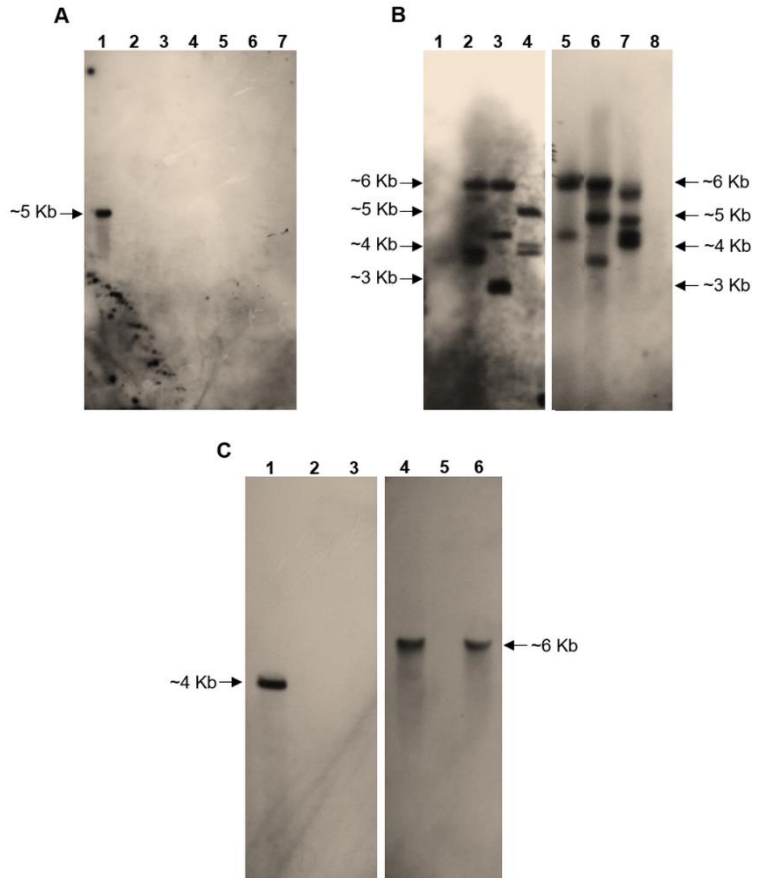

Fig. S1.5. High-stringency Southern Blot analysis of genomic DNA from *Fusarium graminearum* wild type (WT:8/1), Δ*fgcpp*$_1$ and ΔΔ*fgcpp*$_{1,2}$ mutant strains. (A) DNAs from WT and Δ*fgcpp*$_1$ mutant strains were digested with *Vsp*I (Promega) and hybridized with a fragment of the *fgcpp1* gene as probe. The WT strain (lane 1) showed an hybridization signal of ~5 kb, while the Δ*fgcpp*$_1$ mutant strains (lane 2: strain 1.8; lane 3: strain 1.16; lane 4: strain 1.19; lane 5: strain 1.14; lane 6: strain 1.44; lane 7: strain 1.47) did not show any hybridization signal. (B) DNAs from WT and Δ*fgcpp*$_1$ mutant strains were digested with *Vsp*I and hybridized with a fragment of the *Hyg* resistance gene as probe. The presence of the hybridization band of about 6 kb, corresponding to the targeted integration of the *Hyg* gene in the *fgcpp1* locus, was observed in three mutant strains (lane 3: strain 1.16; lane 5: strain 1.14; lane 6: strain 1.44). Other bands corresponding to ectopic integrations of the deletion construct were also present in these as well as in the other mutant strains (lane 2: strain 1.8; lane 4: strain 1.19; lane 7: strain 1.47). The WT strain (lanes 1 and 8) gave no hybridization signal. (C) Lanes 1-3: DNAs from WT and ΔΔ*fgcpp*$_{1,2}$ mutant strains were digested with *Bam*HI and *Kpn*I (Promega) and hybridized with a fragment of the *fgcpp2* gene as probe. The WT strain (lane 1) showed a hybridization signal of ~4 kb, while the mutant strains (lane 2: strain 1.1; lane 3: strain 1.4) did not show any hybridization signal. Lanes 4-6: DNAs from WT and ΔΔ*fgcpp*$_{1,2}$ mutant strains were digested with *Bgl*II (Promega) and hybridized with a fragment of the *GEN* resistance gene as probe. The presence of the hybridization band of ~6 kb, corresponding to the targeted integration of the *GEN* gene in the *fgcpp2* locus, was observed in both ΔΔ*fgcpp*$_{1,2}$ mutant strains analysed (lane 4: strain 1.1; lane 6: strain 1.4). The WT strain (lane 5) gave no hybridization signal.

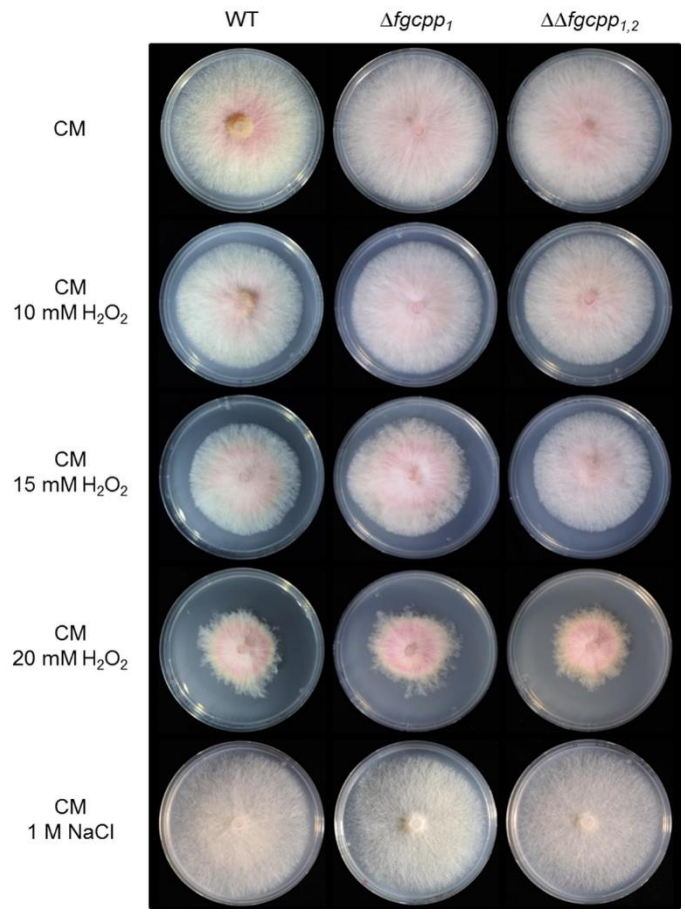

Fig. S1.6. Colony morphology of *Fusarium graminearum* wild type (WT:8/1) and the Δ*fgcpp*$_1$, ΔΔ*fgcpp*$_{1,2}$ mutants after 3 days of growth on complete medium (CM) and CM containing 10, 15, and 20 mM H_2O_2 or 1 M NaCl. Agar plates were inoculated with mycelial plugs from 3-day-old cultures. The analyses were performed with three replicates.

Table S1.1. Oligonucleotide primers used in this study.

Primer name	Sequence (5'-3')
Primers for *fgcpp1* and *fgcpp2* qPCR gene expression analysis in planta and in vitro	
β–tub FGSG_06611 for	CCCAACAACGTCCAAACTTCC
β–tub FGSG_06611 rev	CCTCGGTGAATTCCATCTCGTC
INT10212for	TTCACTGGTATCCTCTCTGC
INT10212rev	GTTGACACCACCGATGTACT
INT11205for	ACCAACCCCTCTCTCAATAC
INT11205rev	GATGCTCTTGCCCTTGTAG
Primers to produce the *fgcpp1* gene disruption construct (Δ*fgcpp*$_1$) (tail sequences underscored)	
UP10212for	ATGCCACAGCATTGAAAACA
UP10212rev	AGATGCCGACCGAACAAGAGCTGTCCCCC ACGGTTGTGGGTTTTTGTGT
DOWN10212for	TCAATGCTACATCACCCACCTCGCTCCCCC ACGGCTGCAACTCTACGACT
DOWN10212rev	TTGTTGAAGTGCTCCAGTGC
NEST10212for	GCGGTGGAACTTCGATTTTA
NEST10212rev	TCATCGTGCATCAGCTAACA
Primers to produce the double knock-out mutant (ΔΔ*fgcpp*$_{1,2}$) (tail sequences underscored)	
UP11205for	GAAGAGATGGTTGATGGGACA
UPGEN11205rev	AACAACTGGCATGAATTCATCGATGATATCAGATC GAAGGTTGTTTGGTTGTGTTGA
DOWNGEN11205for	GATCCTCTAGAGTCGACCTGCAGGCATGCA GATGGGACGGGATACGTTTA
DONW11205rev	TTTTCCGAGGTACCTTGCTG
NESTGEN11205for	GCTGCATGGGTACAAGGTTT
SPLITUPGENrev	AATATCACGGGTAGCCAACG
SPLITDOWNGENfor	GAAAGCGCGTTGGATTAGAG
NESTGEN11205rev	ATGCGTTCGAAAATGTCTCC
Primers for preliminary screening of Δ*fgcpp*$_1$ and ΔΔ*fgcpp*$_{1,2}$ mutants and for DIG-labeled probes	
INT10212for	TTCACTGGTATCCTCTCTGC
INT10212rev	GTTGACACCACCGATGTACT
INT11205for	ACCAACCCCTCTCTCAATAC
INT11205rev	GATGCTCTTGCCCTTGTAG
HygPRB2for	AGAGTGATGCTTTGAGAGAG
HygPRB2rev	TAGTGTACCACTTGACCAAA
GenPRBf	AGGATCTCCTGTCATCTCA
GenPRBr	CCAAGCTCTTCAGCAATA
Primers for *FGSG_03971* and *FGSG_04471* qPCR expression analysis in planta and in vitro	
BetaTubFGfor	ACTTCCGTCTGTTCCGTG
BetaTubFGrev	TTCCATCTCGTCCATACCCT
Fg03971for	GACAGCAATAGCAATAGCAACAG
Fg03971rev	GAGGTAATTCCAGGCATCGT
Fg04471for	CCTCACGACATGTACTCCAG
Fg04471rev	GTAGTTCCAGGCATCGTAAGAG

Chapter II

The *Fusarium graminearum* cerato-platanin proteins interact with carboxymethyl cellulose reducing its viscosity and favor cellulase activity

Abstract

Cerato-platanin proteins (CPPs) belong to a family of small secreted fungal proteins with phytotoxic activity. The genome of *Fusarium graminearum*, the causal agent of *Fusarium* head blight disease (FHB) of wheat, barley and other cereal grains, contains two genes putatively encoding for CPPs. To better characterize their role, the two putative FgCPPs have been heterologously expressed in the *Pichia pastoris* yeast. In a viscosimetric assay, the recombinant FgCPPs showed the ability to reduce the viscosity of carboxymethyl cellulose (CMC), with higher affinity for substrates with medium/high viscosity, and this activity was shown as mainly non-enzymatic. The same effect was not observed on other polysaccharide substrates such as chitin, xylan and pectin. Indeed, a carbohydrate binding assay showed that the FgCPPs are trapped by cellulose and not by chitin, thus suggesting that the recombinant proteins could interact to cellulose. Besides, the incubation of a β-1,4-glucanase in presence or absence of the two FgCPPs showed that the enzyme was able to release more reducing sugars from the CMC substrate in presence of the recombinant fungal proteins, thus indicating that the FgCPPs could favour fungal cellulase activity. A double knock-out mutant deleted of both FgCPPs encoding genes (ΔΔ*fgcpp*$_{1,2}$) grown on CMC produced more cellulase activity than the corresponding wild-type strain, mainly on medium and high viscosity CMC. This result suggests that the higher enzymatic activity produced by the mutant could compensate for the absence of the FgCPPs. Finally, the demonstration that FgCPPs act also loosening filter paper cellulose could suggest a possible future biotechnological application in biofuel production from plant substrates rich in cellulose.

2.1. Introduction

Cerato-platanin proteins (CPPs) are small non-catalytic, cysteine-rich and moderately hydrophobic proteins produced by filamentous fungi (Chen et al., 2013). These proteins contain a signal peptide and are thus secreted by fungi, but they can also bind N-acetylglucosamine oligomers and chitin (de Oliveira et al., 2011), being possibly localized at the fungal cell walls (Gaderer et al., 2014; Pazzagli et al., 2014). Genes encoding for CPPs have been found in several fungal genomes, with Ascomycete genomes usually containing one or two encoding genes (Chen et al., 2013; Gaderer et al., 2014).

In particular, the genome of *Fusarium graminearum* Schwabe [teleomorph *Gibberella zeae* (Schwein) Petch], a hemibiotrophic fungal plant pathogen responsible of the *Fusarium* head blight (FHB) disease of monocot cereal species such as wheat that causes yield reduction and contamination of seeds with mycotoxins belonging to the trichothecenes group (Goswami and Kistler, 2004; O'Donnell et al., 2004; Brown et al., 2010), contains two genes encoding for proteins with the cerato-platanin domain (Pfam07249). A role played by these two proteins, named FgCPP1 and FgCPP2, has been recently demonstrated by producing and characterizing single and double *F. graminearum* knock-out mutants; the two FgCPPs, probably located at the fungal cell wall, protect fungal cell wall polysaccharides from enzymatic degradation by β-1,3-glucanase and chitinase, while they do no contribute to fungal virulence (Quarantin et al., 2016). However, these proteins are also predicted to be secreted and phytotoxic (Lu and Edwards, 2016) and could therefore play other roles during fungal growth and plant infection.

Fungal CPPs seem to be structurally related to plant expansins, small proteins of about 26 kDa secreted by plant cells during growth that loosen and disrupt the non-covalent bonding networks of cell wall polysaccharides and are involved in “acidic-induced growth” and other various processes (Cosgrove, 2000; Sampedro and Cosgrove, 2005; Baccelli et al., 2014b; Gaderer et al., 2014). Structurally, expansins consist of two domains: i) the N-terminal domain (D1) featuring the double ψ-β-barrel fold, distantly related to the catalytic domain of the glycoside hydrolase family 45 (GH45) proteins, most of which are fungal β-1,4-D-endoglucanases; ii) the C-terminal domain (D2), which

forms an Ig-like β-sandwich fold and is homologous to a family of grass-pollen allergens (Sampedro and Cosgrove, 2005; Marowa et al., 2016). Proteins similar to expansins able to loosen cellulose fibrils have been also reported in fungi and bacteria (Georgelis et al., 2011; Cosgrove, 2015). In particular, a single domain containing the double-ψ/β-barrel fold quite similar to that found in expansins has been identified in the solved 3D structures of *Ceratocystis platani* CP, *Moniliophthora perniciosa* MpCP and *Trichoderma virens* Sm1 (de Oliveira et al., 2011; de O Barsottini et al., 2013). Furthermore, the EXLX1 protein secreted by *Bacillus subtilis*, a Gram-positive soil bacterium capable of colonizing the surface of plant roots, has been shown to have structure similarity to plant expansins (Kerff et al., 2008), binding ability to plant and bacterial cell walls, extension activity on plant cell wall and no-hydrolytic activity against major cell wall polysaccharides (Kerff et al., 2008; Georgelis et al., 2015). However, these proteins have been classified as "expansins-like" because of a distantly related phylogenetic origin and lack of the C-terminal binding domain (D2) (Baccelli et al., 2014b; Olarte-Lozano et al., 2014; Baccelli, 2015).

Interestingly, a correlation between the ability to weaken cellulose and the capacity to induce defence responses in plants have been identified in expansins and expansin-like proteins, whose sequences contain a conserved carboxyl group of the Asp-77 residue (D77) crucial for loosening and PAMP activities (Kim et al., 2013; Liu et al., 2015; Luti et al., 2017). Besides, the specific residues D77 and Asn-84 (N84), identified in the *C. platani* CP mature sequence, have been shown to be involved in the lack of glycoside hydrolase activity and in the oligosaccharide-binding capability of fungal CPPs, respectively. Indeed, it is known that the *C. platani* CP binds to *N*-acetylglucosamine oligomers of chitin (de Oliveira et al., 2011) because of the presence of residues involved in oligosaccharide binding, which seem to be conserved among the members of the CPPs family (de Oliveira et al., 2011).

The ability of the *C. platani* CP and other fungal CPPs to loosen cellulose in an expansin-like manner without lytic activity (Baccelli et al., 2014b) and its association to cell wall chitin (de Oliveira et al.,

2011), suggest that CPPs could loosen fungal or plant cell walls, thus favoring fungal hyphae growth or its advancement in the plant tissue during infection (Baccelli, 2015).

The observation that treatments of plant tissues with the CPPs of some pathogenic and beneficial biocontrol fungi seem to elicit defense responses and/or necrosis in host and non-host plants (Gaderer et al., 2014; Pazzagli et al., 2014) indicate that fungal CPPs could act also as microbe/pathogen-associated molecular patterns (MAMPs/PAMPs) or assist tissue colonization of necrotrophic pathogens with their necrosis-inducing activity (Gaderer et al., 2014; Pazzagli et al., 2014; Gaderer et al., 2015; Luti et al., 2016).

In particular, Sm1 from *T. virens*, Epl1 from *T. atroviride*, EPL1 from *Colletotrichum falcatum* and VdCP1 from *Verticillium dahliae* elicit defence responses in several host tissues (rice, cotton, sugarcane and maize), production of reactive oxygen species (ROS), up-regulation of defense-related genes and localized or systemic acquired resistance (SAR), which are effective against fungal and bacterial pathogens (Djonović et al., 2006, 2007; Gaderer et al., 2015; Salas-Marina M.A. et al., 2015; Ashwin et al., 2017; Zhang et al., 2017a). Moreover, the BcSpl1 of *Botrytis cinerea* induces symptoms of hypersensitive response (HR) in multiple hosts such as tobacco, tomato and *Arabidopsis thaliana* (Frías et al., 2011) and systemic resistance in tobacco (Frías et al., 2013). MoSM1 of *Magnaporthe oryzae* is also able to induce HR in leaves and enhances disease resistance against *B. cinerea* and *Pseudomonas syringae* when transiently expressed in *A. thaliana* (Yang et al., 2009). Furthermore, the overexpression in rice plants of MoSM1 confers broad-spectrum resistance against blast disease caused by *M. oryzae* and bacterial blight disease caused by *Xanthomonas oryzae* pv. *oryzae*, probably through modulating the salicylic acid (SA) and jasmonic acid (JA) signalling pathways; however, MoSM1 overexpression does not affect drought and salt stress tolerance and some of the important agronomic traits such as grain yield (Wang et al., 2016; Hong et al., 2017). The CP of *C. platani*, the first member of the CPPs family, plays also a role as PAMP in host-fungus interaction. CP is able to induce mitogen-activated protein kinase (MAPK) cascades, up-regulation of SA and ethylene (Et)-signalling genes, accumulation of nitric oxide (NO) and reactive oxygen

species (ROS), HR, accumulation of phenolic compounds such as phytoalexins, and has been shown to induce resistance, through stomatal perception, against *B. cinerea* and *Pseudomonas syringae* pv. *tomato* (Pazzagli et al., 1999; Baccelli et al., 2014a).

Protein regions recognized as PAMPs by the plant immune system are usually very well conserved in the corresponding protein families, such as in the case of bacterial flagellin (Felix et al., 1999). Accordingly, the alignment of 146 putative CPP sequences showed the presence of two regions with high degree of conservation corresponding to two loops interacting with each other, forming a small protrusion in the protein surface (de Oliveira et al., 2011). In the BcSpl1 protein, these two regions of 10 residues are included in a 40-amino acid (aa) conserved region and the necrosis-inducing activity seems to reside on these two-peptide motives (Frías et al., 2014). These observations indicate that members of the CPPs family represent a novel class of proteins with potential PAMP activity as plant defense elicitors (Gaderer et al., 2014; Pazzagli et al., 2014; Baccelli, 2015).

Despite all this information, the mechanism by which CPPs interact with the plant cell wall acting by PAMP is not available yet. In fact, no pattern recognition receptor has been identified to date and only some pieces of evidence have been reported to support the interaction between CP and the plant cuticle (Martellini et al., 2012).

In order to investigate if the *F. graminearum* CPPs (named FgCPP1 and FgCPP2) are able to loosen plant or fungal cell wall polysaccharides and to induce necrotic symptoms of defense responses in planta, we heterologously expressed these two proteins in the *Pichia pastoris* yeast. The recombinant proteins have been therefore characterized by enzymatic assays on different cell wall polysaccharides such as cellulose, xylan, pectin and chitin and by in vivo treatments on the model plant *A. thaliana*.

2.2. Materials and methods

2.2.1. Sequences analysis and primers design

All the primers used were designed by using PRIMER3 (http://primer3.ut.ee/) and PerlPrimer v.1.1.17 softwares (Table S1). Post-translational modifications of heterologously expressed proteins were predicted using proteomic tools (NetNGlyc 1.0 and NetOGlyc 4.0; http://expasy.org/tools/) and signal peptides (SP) were identified with the SignalP program (http://www.cbs.dtu.dk/services/SignalP/).

2.2.2. Cloning and expression of the FgCPPs in P. pastoris

The cDNAs of the entire coding sequences of the *fgcpp1* and *fgcpp2* genes were obtained from total RNA extracted from infected wheat spikelets collected at 5 dpi. RNA extraction, DNase treatment and reverse transcription were performed as reported in Quarantin et al. (2016). The genes were amplified from the obtained cDNAs with the ORF primers pair (Table S2.1) by using the "REDTaq ReadyMix PCR Reation Mix" (Sigma-Aldrich). The PCR was performed by repeating for 35 times the following cycle: 30 s at 94 °C; 30 s at 50 or 52 °C; 1 min at 72 °C. The amplification products of the expected size (*fgcpp1* ORF: 420 bp; *fgcpp2* ORF: 423 bp) were purified using the "Wizard SV Gel and PCR Clean-Up System kit" (Promega) and then cloned into the pGEM-T Easy vector (Promega) following manufacturer's instructions. The cloned cDNAs were sequenced in order to check the correctness of the nucleotide sequence and then amplified with Pfu DNA polymerase (Promega) by using specific primers (*pPICZαA*for/rev, Table S2.1) containing adaptors for *Eco*RI and *Xba*I recognition sequences for amplification of the coding sequence without signal peptide (*WSP*). The amplifications were performed by repeating for 35 times the following cycle: 30 s at 94 °C; 30 s at 50 °C; 1 min at 72 °C. The PCR amplicons, purified as above reported, were ligated into the *Eco*RI and *Xba*I sites of the pPICZαA expression vector (Invitrogen Life Technologies) and the ligation mixtures were then used to transform *Escherichia coli* competent cells, selected in low salt lysogeny broth medium (Fluka) supplemented with 25 μg mL^{-1} Zeocin (InvivoGen). The two

recombinant plasmids (named *pPIC1 WSP* and *pPIC2 WSP*) were extracted and purified from one PCR positive colony using the "GenElute HP Plasmid Midiprep" (Sigma-Aldrich kit, linearized with *Sac*I (Fig. S2.1), precipitated with 2 volumes of absolute ethanol and 1/10 volume of sodium acetate 3M pH 5.2 and resuspended in 20 µL of water. *P. pastoris* transformation was performed as reported in Sella et al. (2013). Some positive colonies were tested by PCR using the specific primers *pPICZαA*for/rev (Table S2.1) and the "REDTaq ReadyMix PCR Reaction Mix", repeating for 35 times the following cycle: 30 s at 94 °C; 30 s at 50 °C; 1 min at 72 °C. The colonies showing the expected band were grown and induced with methanol according to the Invitrogen Life Technologies manual. After 72 h, liquid cultures were centrifuged at 10,000 x g for 10 min and supernatants were subjected to SDS-PAGE.

2.2.3. SDS-PAGE analysis and preparation of the F. graminearum *recombinant CPPs*

The culture filtrates of *P. pastoris* containing the FgCPPs of interest (FgCPP1 and FgCPP2) and a *P. pastoris* wild type (WT) culture filtrate also induced with methanol were subjected to precipitation with ammonium sulphate 20% (w/v) and dissolved under stirring by incubating for 1 h at 4 °C. After centrifugation at 8,000 x g for 20 min at 4 °C, the recovered supernatants were precipitated again with ammonium sulphate 80% (w/v) as above reported. The pellets were resuspended in 20 mL of water and centrifuged at 5,000 x g for 10 min at 4 °C. The recovered supernatants were then dialyzed against water (1:100 dilution) overnight at 0 °C using Nominal MWCO 3500 membranes (Orange Scientific) and finally stored at -20 °C.

SDS-PAGE was performed on a 16% polyacrylamide gel according to Laemmli (1970) by a Mini Protean II unit (Bio-Rad). Electrophoresis was run at constant 200 V for about 45 min. Proteins were stained with Coomassie Blue G250 (Sigma-Aldrich) and the bands obtained were compared with 10 µL of marker Low Range (Bio-Rad). Protein concentration was evaluated by comparison with known amounts of bovine serum albumin (BSA) protein.

2.2.4. Effect of FgCPPs on polysaccharide substrates

The activity of the FgCPPs on polysaccharide substrates was determined by a viscosimetric method. Viscosimetric activity was assayed by measuring the decrease in relative viscosity at 30 °C of a 2 mL reaction mixture containing 0.25% (w/v) high, medium or low viscosity carboxymethyl cellulose (CMC; Sigma-Aldrich, Milano, Italy, codes C-8758, C-4888 and C-5013, respectively), chitin (Sigma-Aldrich, code C-7170), larchwood xylan (Sigma-Aldrich, code X-3875) or apple pectin (Sigma-Aldrich, code 76282) dissolved in 50 mM phosphate buffer (pH 6.0) and 0.1 μM of recombinant FgCPPs native or boiled for 30 min. Equal volumes of a *P. pastoris* WT preparation or 0.1 μM bovine serum albumin (BSA) were used as negative control. Micro-Ostwald capillary viscosimeters (i.d. = 0·70 mm), connected to AVS 310 systems, were used. Experiments were performed by measuring the percentage of viscosity reduction after 30 min or the time (sec) employed by the FgCPPs to decrease the initial relative viscosity by 10% (T_{10}), 15% (T_{15}) and 50% (T_{50}). To investigate whether the two FgCPPs possess enzymatic activity on cellulose, 100 μL of each reaction mixture were assayed as reported by Nelson et al. (1944) to determine reducing sugars released by using D-(+)-glucose as standard.

Moreover, to test the effect of the two FgCPPs on fungal cellulase activity, a viscosimetric assay was performed by incubating 0.04 U of a β-1,4-glucanase from *T. longibrachiatum* (Sigma-Aldrich) at 30 °C for 30 min in a 2 mL reaction mixture containing 0.25% (w/v) medium viscosity CMC dissolved in 50 mM phosphate buffer (pH 6.0) with 0.1 μM of the recombinant native FgCPP1 and FgCPP2 or with an equal volume of a *P. pastoris* WT preparation as negative control. Experiments were performed by measuring the time (sec) employed by the mixture of β-1,4-glucanase and FgCPPs to decrease the initial relative viscosity by 50% (T_{50}).

Besides, the same amount of β-1,4-glucanase was tested at the same assay conditions in the presence of 0.15 μM of each of the recombinant native FgCPP1 and FgCPP2 or with an equal volume of *P. pastoris* WT preparation as negative control and reducing sugars released in the mixtures were determined as above reported.

2.2.5. Effect of FgCPPs on filter paper

The effect of the FgCPPs was tested on Whatman 3MM filter paper (Whatman-GE Healthcare, Milan, Italy) as substrate as reported in Baccelli et al. (2014b). Filter papers were cut into 1-cm-diameter discs (6 mg each), and a single disc was incubated in 1 mL of 50 mM sodium acetate buffer (pH 5) containing 0.25 µM of FgCPPs. Buffer only or buffer containing 0.25 µM BSA or an equal volume of *P. pastoris* WT preparation were used as negative controls. The experiments were performed at 38 °C for 48 h and 72 h onto an orbital shaker at 150 rpm. At the end of the incubation period, discs were removed and the absorbance at 500 nm was measured to quantify the paper fragments produced. Data are presented as net absorbance calculated by subtracting for each sample the absorbance at T_0 and the background absorbance of the buffer incubated alone with filter paper.

2.2.6. Cellulase activity produced by F. graminearum *WT and* ΔΔfgcpp$_{1,2}$ *mutant in CMC containing medium*

The *F. graminearum* wild type (WT:8/1) and the Δ*Δfgcpp$_{1,2}$* mutant strain were cultured at 25 °C on potato dextrose agar (PDA, Difco). Conidia were obtained by culturing *F. graminearum* strains in carboxymethyl cellulose (CMC; Sigma-Aldrich) as reported in Sella et al. (2016).

For cellulase activity, 10^4 conidia mL^{-1} of the *F. graminearum* wild type (WT:8/1) and the Δ*Δfgcpp$_{1,2}$* mutant were inoculated in flasks containing 20 mL of Szécsi medium (Szécsi, 1990) supplemented with 1% (w/v) low, medium and high viscosity CMC (Sigma-Aldrich) or 1% (w/v) D-(+)-glucose (Sigma-Aldrich) as control. Flasks were incubated at 25 °C on an orbital shaker at 150 rpm in the dark for 4 days. The cellulase activity produced during growth on CMC media by the *F. graminearum* WT and the Δ*Δfgcpp$_{1,2}$* mutant was determined by a viscosimetric assay as above reported. In particular, cellulase activity was assayed by measuring the decrease in relative viscosity at 30 °C of a 2 mL reaction mixture containing 0.25% (w/v) medium viscosity CMC (Sigma-Aldrich) dissolved in 50 mM phosphate buffer (pH 6.0) and 500 µL of culture filtrates. Experiments were performed by measuring the time (sec) necessary to decrease the initial relative viscosity by 30% (T_{30}). Mycelia of

the *F. graminearum* WT and double mutant was then collected after 4 days of culture, treated and weighed as reported in Quarantin et al. (2016).

2.2.7. Binding assay of FgCPPs with CMC and chitin

The carbohydrate binding assay was performed as reported in Baccelli et al. (2014b) with some modifications. In details, the heterologously expressed FgCPP1 and FgCPP2 proteins (about 4 µg) were incubated in 1 mL of 50 mM sodium acetate reaction mixture buffered at pH 5 containing 0.25% (w/v) chitin (Sigma-Aldrich) or 0.25% (w/v) medium viscosity CMC (Sigma-Aldrich). As control, the proteins were incubated only with the buffer solution. After 48 h of incubation at 38 °C with shaking (250 rpm), the samples were centrifuged at 14,000 rpm for 2 min and the unbound proteins present in the supernatants were precipitated by using four volumes of absolute ethanol. Proteins were then resuspended in 100 µL sample buffer and for SDS-PAGE analysis 50 µL were loaded on a 16% (w/v) polyacrylamide gel as above reported.

2.2.8. Plants growth and detection of hydrogen peroxide and necrotic symptoms

A. thaliana seeds (cv. Col-0) were sown in 9 cm plastic pots and plants were grown into a climatic chamber with a 14 h photoperiod and 22/20°C day/night temperature up to 4-week-old.

The production of hydrogen peroxide (H_2O_2) in *A. thaliana* leaves infiltrated with the *F. graminearum* recombinant CPPs was assayed with 3,3'-diaminobenzidine (DAB, Sigma-Aldrich). Leaves were first infiltrated using a 1 mL syringe without needle through stomata in the lower surface of the leaf with 1.5 µM FgCPP1 and FgCPP2 protein solutions; as negative control, leaves were infiltrated with an equal volume of the *P. pastoris* WT preparation as control. Plants were incubated into the climatic chamber and after 4 h leaves were cut and dipped into 1 mg mL^{-1} DAB solution (pH 3.8) and incubated overnight at room temperature in the dark. Leaves were then removed, placed into acetic acid/glycerol/ethanol (1/1/1, v/v/v) solution and boiled for 5 min in water bath to eliminate chlorophyll. Subsequently, leaves were maintained in 60% glycerol and photographed. Some *A.*

thaliana plants were also treated with the *F. graminearum* recombinant CPPs (1.5 μM) or with an equal volume of the *P. pastoris* WT preparation as control and incubated into the climatic chamber to monitor the development of macroscopic necrotic symptoms up to 5 days after treatment.

2.3. Results

2.3.1. Features of the FgCPPs

The deduced amino acid sequences of the *F. graminearum* CPPs (FgCPP1 and FgCPP2) have 61.4% of identity and 76% of similarity (data not shown).

The structural analysis of the CPPs characterized so far has revealed the presence of conserved aa residues putatively related with the main characteristics identified for this family of proteins. The structural study of the CP of *C. platani* performed by de Oliveira et al. (2011) highlighted the presence of some aa potentially involved in the oligosaccharides binding. Most of these residues are highly conserved among the members of the CPPs family, including the FgCPPs: the SYD motif, Tyr-9 (Y9), Gly-51 (G51), Ser-54 (S54), Asp-77 (D77) (Fig. 2.1). In particular, the residue Asp-77 is known to be co-responsible for the oligosaccharides binding and is essential for the maintenance of PAMP and cellulose weakening activities of the CP protein (Luti et al., 2017). Furthermore, the residue Asn-84 (N) is responsible for the lack of glycoside hydrolase activity (de Oliveira et al., 2011; Fig. 2.1). Since Asp-77 and Asn-84 are conserved among the members of the CPPs family, they could be responsible for the same features in all the proteins of this family.

The two conserved regions (PepA and PepB) identified in the BcSpl1 protein of *B. cinerea* as putatively responsible of the necrotizing activity (Frías et al., 2014), including the two cysteine residues forming the disulphide bond connecting the two loops, were also found as highly conserved in the aa sequences of the FgCPPs and other seven CPPs known to elicit defence responses and HR in plants (Fig. 2.1). In particular, the PepA region of FgCPP1 is identical to that of BcSpl1, while that of FgCPP2 has a 90% aa identity with that of BcSpl1 and also with those of Sm1, Epl1, MoSM1, VdCP1 and Sp1. Differently, the PepB regions of FgCPP1 and FgCPP2 have a 60% and 50% aa identity, respectively, with that of BcSpl1 (Fig. 2.1). Besides, the PepB region of FgCPP1 has a maximum of 80% aa identity with that of VdCP1, while the PepB of FgCPP2 has 90% aa identity with Epl1 (Fig. 2.1).

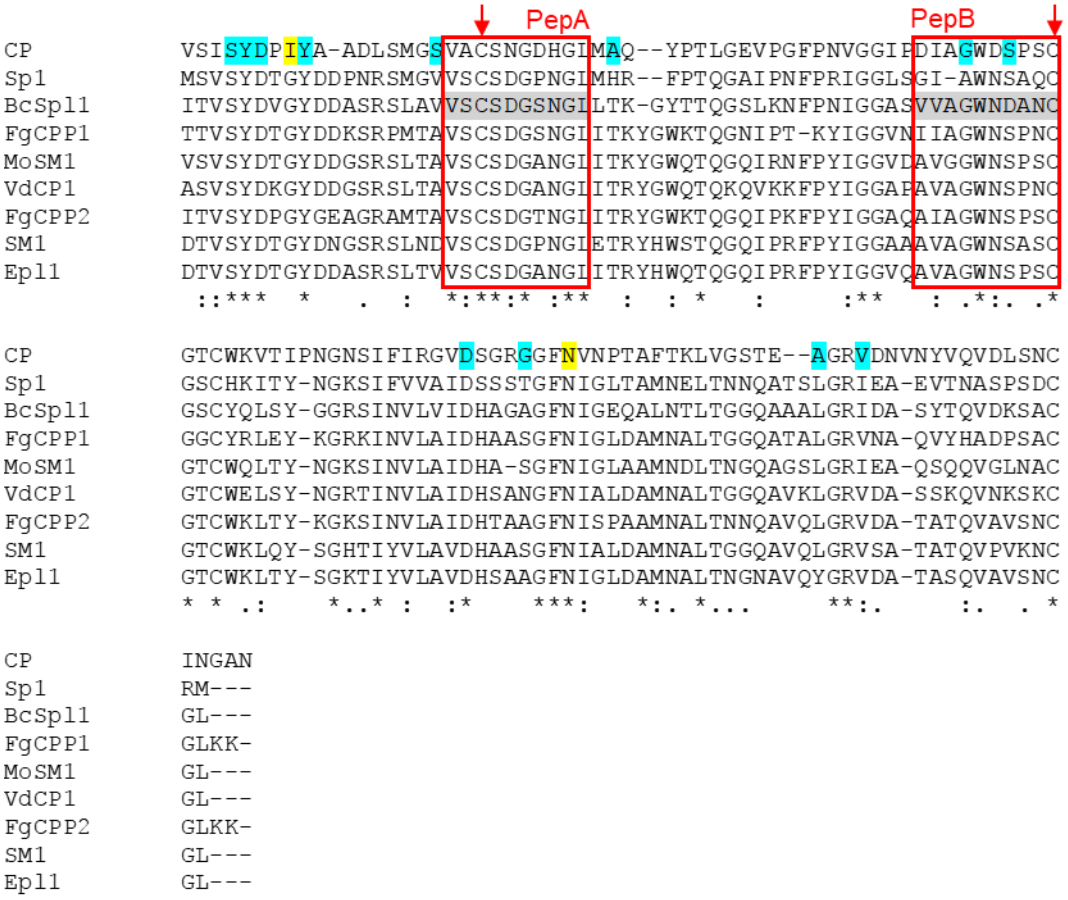

Fig. 2.1. Alignment of the aa sequences without signal peptide of the *Fusarium graminearum* CPPs with other six cerato-platanin known to elicit defense responses in plant tissues. The alignment includes FgCPP1 and FgCPP2 of *F. graminearum*, SM1 of *Trichoderma virens* (Buensanteai et al., 2010); Epl1 of *T. atroviride* (Vargas et al., 2008); MoSM1 of *Magnapothe oryzae* (Yang et al., 2009); VdCP1 of *Verticillium dahliae* (Zhang et al., 2017a); BcSpl1 of *Botrytis cinerea* (Frías et al., 2011); Sp1 of *Leptosphaeria maculans* (Wilson et al., 2002) and CP of *Ceratocystis platani* (Pazzagli et al., 1999). The necrosis-inducing motifs, PepA and PepB, are framed in red and the BcSpl1 corresponding sequences are highlighted in grey (Frías et al., 2014). The two cysteine residues which form a disulphide bond connecting the two loops are indicated with a red arrow. The aa residues identified in CP putatively responsible for oligosaccharide-binding capability, in particular the Asp-77 (D), are highlighted in blue (de Oliveira et al., 2011). The Asn-84 (N), which represents the main conserved residual hypothesized to be the cause of the lack of glycoside hydrolase activity of the CPPs, is highlighted in yellow. These residues identified are conserved among the members of the CPPs family. The alignment was created using the Clustal Omega multiple sequence alignment software. (*) conserved residue; (:) aa with conservative substitution; (.) aa with some non-conservative substitution.

2.3.2. Heterologous expression of the FgCPPs

The *fgcpp1* and *fgcpp2* sequences encoding the mature protein (*WSP)* were obtained by PCR using specific primer pairs with adapters for cloning in the *pPICZαA* vector. Ten *pPIC1 WSP* and ten *pPIC2 WSP* transformed colonies were selected and tested by colony PCR and the presence of amplicons of the expected size (366 bp for *fgcpp1 WSP* and 372 bp for *fgcpp2 WSP*) was detected in all the colonies analyzed (data not shown). The *pPIC1 WSP* and *pPIC2 WSP* constructs obtained were used to transform *P. pastoris* cells. Thirty transformed colonies for both constructs were obtained, and for each construct five were tested by PCR. The expected amplicon was present in the genome of all the selected colonies (data not shown). The presence of the recombinant proteins in the secretome of *P. pastoris* was verified by subjecting aliquots of the cultures broths of 2 recombinant colonies grown for 72 h in presence of methanol to SDS-PAGE. Compared to culture filtrate of the *P. pastoris* WT loaded as control, bands of approximately 20 kDa, corresponding to the FgCPP1 and FgCPP2 proteins were observed (Fig. 2.2). Since the expected molecular mass is about 15 kDa, probably the proteins are in glycosylated form. In fact, both protein sequences possess a putative site of O-glycosylation.

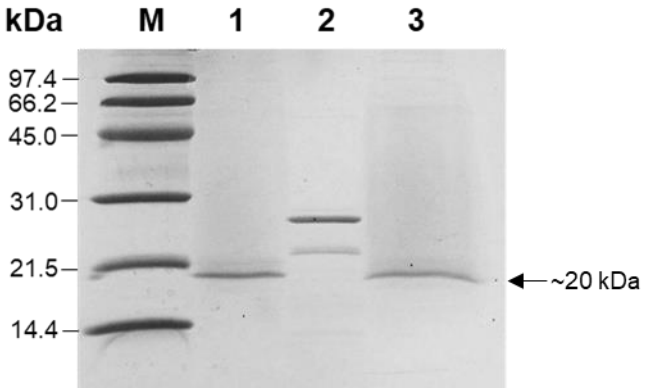

Fig. 2.2. SDS-PAGE analysis of the secretome of two *Pichia pastoris* colonies transformed to express the FgCPPs (FgCPP1 and FgCPP2) and the *P. pastoris* WT culture filtrate as control induced with methanol for 72 h. Aliquots of *P. pastoris* liquid cultures were loaded on a 16% polyacrylamide gel and then stained with Coomassie Brilliant Blue G250. Lane M: molecular weight standards (Low Range; Bio-Rad Laboratories); lane 1: 5 µL of culture filtrate containing the recombinant FgCPP1; lane 2: 5 µL of the *P. pastoris* WT culture filtrate as control; lane 3: 5 µL of culture filtrate containing the recombinant FgCPP2. Size of the molecular mass standards is reported on the left.

2.3.3. The FgCPPs reduce the CMC viscosity

The effect of the FgCPPs on the viscosity of different high, medium or low viscosity CMC preparations was analyzed by a viscosimetric assay. Both recombinant FgCPPs resulted able to decrease the substrate viscosity, although with different efficacy. Interestingly, the activity of the FgCPPs was affected by the initial viscosity of the substrate, with higher affinity observed for high and medium viscosity substrates. In particular, viscosity was monitored with time: on the whole, the FgCPP2 was ~2-folds more effective in decreasing the substrate viscosity compared to the FgCPP1 on both medium and high viscosity CMC preparations, and ~3-folds more effective in the low viscosity CMC (Table 2.1). Besides, the boiled FgCPP1 and FgCPP2 preparations retained about 18% and 15% activity, respectively, after 30 min of incubation (Table 2.1). Experiments were also performed by incubating the recombinant FgCPPs on other polysaccharide substrates such as chitin, xylan and pectin. However, no viscosity reduction was observed on these polysaccharides (data not shown).

Table 2.1. Viscosimetric assay performed with *Fusarium graminearum* CPPs on carboxymethyl cellulose (CMC) with different viscosity. The assay was performed at 30 °C in a 2 mL reaction mixture containing 0.25% (w/v) high, medium or low viscosity CMC dissolved in 50 mM sodium phosphate buffer (pH 6.0) and 0.1 µM recombinant native or boiled (B) FgCPPs, 0.1 µM bovine serum albumin (BSA) or an equal volume of a *Pichia pastoris* WT preparation as negative controls. At least three independent experiments were performed. Data after 30 min of incubation represent the average ± standard deviation of the percentage (%) of decrease of the initial relative viscosity. T_{15} or T_{10} data represent the mean ± standard deviation of the time (expressed in sec) necessary to decrease the initial relative viscosity by 15% or 10%, respectively.

High viscosity CMC

Sample	30 min (%)	T_{15} (s)
BSA	0.0 ± 0.0	∞
WT	0.8 ± 0.7	∞
FgCPP1	27.2 ± 0.7	714.3 ± 75.1
FgCPP2	43.7 ± 0.7	338.7 ± 24.7
FgCPP1B	3.8 ± 0.1	11812.5 ± 1412.1
FgCPP2B	7.9 ± 0.3	4470.0 ± 161.2

Medium viscosity CMC

Sample	30 min (%)	T_{15} (s)
BSA	0.0 ± 0.0	∞
WT	0.9 ± 1.1	∞
FgCPP1	24.4 ± 0.3	909.0 ± 11.4
FgCPP2	40.8 ± 0.7	357.7 ± 22.1
FgCPP1B	3.6 ± 0.6	13414.7 ± 308.1
FgCPP2B	7.1 ± 0.7	5354.8 ± 442.2

Low viscosity CMC

Sample	30 min (%)	T_{10} (s)
BSA	0.0 ± 0.0	∞
WT	0.0 ± 0.0	∞
FgCPP1	5.7 ± 0.6	4360.0 ± 427.1
FgCPP2	13.3 ± 1.1	1216.0 ± 84.8

2.3.4. The FgCPPs are trapped by CMC and not by chitin

A carbohydrate binding assay was performed by incubating the FgCPP1 and FgCPP2 proteins with chitin or CMC to verify if these proteins can bind to these polysaccharides. After incubation, the

mixtures were centrifuged and the supernatants containing the proteins not bound to polysaccharides were precipitated and analysed by SDS-PAGE. Compared to the control sample, consisting of proteins incubated without polysaccharides, a similar amount of FgCPPs was present in the supernatant previously incubated with chitin (Fig. 2.3). Differently, the intensity of the band corresponding to the FgCPPs was drastically reduced in the CMC-containing sample (Fig. 2.3).

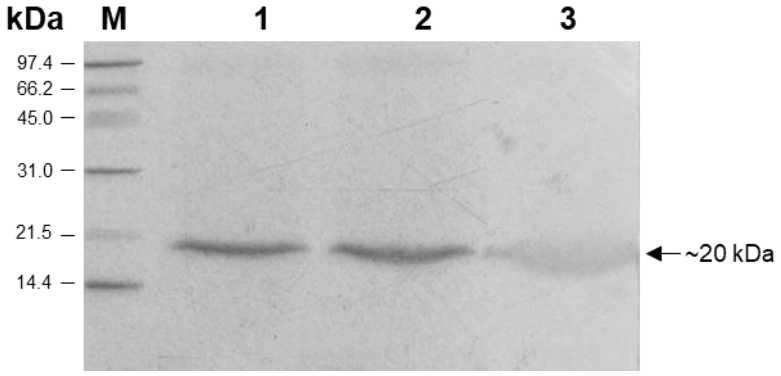

Fig. 2.3. SDS-PAGE analysis of the carbohydrate binding assay. The *Fusarium graminearum* CPPs were incubated with 0.25% (w/v) chitin or medium viscosity carboxymethyl cellulose (CMC) or with 50 mM sodium acetate buffer (pH 5) as control at 38 °C for 48 h with shacking (250 rpm). The samples were then centrifuged at 14,000 rpm for 2 min and the unbound proteins present in the supernatants were precipitated, resuspended in 100 µL sample buffer and loaded on a 16% polyacrylamide gel. Staining was performed with Coomassie Brilliant Blue G250. Lane M: molecular weight standards (Low Range; Bio-Rad Laboratories); lane 1: 50 µL of control sample; lane 2: 50 µL of sample incubated with chitin; lane 3: 50 µL of sample incubated with CMC. Size of the molecular mass standards is reported on the left.

2.3.5. The FgCPPs favour the cellulase activity

Since the FgCPPs have been shown to affect CMC viscosity, we investigated their effect on fungal cellulase activity. To this aim, a β-1,4-glucanase was incubated on the medium viscosity CMC substrate in presence or absence of the heterologously expressed FgCPPs. In a viscosimetric assay, the β-1,4-glucanase resulted ~2.5-folds faster in halving the initial relative viscosity (T_{50}) in the presence of the FgCPPs compared to the control thesis in which the enzyme was supplemented with the *P. pastoris* WT preparation (Table 2.2).

Table 2.2. Viscosimetric assay performed to investigate the effect of the *Fusarium graminearum* CPPs on fungal cellulase activity. The two recombinant native FgCPPs (0.1 µM) or an equal volume of a *Pichia pastoris* WT preparation as negative control were incubated in the presence or absence of 0.04 U of β-1,4-glucanase from *Trichoderma longibrachiatum* (Sigma-Aldrich) at 30 °C in a 2 mL reaction mixture containing 0.25% (w/v) medium viscosity carboxymethyl cellulose (CMC) dissolved in 50 mM phosphate buffer (pH 6.0). T_{50} data represent the mean ± standard deviation of the time (expressed in sec) necessary to decrease the initial relative viscosity by 50%. At least three independent experiments were performed. Data were statistically analyzed by the ANOVA Tukey-Kramer test. Different letters (a, b, c) indicate significant differences at $P<0.05$.

Sample	T_{50} (s)
Control	∞
FgCPPs	$3032.7^{b} \pm 265.0$
β-1,4-glucanase	$3828.5^{bc} \pm 43.1$
β-1,4-glucanase + FgCPPs	$1815.3^{c} \pm 47.6$
β-1,4-glucanase + Control	$4349.0^{a} \pm 562.6$

Reducing sugars released in the mixtures were determined by the Nelson assay. In the presence of the FgCPPs, the β-1,4-glucanase was able to release about 3 µg more glucose equivalents (27% increase) compared to the control thesis containing only the enzyme supplemented with the *P. pastoris* WT preparation (Fig. 2.4). Since the heterologously expressed proteins alone seem to release only about 1 µg of glucose equivalents from the CMC substrate (Fig. 2.4), it appears that the FgCPPs positively affects the enzymatic activity of the β-1,4-glucanase.

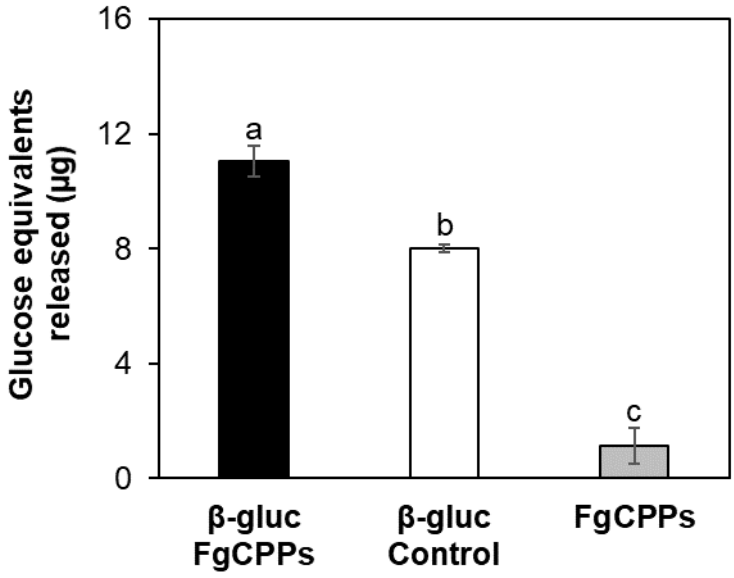

Fig. 2.4. Glucose equivalents released from carboxymethyl cellulose (CMC) substrate by 0.04 U of β-1,4-glucanase from *Trichoderma longibrachiatum* (Sigma-Aldrich) in combination with the recombinant *Fusarium graminearum* CPPs (0.1 μM) or with an equal volume of a *Pichia pastoris* WT preparation as negative control, or by the FgCPPs alone. One hundred μL of a reaction mixture containing 0.25% (w/v) CMC dissolved in 50 mM phosphate buffer (pH 6.0) were incubated at 30 °C for 30 min and assayed as reported by Nelson et al. (1944). D-(+)-glucose was used as standard. Data were obtained from three independent experiments. Error bars correspond to the standard error. Data were statistically analyzed by the ANOVA Tukey-Kramer test. Different letters (a, b, c) indicate significant differences at $P<0.05$.

2.3.6. The FgCPPs weaken filter paper cellulose

The FgCPPs were incubated with Whatman filter paper to verify their ability to affect this substrate. The spectrophotometric analysis after 48 h of incubation allowed to demonstrate that only the FgCPPs were able to release a clearly detectable amount of paper fragments in suspension (Fig. 2.5). Fragments released by FgCPPs increased after 72 h while BSA, used as negative control, was able to release a very poor quantity of paper fragments (Fig. 2.5).

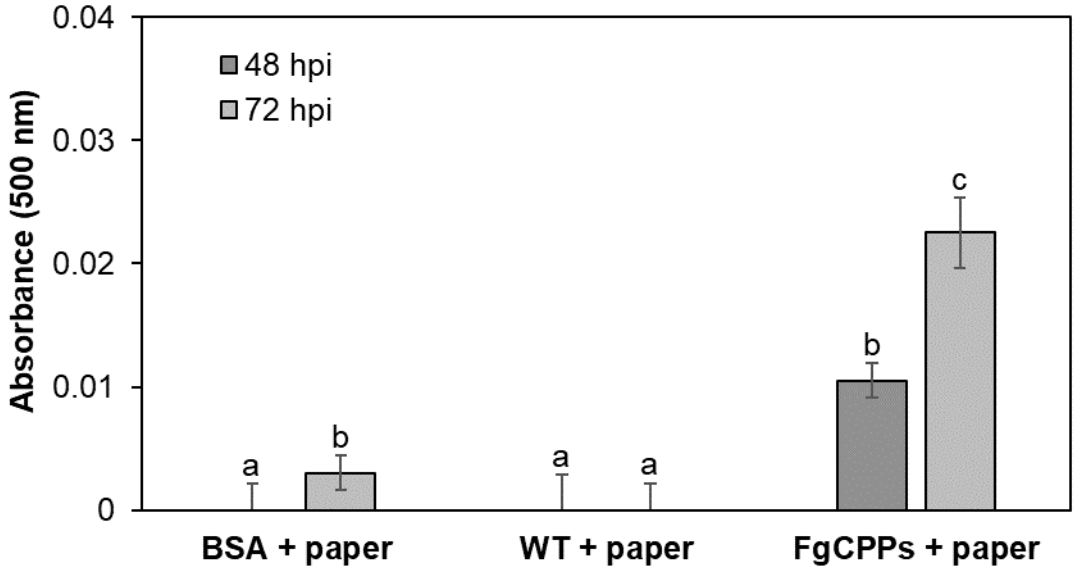

Fig. 2.5. Effect of FgCPPs on Whatman 3MM filter paper. Filter papers (1-cm-diameter discs) were incubated in 1 mL of 50 mM sodium acetate buffer (pH 5) containing 0.25 μM of FgCPPs. Buffer only or buffer containing 0.25 μM bovine serum albumin (BSA) or an equal volume of *Pichia pastoris* WT (WT) preparation were used as negative controls. After 48 h and 72 h at 38 °C the absorbance was measured at 500 nm to quantify the paper fragments produced. Data, obtained from two independent experiments, are presented as net absorbance calculated by subtracting for each sample the absorbance at T_0 and the background absorbance of the buffer incubated alone with filter paper. Error bars correspond to the standard error. Data were statistically analyzed by the ANOVA Tukey-Kramer test. Different letters (a, b, c) indicate significant differences at $P<0.05$.

2.3.7. The ΔΔfgcpp$_{1,2}$ *mutant produces higher cellulase activity than WT in CMC containing medium*

The cellulase activity produced by the *F. graminearum* WT and the Δ*Δfgcpp$_{1,2}$* mutant grown for 4 days in liquid culture containing high, medium or low viscosity CMC as the sole carbon source was measured by a viscosimetric assay. Both WT and double mutant strains were able to produce about 3 folds more cellulase activity when grown on low viscosity CMC compared to their growth on medium and high viscosity CMC, as demonstrated by the lower time needed to decrease the initial relative viscosity by 30% (T_{30}) (Fig. 2.6). However, the double mutant was able to produce higher cellulase activity than WT in all the three CMC substrates; in particular, on medium and high viscosity substrates the mutant produced about 3.5-4 folds more cellulose activity than WT, while the difference was reduced (about 2-folds) on low viscosity CMC (Fig. 2.6).

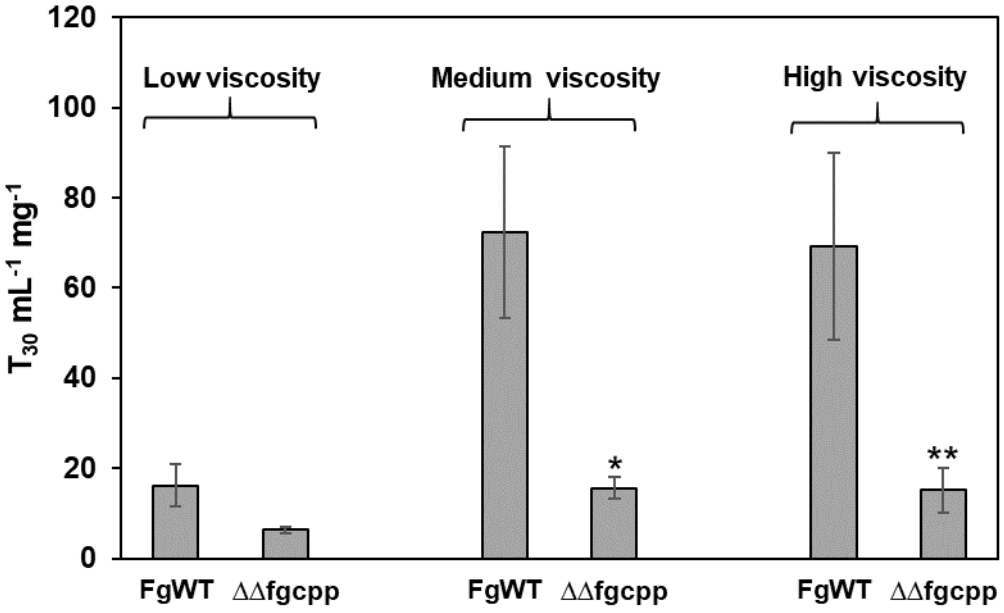

Fig. 2.6. Cellulase activity produced by *Fusarium graminearum* wild type (FgWT:8/1) and Δ*Δfgcpp$_{1,2}$* mutant in carboxymethyl cellulose (CMC) containing medium. Viscosimetric assay was performed to detect cellulase activity released from the *F. graminearum* WT and mutant grown on low, medium and high viscosity CMC as the sole carbon source. After 4 days of growth at 25 °C, 500 µL of culture supernatants, previously filtered, were added in a 2 mL reaction mixture containing 0.25% (w/v) medium viscosity CMC dissolved in 50 mM phosphate buffer (pH 6.0) at 30 °C. Three independent experiments were performed. Data represent the mean ± standard error of the time (expressed in sec) necessary to decrease the initial relative viscosity by 30% (T_{30}) per mL of culture filtrate per mg of dry weight. Data were statistically analyzed by the Student's t-test. * indicates that the difference is significant at $P<0.05$, ** indicates that the difference is significant at $P<0.01$.

2.3.8. FgCPPs do not elicit defense responses in A. thaliana *leaves*

To investigate the ability of the FgCPPs to elicit defense responses and/or necrosis, *A. thaliana* leaves were infiltrated with the recombinant FgCPP proteins or with an equal volume of *P. pastoris* WT preparation, used as control. After 4 h from infiltration, none of the FgCPPs was able to induce the formation of the brown precipitate typical of H_2O_2 accumulation (Fig. 2.7A). Besides, the FgCPPs were not able to induce macroscopic necrotic symptoms in treated leaves (Fig. 2.7B). The same results were observed in the leaves infiltrated or treated with the *P. pastoris* WT preparation used as control (Fig. 2.7A-B).

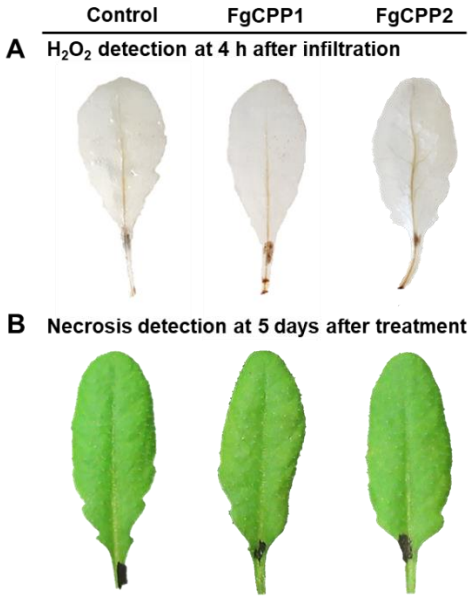

Fig. 2.7. Detection of H_2O_2 production and necrotic symptoms in *Arabidopsis thaliana* (cv. Col-0) leaves infiltrated or treated in the lower surface with the recombinant native FgCPP1 and FgCPP2, or with an equal volume of the *Pichia pastoris* WT preparation as control. To reveal the production of H_2O_2 leaves were treated with 3,3'-diaminobenzidine (DAB). (A) H_2O_2 detection on leaves 4 h after infiltration; (B) detection of necrotic symptoms on leaves 5 days after treatment.

2.4. Discussion

In order to characterize the role of the *F. graminearum* cerato-platanins (FgCPPs), single and multiple knock-out mutants of the corresponding encoding genes have been previously produced and characterized, demonstrating that the FgCPPs contribute to protect fungal cell wall polysaccharides from enzymatic degradation by β-glucanase and chitinase but do not contribute to fungal virulence (Quarantin et al., 2016). However, fungal CPPs could play other roles during fungal growth and plant infection, so we heterologously expressed the FgCPPs in the *P. pastoris* yeast to investigate their properties.

Since FgCPPs share important amino acid residues with other CPPs (Fig. 2.1), which have been reported to cause several effects on plant and fungal cell wall polysaccharides, we initially investigated the effects of FgCPPs on polysaccharide substrates. Both recombinant FgCPPs resulted able to reduce the viscosity of cellulose substrates, and the reduction was faster on CMC substrates with medium and high viscosity, probably due to a higher affinity of FgCPPs for these substrates. In particular, the FgCPP2 was about 2 to 3-folds more effective in weakening cellulose viscosity than the FgCPP1 depending on the viscosity of the substrate. Differently, the FgCPPs were ineffective against other polysaccharide substrates such as chitin, xylan and pectin.

These findings are similar to those obtained with the *C. platani* CP, which has been shown to weaken cellulose via a non-enzymatic mechanism while it is ineffective against other polysaccharides (de Oliveira et al., 2011). Similarly, the mechanism by which the FgCPPs reduce the CMC viscosity seems to be ascribed mainly to a non-enzymatic mechanism, as also suggested by the presence in the FgCPP aa sequences of the Asn-84 residue responsible of the lack of glycoside hydrolase activity (de Oliveira et al., 2011) and by the observation that the boiled FgCPPs partially retain their ability to reduce cellulose viscosity. In fact, the Nelson assay performed in our paper revealed that the FgCPPs can release a little amount of reducing sugars; however, if this is due to a real enzymatic activity or it is an indirect effect due to the exposure of additional reducing ends in the polysaccharide modified by the activity of the FgCPPs remains to be elucidated. In this regard, it is worth noting that

electrostatic interactions are one of the key factors shown to be responsible of the viscous properties of the CMC solution (Yang and Zhu, 2007). Since ion binding and hydrogen bonding are the major forms of electrostatic interaction identified in CMC (Yang and Zhu, 2007), it can be speculated that the FgCPPs are able to interfere in some way with these interactions, thus loosening the cellulose structure. Besides, a role of the FgCPPs in the CMC transition from crystalline to amorphous structure could also be hypothesized. Although the structure of CMC is slightly different from that of plant cellulose, the observation that the FgCPPs act also on filter paper, an insoluble natural cellulose, suggests that these proteins could act with a similar mechanism on plant cellulose.

The observation that the FgCPPs are trapped by cellulose and not by chitin, as shown by a carbohydrate binding assay, supports the hypothesis that the non-enzymatic activity of the FgCPPs on cellulose could depend on their ability to interact with cellulose. This result is similar to that observed with the *B. subtilis* expansin-like EXLX1 protein (Kerff et al., 2008), but is in contradiction to previous data indicating that the *C. platani* CP, *B. cinerea* BcSpl1 and *V. dahliae* VdCP1 are able to bind to chitin and not to CMC (de Oliveira et al., 2011; Baccelli et al., 2014b; Zhang et al., 2017a and 2017b).

Interestingly, the *C. platani* CP and those of three other fungi are also able to induce HR on leaves of several plants (Baccelli et al., 2014a; Frías et al., 2011; Yang et al., 2009). Besides, Frías et al. (2014) identified at the surface of the *B. cinerea* BcSpl1 two conserved regions interacting each other and involved in the necrosis-inducing activity. These regions seem conserved among CPPs and have been previously proposed as also involved in the binding to N-acetylglucosamine oligosaccharides (de Oliveira et al., 2011). Therefore, the binding with polysaccharides and the necrosis-inducing activity appear strictly associated features and related to the same region of the protein surface. However, treatments of *A. thaliana* leaves with the FgCPPs did not induce H_2O_2 accumulation nor necrotic symptoms, although their alignment with the BcSPl1 and other CPPs known to elicit necrosis highlighted the presence of these two homologous regions also in the FgCPPs. Nevertheless, the PepA and PepB aa sequences of the FgCPPs differed for a single amino acid from the conserved sequences

of the other CPPs, so we cannot rule out that single amino acid mutations could affect the elicitor and polysaccharide binding activity of the FgCPPs, as recently demonstrated with the *C. platani* CP (Luti et al., 2017). However, it is worth nothing that the concentration of FgCPPs used in our assay (1.5 µM) is lower than the high concentrations used for in vivo treatments with other fungal CPPs shown as able to induce H_2O_2 and necrosis (Baccelli et al., 2014a; Frías et al., 2011, 2013).

To investigate a possible role of the FgCPPs in vivo during plant infection, we incubated a β-1,4-glucanase in the presence or absence of the heterologously expressed FgCPPs. Our enzymatic assays show that the β-1,4-glucanase has an increased capacity to release reducing sugars from cellulose in presence of the FgCPPs, and this effect is only partially due to a direct activity of the FgCPPs on the substrate. In fact, at least 60% of the increased activity of the β-1,4-glucanase depends on an indirect effect of the FgCPPs that, probably by reducing the CMC viscosity, could modifying the structure of the polysaccharide substrate making it more easily accessible for β-1,4-glucanase enzymatic activity. From these results it could be therefore inferred that the FgCPPs could increase the degradation of plant cellulose, a polysaccharide abundantly present in the primary and secondary cell walls of grass monocot and dicot species (Vogel, 2008), thus facilitating wheat tissue colonization. However, from our previous paper it appears that the *F. graminearum* double knock-out mutant (ΔΔ*fgcpp*$_{1,2}$) is as virulent as the WT strain (Quarantin et al., 2016). Nevertheless, it should be considered that the ΔΔ*fgcpp*$_{1,2}$ mutant grown on CMC produced more cellulase activity than WT, and this higher enzymatic activity could compensate for the absence of the FgCPPs. Therefore, a role of these proteins during plant infection cannot be conclusively ruled out.

In conclusion, the FgCPPs can reduce the viscosity of carboxymethyl cellulose mainly by a non-enzymatic mechanism, with higher affinity for medium/high viscosity substrates, while they are ineffective against other polysaccharides. Besides, the FgCPPs weaken filter paper and, probably by binding to cellulose, could favor the enzymatic activity of β-1,4-glucanase making the substrate more accessible. These features could be further investigated in order to verify if these proteins can find a biotechnological application in the production of biofuel from cereal straw, a potential biofuel

resource abundantly produced worldwide. In fact, this plant waste tissue is particularly rich in lignocellulose materials, consisting mainly of cellulose, hemicellulose, and lignin polymers, which are particularly recalcitrant to digestion. In particular, the FgCPPs could contribute to cellulose degradation by increasing the activity of cellulolytic enzymes.

References

Ashwin, N.M.R., Barnabas, L., Ramesh Sundar, A., Malathi, P., Viswanathan, R., Masi, A., Agrawal, G.K., Rakwal, R., 2017. Comparative secretome analysis of *Colletotrichum falcatum* identifies a cerato-platanin protein (EPL1) as a potential pathogen-associated molecular pattern (PAMP) inducing systemic resistance in sugarcane. J. Proteomics. Doi: 10.1016/j.jprot.2017.05.020.

Baccelli, I., Lombardi, L., Luti, S., Bernardi, R., Picciarelli, P., Scala, A., Pazzagli, L., 2014a. Cerato-platanin induces resistance in *Arabidopsis* leaves through stomatal perception, overexpression of salicylic acid- and ethylene-signalling genes and camalexin biosynthesis. PLoS One. 9, e100959.

Baccelli, I., Luti, S., Bernardi, R., Scala, A., Pazzagli, L., 2014b. Cerato-platanin shows expansin-like activity on cellulosic materials. Appl. Microbiol. Biotechnol. 98, 175-184.

Baccelli, I., 2015. Cerato-platanin family proteins: one function for multiple biological roles? Front. Plant Sci. 5.

Brown, N.A., Urban, M., van de Meene, A.M.L., Hammond-Kosack, K.E., 2010. The infection biology of *Fusarium graminearum*: Defining the pathways of spikelet to spikelet colonisation in wheat ears. Fungal Biol. 114, 555-571.

Buensanteai, N., Mukherjee, P.K., Horwitz, B.A., Cheng, C., Dangott, L.J., Kenerley, C.M., 2010. Expression and purification of biologically active *Trichoderma virens* proteinaceous elicitor Sm1 in *Pichia pastoris*. Protein Expr. Purif. 72, 131-138.

Chen, H., Kovalchuk, A., Keriö, S., Asiegbu, F.O., 2013. Distribution and bioinformatic analysis of the cerato-platanin protein family in Dikarya. Mycol. 105, 1479-1488.

Cosgrove, D.J., 2000. Loosening of plant cell walls by expansins. Nature. 407.

Cosgrove, D.J., 2015. Plant expansins: diversity and interactions with plant cell walls. Curr. Opin. Plant Biol. 25, 162-72.

de O Barsottini, M.R., de Oliveira, J.F., Adamoski, D., Teixeira, P.J., do Prado, P.F., Tiezzi, H.O., et al., 2013. Functional diversification of cerato-platanins in *Moniliophthora perniciosa* as seen by

differential expression and protein function specialization. Mol. Plant-Microbe Interact. 26, 1281-1293.

de Oliveira, A.L., Gallo, M., Pazzagli, L., Benedetti, C.E., Cappugi, G., Scala, A., Pantera, B., Spisni, A., Pertinhez, T.A., Cicero, D.O., 2011. The structure of the elicitor Cerato-platanin (CP), the first member of the CP fungal protein family, reveals a double ψβ-barrel fold and carbohydrate binding. J. Biol. Chem. 286, 17560-17568.

Djonović, S., Pozo, M.J., Dangott, L.J., Howell, C.R., Kenerley, C.M., 2006. Sm1, a proteinaceous elicitor secreted by the biocontrol fungus *Trichoderma virens* induces plant defense responses and systemic resistance. Mol. Plant-Microbe Interact. 19, 838-853.

Djonović, S., Vargas, W.A., Kolomiets, M.V., Horndeski, M., Wiest, A., Kenerley, C.M., 2007. A proteinaceous elicitor Sm1 from the beneficial fungus *Trichoderma virens* is required for induced systemic resistance in maize. Plant Physiol. 145, 875-889.

Felix, G., Duran, J.D., Volko, S., and Boller, T., 1999. Plants have a sensitive perception system for the most conserved domain of bacterial flagellin. Plant J. 18, 265-276.

Frías, M., González, C., Brito, N., 2011. BcSpl1, a cerato-platanin family protein, contributes to *Botrytis cinerea* virulence and elicits the hypersensitive response in the host. New Phytol. 192, 483-495.

Frías, M., Brito, N., González, C., 2013. The *Botrytis cinerea* cerato-platanin BcSpl1 is a potent inducer of systemic acquired resistance (SAR) in tobacco and generates a wave of salicylic acid expanding from the site of application. Mol. Plant Pathol. 14, 191-196.

Frías, M., Brito, N., González, M., González, C., 2014. The phytotoxic activity of the cerato-platanin BcSpl1 resides in a two-peptide motif on the protein surface. Mol. Plant Pathol. 15, 342-351.

Gaderer, R., Bonazza, K., Seidl-Seiboth, V., 2014. Cerato-platanins: a fungal protein family with intriguing properties and application potential. Appl. Microbiol. Biotechnol. 98, 4795-4803.

Gaderer, R., Lamdan, N., Frischmann, A., Sulyok, M., Krska, R., Horwitz, B. A., Seidl-Seiboth, V., 2015. Sm2, a paralog of the *Trichoderma* cerato-platanin elicitor Sm1, is also highly important for

plant protection conferred by the fungal-root interaction of *Trichoderma* with maize. BMC Microbiol. 15, 2.

Georgelis, N., Nikolaidis, N., Cosgrove, D.J., 2015. Bacterial expansins and related proteins from the world of microbes. Appl. Microbiol. Biotechnol. 99, 3807-3823.

Georgelis, N., Tabuchi, A., Nikolaidis, N., Cosgrove, D.J., 2011. Structure-function analysis of the bacterial expansin EXLX1. J. Biol. Chem. 286, 16814-16823.

Goswami, R.S., Kistler, H.C., 2004. Heading for disaster: *Fusarium graminearum* on cereal crops. Mol. Plant Pathol. 5, 515-525.

Hong, Y., Yang, Y., Zhang, H., Huang, L., Li, D., Song, F., 2017. Overexpression of *MoSM1*, encoding for an immunity-inducing protein from *Magnaporthe oryzae*, in rice confers broad-spectrum resistance against fungal and bacterial diseases. Sci. Rep. 7, 41037.

Kerff, F., Amoroso, A., Herman, R., Sauvage, E., Petrella, S., Filée, P., Charlier, P., Joris, B., Tabuchi, A., Nikolaidis, N., Cosgrove, D.J., 2008. Crystal structure and activity of *Bacillus subtilis* YoaJ (EXLX1), a bacterial expansin that promotes root colonization. PNAS. 105, 16876-16881.

Kim, I.J., Ko, H.J., Kim, T.W., Nam, K.H., Choi, I.G., Kim, K.H., 2013. Binding characteristics of a bacterial expansin (BsEXLX1) for various types of pretreated lignocellulose. Appl. Microbiol. Biotechnol. 97, 5381-5388.

Laemmli, U.K., 1970. Cleavage of structural proteins during the assembly of the head of bacteriophage T4. Nature. 227, 680-685.

Liu, X., Ma, Y., Zhang, M., 2015. Research advances in expansins and expansion-like proteins involved in lignocellulose degradation. Biotechnol. Lett. 37, 1541-1551.

Lu, S., Edwards, M.C., 2016. Genome-Wide Analysis of Small Secreted Cysteine-Rich Proteins Identifies Candidate Effector Proteins Potentially Involved in *Fusarium graminearum*-Wheat Interactions. Phytopathol. 106, 166-176.

Luti, S., Caselli, A., Taiti, C., Bazihizina, N., Gonnelli, C., Mancuso, S., Pazzagli, L., 2016. PAMP Activity of Cerato-Platanin during Plant Interaction: An -Omic Approach. Int. J. Mol. Sci. 17, 866.

Luti, S., Martellini, F., Bemporad, F., Mazzoli, L., Paoli, P., Pazzagli, L., 2017. A single amino acid mutation affects elicitor and expansins-like activities of cerato platanin, a non-catalytic fungal protein. PLoS One. 12, e0178337.

Marowa, P., Ding, A., Kong, Y., 2016. Expansins: roles in plant growth and potential applications in crop improvement. Plant Cell. Rep. 35, 949-965.

Martellini, F., Faoro, F., Carresi, L., Pantera, B., Baccelli, I., Maffi, D., et al., 2012. Cerato-populin and cerato-platanin, two non-catalytic proteins from phytopathogenic fungi, interact with hydrophobic inanimate surfaces and leaves. Mol. Biotechnol. 55, 27-42.

Nelson, N., 1944. A photometric adaptation of the Somoyi method for the determination of glucose. J. Biol. Chem. 153, 275-280.

O'Donnell, K., Ward, T.J., Geiser, D.M., Kistler, H.C., Aoki, T., 2004. Genealogical concordance between the mating type locus and seven other nuclear genes supports formal recognition of nine phylogenically distinct species within the *Fusarium graminearum* clade. Fungal Genet. Biol. 41, 600-623.

Olarte-Lozano, M., Mendoza-Nuñez, M.A., Pastor, N., Segovia, L., Folch-Mallol, J., MartõÂnez-Anaya, C., 2014. PcExl1 a novel acid expansin-like protein from the plant pathogen *Pectobacterium carotovorum*, binds cell walls differently to BsEXLX1. PLoS One. 9, e95638.

Pazzagli, L., Cappugi, G., Manao, G., Camici, G., Santini, A., Scala, A., 1999. Purification, Characterization, and Amino Acid Sequence of Cerato-platanin, a New Phytotoxic Protein from *Ceratocystis fimbriata* f. sp. *platani*. J. Biol. Chem. 274, 24959-24964.

Pazzagli, L., Seidl-Seiboth, V., Barsottini, M., Vargas, W.A., Scala, A., Mukherjee, P.K., 2014. Cerato-platanins: elicitors and effectors. Plant Sci. 228, 79-87.

Quarantin, A., Glasenapp, A., Schäfer, W., Favaron, F., Sella, L., 2016. Involvement of the *Fusarium graminearum* cerato-platanin proteins in fungal growth and plant infection. Plant Physiol. Biochem. 109, 220-229.

Salas-Marina, M.A., Isordia-Jasso, M.I., Islas-Osuna, M.A., Delgado-Sánchez, P., Jiménez-Bremont, J.F., Rodríguez-Kessler, M., et al., 2015. The Epl1 and Sm1 proteins from *Trichoderma atroviride* and *Trichoderma virens* differentially modulate systemic disease resistance against different life style pathogens in *Solanum lycopersicum*. Front. Plant Sci. 6, 77.

Sampedro, J., Cosgrove, D.J. 2005. The expansin superfamily. Genome Biol. 6, 242.

Sella, L., Gazzetti, K., Faoro, F., Odorizzi, S., D'Ovidio, R., Schäfer, W., Favaron, F., 2013. A *Fusarium graminearum* xylanase expressed during wheat infection is a necrotizing factor but is not essential for virulence. Plant Physiol. Biochem. 64, 1-10.

Sella, L., Gazzetti, K., Castiglioni, C., Schäfer, W., D'Ovidio, R., Favaron, F., 2016. The *Fusarium graminearum* Xyr1 transcription factor regulates xylanase expression but is not essential for fungal virulence. Plant Pathol. 65, 713-722.

Szécsi, A., 1990. Analysis of Pectic Enzyme Zymograms of *Fusarium* species II. Comparison of polygalacturonase zymograms of *Fusarium culmorum* and *Fusarium graminearum*. J. Phytopathol. 130, 188-196.

Vargas, W.A., Djonović, S., Sukno, S.A., Kenerley, C.M., 2008. Dimerization controls the activity of fungal elicitors that trigger systemic resistance in plants. J. Biol. Chem. 283, 19804–19815.

Vogel, J., 2008. Unique aspects of the grass cell wall. Curr. Opin. Plant Biol. 11, 301-307.

Wang, Y., Wu, J., Kim, S.G., Tsuda, K., Gupta, R., Park, S.Y., Kim, S.T., Kang, K.Y., 2016. *Magnaporthe oryzae*-secreted protein MSP1 induces cell death and elicits defense responses in rice. Mol. Plant-Microbe Interact. 29, 299-312.

Wilson, L.M., Idnurm, A., Howlett, B.J., 2002. Characterization of a gene (sp1) encoding a secreted protein from *Leptosphaeria maculans*, the blackleg pathogen of *Brassica napus*. Mol. Plant Pathol. 3, 487-493.

Yang, X.H., Zhu, W.L., 2007. Viscosity properties of sodium carboxymethylcellulose solutions. Cellulose. 14, 409-417.

Yang, Y., Zhang, H., Li, G., Li, W., Wang, X., Song, F., 2009. Ectopic expression of MgSM1, a Cerato-platanin family protein from *Magnaporthe grisea*, confers broad-spectrum disease resistance in *Arabidopsis*. Plant Biotechnol. J. 7, 763-777.

Zhang, Y., Gao, Y., Liang, Y., Dong, Y., Yang, X., Yuan, J., Qiu, D., 2017a. The *Verticillium dahliae* SnodProt1-Like Protein VdCP1 Contributes to Virulence and Triggers the Plant Immune System. Front. Plant Sci. 8, 1880.

Zhang, Y., Liang, Y., Qiu, D., Yuan, J., Yang, X. 2017b. Comparison of cerato-platanin family protein BcSpl1 produced in *Pichia pastoris* and *Escherichia coli*. Protein Expr. Purif. 136:20-26.

Supplementary figure captions

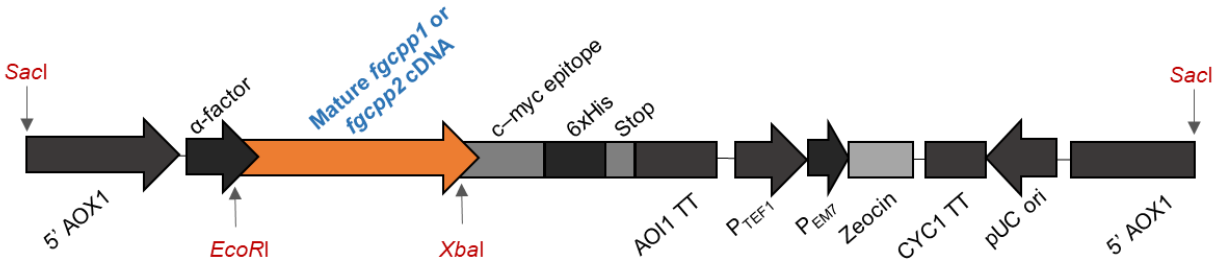

Fig. S2.1. pPICZαA (3.6 Kb) expression vector (Invitrogen Life Technologies, Milano, Italy) containing the *Fusarium graminearum fgcpp1* or the *fgcpp2* cDNAs coding for the mature protein cloned using the *Eco*RI and *Xba*I restriction sites. The vector was linearized for transformation using *Sac*I.

Table S2.1. Oligonucleotide primers used in this study.

Primer name	Sequence (5'-3')
Primers for cloning the *fgcpp1* and *fgcpp2* genes in *Pichia pastoris* (adaptor sequences underscored)	
ORF10212for	ATGAAGTTCACTGGTATCCT
ORF10212rev	TTACTTCTTGAGGCCACA
ORF11205for	ATGCAGCTGACCAACCTC
ORF11205rev	CTATTTCTTCAATCCACAGTTGC
*pPICZαA*10212for	ATGCA GAATTC ACCACTGTCTCCTACGA
*pPICZαA*10212rev	ATGCA TCTAGA TTACTTCTTGAGGCCACA
*pPICZαA*11205for	ATGCA GAATTC GCAATCACCGTATCCTAC
*pPICZαA*11205rev	ATGCA TCTAGA CTATTTCTTCAATCCACAGTTG

Chapter III

Fusarium graminearum hydrophobins are involved in water-air interface penetration, maturation of perithecia and plant infection

Abstract

Hydrophobins (HPs) are small secreted fungal proteins covering the surface of conidia, spores, hyphae and fruiting structures with a hydrophobic layer. HPs may play a role in several processes such as formation of fungal aerial structures, attachment to hydrophobic surfaces, interaction with the environment and protection against the host defense system by masking the fungal cell wall. The genome of the hemi-biotrophic plant pathogen *Fusarium graminearum* contains five genes encoding for hydrophobin proteins, named FgHyd1-5. Expression analysis revealed that the FgHyd3 is dramatically upregulated during initial epiphytical growth on wheat paleas and glumes. Single and triple FgHyd mutants were therefore produced and characterized. A reduced growth was registered when the Δ*hyd2* and all the three triple mutants including the deletion of FgHyd2 were grown in complete or minimal medium. Surprisingly, the reduced growth was recovered when these mutants were grown under osmotic stress conditions or in the presence of H_2O_2. A reduction in the ability of hyphae to penetrate through the water-air interface was observed for the single mutants Δ*hyd2* and Δ*hyd3* as well as the triple mutants including Δ*hyd2* and Δ*hyd3*. Indeed, infection experiments on *Triticum aestivum* showed a reduction of symptomatic spikelets with the Δ*hyd2* and Δ*hyd3* mutants only when spray inoculation was performed, thus indicating that Hyd2 and Hyd3 are involved in adhesion of conidia to the host surface during the early stages of the infection process. This hypothesis is strengthened by a histological analysis, performed by fluorescence microscopy, that showed no differences in the morphology of infection structures produced by wild type and mutant strains during wheat spikelets infection. To verify possible defects at the cell wall level, the mutants were grown in the presence of β-1,3-glucanase and a systemic triazole fungicide containing an ergosterol biosynthesis inhibitor. Results showed that the triple mutants were significantly more inhibited than wild type by β-1,3-glucanase, and one of them was also more susceptible to the fungicide treatment. All the mutant strains confirmed the ability to develop perithecia, but the triple mutants produced a reduced number of mature perithecia, suggesting that the FgHyds could also be involved in the normal development of this sexual structure.

3.1. Introduction

Hydrophobins (HPs) are small secreted cysteine-rich amphiphilic proteins of about 100 amino acids, found only in filamentous fungi (Wessels, 2000; Wösten, 2001). The name hydrophobin was coined after the examination of genes encoding small hydrophobic proteins expressed during fruiting body formation in *Schizophyllum commune* (Wessels et al., 1991a, b). After that, hydrophobins have been identified in several other fungi (Lauter et al., 1992; Beckerman and Ebbole, 1996; Segers et al., 1999; Fuchs et al., 2004; Izumitsu et al., 2010).

HPs are characterised by the presence of eight cysteine residues in their amino acid sequences which are arranged in a conserved pattern and form four disulphide bridges. Nevertheless, HP amino acid sequences usually show a low structural similarity level. HPs have been isolated from Ascomycetes, Basidiomycetes and Zygomycetes as well, and they have been divided into two classes according to their physical properties, which differ in hydropathy patterns and solubility characteristics. Class I hydrophobins have been identified in both Ascomycetes and Basidiomycetes while Class II hydrophobins have been found only in Ascomycetes (Wessels, 1994). Class I and Class II hydrophobins can be distinguished by the amino acids spacing between the cysteine residues, which is more conserved in the Class II hydrophobins (Kershaw and Talbot, 1998).

Secreted as protein monomers, HPs are able to self-assemble at water-air interphases in response to the environment and to aggregate to amphipathic membranes (Wösten et al., 1999). Although proteins of either Classes are able to form stable aggregates, the Class I hydrophobins form aggregates that can only be dissolved in strong acids (Wessels et al., 1991a; de Vries et al., 1993), while the Class II hydrophobins aggregates can be easily dissolved in aqueous dilutions of organic solvents (Wösten and de Vocht, 2000). Nevertheless, so far, the biological meaning of this prediction remains unclear. By self-assembling at the water-air interphases (Wösten and de Vocht, 2000), HPs would allow fungi to escape their aqueous environment. Indeed, HPs attach to the surface of the hydrophilic cell wall polysaccharides of conidia, spores, hyphae and fruiting structures, where they occur exclusively (Wessels, 1997; Wösten et al., 1999; Wösten et al., 2001), and expose the hydrophobic layer to the

outside, conferring water-repellent properties to these fungal surfaces (Wösten et al., 1994; Kershaw and Talbot, 1998; Wösten, 2001). In fact, several fungal mutants have been described to show "easily wettable" phenotypes, indicating that hydrophobins confer surface hydrophobicity to aerial hyphae and spores (Mosbach et al., 2011).

In aerial conidia and hyphae, this hydrophobic coating has been also proposed to have a protecting role both against desiccation and wetting, also aiding dispersal of conidia (Wösten, 2001; Whiteford and Spanu, 2001 and 2002; Klimes and Dobinson, 2006). Furthermore, HPs could also be involved in many morphogenetic processes, including conidia germination, fruit body development, infection structure formation, attachment of fungi to solid supports and fungal pathogenicity (Talbot et al., 1996; Whiteford and Spanu, 2001; Paananen et al., 2003; Kim et al., 2005; Klimes et al., 2006).

The role of hydrophobins has been characterized in several fungal pathogens. The Class I Mpg1 hydrophobin of the rice blast fungus *Magnaporthe oryzae* is important for efficient conidiogenesis and for pathogenicity on host plants (Talbot et al., 1993) and is required for attachment to the leaf surface (Talbot et al., 1996; Whiteford and Spanu, 2002). Indeed, the ΔMpg1 mutant have impaired ability to form appressoria, probably due to the inability of the germ tubes to firmly attach to the hydrophobic plant cuticle and to appropriately sense surface features (Talbot et al., 1993). Besides, the Class II hydrophobin of *M. oryzae*, named MHP1, is required for conidial development and viability and for surface hydrophobicity; indeed, the Δmhp1 mutant show a reduced appressorium formation and thus a significant reduction in pathogenicity (Kim et al., 2005). The *Botrytis cinerea* genome contains three gene encoding for hydrophobins, one (Bhp1) belonging to Class I and two (Bhp2 and Bhp3) to Class II. While Izumitsu et al. (2010) attributed a role for Hpb1 in conidia hydrophobicity and adhesion to hydrophobic surfaces, Mosbach et al. (2011) showed that the *B. cinerea* hydrophobins are neither involved in conferring surface hydrophobicity to conidia and aerial hyphae, nor they are required for virulence. Finally, Terhem et al. (2014) demonstrated that sclerotia produced by a double knock-out mutant (ΔBhp1/ΔBhp3) and by a triple knock-out mutant were "easily wettable", thus indicating that both Class I and Class II hydrophobins are involved in normal

development of *B. cinerea* apothecia. In *Aspergillus nidulans* two hydrophobins named RodA and DewA, have been shown to contribute to conidiospore surface hydrophobicity (Grunbacher et al., 2014). Differently, the deletion of the hydrophobin encoding gene of the rye pathogen *Claviceps purpurea* (cpph1) did not lead to differences compared to wild type (Mey et al., 2003).

The genome of the plant pathogen *Fusarium graminearum*, a hemi-biotrophic fungus causing the *Fusarium* head blight (FHB) disease of wheat, barley and other cereal grains, contains five different genes encoding for hydrophobin proteins, named FgHyd1-5. Four of them were predicted to belong to Class I hydrophobins while the FgHyd5 seems to be the only gene coding for a Class II hydrophobin (Sarlin et al., 2012). So far, only the role of the FgHyd5 has been investigated, showing that it does not affect colony and hyphal morphology, it is not involved in the penetration of hyphae through the water-air interface but affects the hydrophobicity of aerial mycelia (Minenko et al., 2014). Therefore, to fully characterize the role played by the *F. graminearum* hydrophobins in fungal growth and plant infection, single and triple mutants of the five genes have been produced and characterized in vitro and in vivo.

3.2. Materials and methods

3.2.1. Sequences analysis and primer design

The genome of *Fusarium graminearum* (Cuomo et al., 2007; MIPS database, http://mips.helmholtz-muenchen.de/genre/proj/fusarium/) contains five genes encoding for Class I and Class II hydrophobin proteins (NCBI database entries: FGSG_01763: FgHyd1, FGSG_01764: FgHyd2, FGSG_09066: FgHyd3, FGSG_03960: FgHyd4 and FGSG_01831: FgHyd5) (Minenko et al., 2014).

Prediction of signal peptides (SP) and hydrophobin conserved domains were performed by SMARTanalysis tool (http://smart.embl-heidelberg.de/) and Motif Scan (MyHits, SIB, Switzerland; http://myhits.isb-sib.ch/cgi-bin/motif_scan), respectively. The five *F. graminearum* hydrophobin proteins were aligned and compared with the already characterized hydrophobins of different Ascomycetes species using the Clustal W program, with the default settings for multiple alignments. A phylogenetic analysis was performed using BOOTSTRAP Neighbour Joining model TREE (1000) with MEGA 5 software.

The hydropathy score was calculated with ProtScale software (http://expasy.org/tools/) by using the Kyle and Doolittle aa scale. All the primers used were designed by using PRIMER3 (http://primer3.ut.ee/) and PerlPrimer v.1.1.17 softwares (Table S3.1).

3.2.2. Fungal strains and growth analysis

The *F. graminearum* wild type (WT:8/1) and the mutant strains used are listed in Table 3.1. Conidia were obtained by culturing the fungal strains in carboxymethyl cellulose sodium salt (CMC; Sigma-Aldrich), as reported in Sella et al. (2016), or wheat medium. For this latter, briefly, 1 L of water containing 15 g of wheat stems and leaves, finely cut, was autoclaved, filtered and autoclaved again; three mL aliquots were inoculated with 10 µL of fungal conidia and incubated with shacking in the dark at 28 °C for three or four days. Conidia were recovered by centrifugation, re-suspended with 1 mL of distilled water and counted with a haemocytometer under a microscope.

Colony morphologies of the fungal strains were analyzed inoculating Complete (CM) and Minimal medium (MM) plates (9-cm diameter) with actively growing mycelium agar plugs. Color and properties of aerial mycelia were visually determined.

3.2.3. Transcriptomic analysis

The expression of the five *F. graminearum* hydrophobin genes was analysed by transcriptomic analysis at the Laboratory of Molecular Phytopathology and Genetics, Biocenter Klein Flottbek, University of Hamburg. RNA was obtained from *F. graminearum* mycelium grown for 3 days on CM medium and from infection cushions and runner hyphae collected from wheat palea and glume tissues previously infected with the fungus (A.L. Martínez-Rocha, personal communication).

3.2.4. Single and triple knock-out mutants production

The constructs to produce single and triple knock-out mutants of the five FgHyd genes by homologous recombination have been generated as reported in Quarantin et al. (2016) by using the oligonucleotides reported in Table S3.1 (see also Fig. S3.1A-E for schemes of the constructs produced). The plasmids used or generated in this work are reported in Table S3.2. The *F. graminearum* strains generated and used in this work and the selection markers used for each construct are reported in Table 3.1. Protoplast preparation and fungal transformation were performed according to van Nguyen et al. (2012). Selection of fungal transformed colonies was performed as reported by Quarantin et al. (2016) using the corresponding antibiotics (Table 3.1). The generation of the single FgHyd knock-out mutants constitutively expressing the green fluorescent protein (GFP) was performed as reported by Martínez-Rocha et al. (2016) by transforming a WT strain constitutively expressing GFP with the FgHyd deletion constructs (Table 3.1). Resistant mutants were single-conidiated and screened by PCR using the primer pairs reported in Table S3.1. Transformants were then confirmed by Southern blot hybridization (A.L. Martínez-Rocha, personal communication) with probes obtained using the primers reported in Table S3.1.

Table 3.1. *Fusarium graminearum* strains generated and used in this work.

Nr	Strain	Transformation Number	Resistance cassette	Reference
1	FgWT 8/1			Miedaner et al., 2000
2	FgWT 8/1 GFP constitutive	#600.25.	HygB	Jansen et al., 2005
3	FgWT 8/1 GFP constitutive		NptII	Martínez-Rocha et al., 2016
	Single knock-out			
4	Δ*hyd1* (FGSG_01763)	#1801.14.	HygB	This study
5	Δ*hyd2* (FGSG_01764)	#1661.3.1.	NptII	This study
6	Δ*hyd3* (FGSG_09066)	#1640.3.	Nat1	This study
7	Δ*hyd4* (FGSG_03960)	#1653.34.	HygB	This study
8	Δ*hyd5* (FGSG_01831)	#1652.28.	HygB	This study
	Double knock-out			
9	Δ*hyd3,2*	#1733.7.	Nat1/NptII	This study
10	Δ*hyd3,4*	#1734.6.	Nat1/HygB	This study
11	Δ*hyd3,5*	#1732.6.	Nat1/HygB	This study
	Triple knock-out			
12	Δ*hyd1,2,3*	#1802.4.	Nat1/HygB/NptII	This study
13	Δ*hyd2,3,4*	#1745.4.	Nat1/HygB/NptII	This study
14	Δ*hyd2,3,5*	#1748.3.	Nat1/HygB/NptII	This study
	Single knock-out GFP constitutive			
15	Δ*hyd2* GFP constitutive	#1697.4.	NptII/HygB	This study
16	Δ*hyd3* GFP constitutive	#1695.1.	Nat1/HygB	This study
17	Δ*hyd4* GFP constitutive	#1698.2.	HygB/NptII	This study
18	Δ*hyd5* GFP constitutive	# 1696.4.	HygB/NptII	This study

HygB = Hygromycin

Nat1 = Nourseothricin acetyltransferase

NptII = Neomycin phosphotransferase

Jansen, C., Von Wettstein, D., Schäfer, W., Kogel, K.H., Felk, A., Maier, F.J., 2005. Infection patterns in barley and wheat spikes inoculated with wild-type and trichodiene synthase gene disrupted *Fusarium graminearum*. PNAS, 102, 16892-16897.

Martínez-Rocha, A.L., Woriedh, M., Chemnitz, J., Willingmann, P., Kröger, C., Hadeler, B., Hauber, J., Schäfer, W., 2016. Posttranslational hypusination of the eukaryotic translation initiation factor-5A regulates *Fusarium graminearum* virulence. Sci. Rep. 6, 24698.

Miedaner, T., Reinbrecht, C., Schilling, A.G., 2000. Association among aggressiveness, fungal colonization, and mycotoxin production of 26 isolates of *Fusarium graminearum* in winter rye head blight. J. Plant Dis. Protect. pp.124-134.

3.2.5. Penetration of fungal hyphae through the air-liquid barrier

The ability of the *F. graminearum* WT and mutant strains hyphae to penetrate through the water-air interface was tested by placing a 5 µL drop of conidia (containing about 2,500 conidia) re-suspended in CM liquid medium on Petri dishes. Inside each plate, a smaller plate (3-cm diameter) containing water was inserted to maintain humidity condition. Plates were incubated at 28 °C in the dark up to 48 hours (h) until observing aerial hyphae growing out of the drops. Pictures were taken after 36 and 48 h with Leica stereo microscope.

3.2.6. Stress response assays

Stress response assays were prepared by adding KCl or sorbitol to CM or MM (final concentration 750 mM and 1.5 M, respectively) prior to autoclaving, while hydrogen peroxide (H_2O_2, final concentration 30 mM) was added to autoclaved CM and MM after cooling to 55 °C. Agar plates were inoculated with agar plugs containing actively growing mycelia of WT or single and triple mutant strains and incubated at 28 °C in the dark. Colony diameters were measured every 24 h up to 3 days. Each assay was performed with three replicates per each strain and the experiments were repeated at least three times.

3.2.7. Calcofluor White assay

To verify possible chitin defects at the cell wall level, CM or MM plates supplemented after autoclaving with 50 µg mL^{-1} of Calcofluor White (CFW) were inoculated with actively growing mycelia plugs of the *F. graminearum* WT, single and triple mutant strains. Plates were incubated at 28 °C in the dark to prevent possible inactivation of CFW by light. The susceptibility to CFW was estimated by measuring colony diameters every 24 h up to 3 days. The assay was performed with three replicates per each strain and the experiments were repeated at least three times.

3.2.8. Inhibition of fungal growth by β-1,3-glucanase treatment

Agar plugs containing actively growing mycelia of *F. graminearum* WT, single and triple hydrophobin mutant strains were inoculated in the middle of CM or MM agar plates. After 2 days of growth at 28 °C in the dark, 8 U of a β-1,3-glucanase enzymatic solution from *Trichoderma longibrachiatum* were loaded on 5 mm diameter wells produced in the agar exactly at 1 cm from the actively growing mycelia. The plates were further incubated at the same conditions, monitored and photographed up to 48 h after the onset of treatment. The β-1,3-glucanase solution was filtered with a 0.22 µm membrane filter prior to application. Three replicates were performed for each strain.

3.2.9. Tebuconazole inhibition assay

To investigate a possible alteration at the plasma membrane in the hydrophobin mutants, a 5 µL drop containing 500 conidia of the *F. graminearum* WT, single and triple mutant strains was added on CM or MM agar plates supplemented with 0.01 µg mL^{-1} of Folicur (Bayer), a systemic triazole fungicide containing the active substance Tebuconazole, an ergosterol biosynthesis inhibitor. Plates were incubated in the dark at 28 °C and the inhibition effect was determined by measuring the radial growth after 4 days of growth. The assay was repeated five times, each one including three replicates per strain.

3.2.10. Perithecia viability assay

To investigate a possible role of the *F. graminearum* hydrophobins in the sexual reproduction of the fungus, five wheat stems autoclaved twice containing a node in the middle were laid in water agar plates (1.6% w/v). Nodes were inoculated with a 10 µL drop containing 1,000 conidia of the *F. graminearum* WT, single and triple mutant strains. Plates were incubated in a UV chamber up to 3 months to induce perithecia production. Perithecia were examined with Leica stereo microscope. The assay was repeated three times with at least three replicates per each strain.

3.2.11. Pathogenicity assays on wheat plants

Wheat plants (*Triticum aestivum* cv. Nandu and Amaretto) were grown as reported in Paccanaro et al. (2017). Point inoculation experiments of wheat spikes were performed at anthesis (Zadoks stage 65 to 67; Zadoks et al., 1974) on cv. Nandu by pipetting 10 µL of a fresh conidial suspension containing approximately 200 conidia of the *F. graminearum* WT, single and triple hydrophobin mutant strains between the glumes of two florets of two opposite central spikelets.

The Δ*hyd2* and Δ*hyd3* mutant strains were also tested with the WT strain on cv. Nandu and Amaretto wheat spikes by spray inoculation to identify differences in the ability of conidia to attach to the wheat spike surface. In this case, each spike was sprayed twice (one spray per side) with approximately 50,000 conidia. At least three independent infection experiments were performed by inoculating at least 10 plants with each strain.

In both infection methods, after inoculation the spikes were covered for 3 days with a plastic bag to maintain a moist environment. Disease symptoms were assessed up to 21 days post inoculation (dpi) by counting the number of visually diseased spikelets and by relating them to the total number of spikelets of the respective head, resulting in a percentage of symptomatic spikelets. Data were statistically analyzed by applying the ANOVA Tukey-Kramer test.

3.2.12. Fluorescence microscopy

Wheat glumes, collected from flowering spikes (cv. Nandu) and washed in water and in 0.01% (v/v) Tween 20 for 20 min, were laid on 1.6% (w/v) water agar plates and inoculated with 10 µL of a fresh conidial suspension containing approximately 500 conidia of the *F. graminearum* WT or single hydrophobin mutant strains expressing the GFP. Plates were incubated in the dark at 28 °C for 6 days. Infection structures produced on paleas by WT and single mutants were investigated by fluorescence microscopy as reported in Quarantin et al. (2016) with some modifications; in details, GFP was detected with an excitation of 488 nm and emission of 500-509 nm, while autofluorescence of the plant was exited at 405 nm and detected at 410-490 nm. Detection of infection structures was

performed using the Zeiss LSM 780 laser scanning microscope (CLSM). Images were taken with Zeiss AxioCam MRm CCD camera.

3.3 Results

3.3.1. Sequence analysis and phylogenetic relationships of the F. graminearum *hydrophobins*

The *F. graminearum* genome contains five hydrophobin encoding genes (FgHyd1: FGSG_01763; FgHyd2: FGSG_01764; FgHyd3: FGSG_09066; FgHyd4: FGSG_03960 and FgHyd5: FGSG_01831) showing similarity with known hydrophobin sequences. Their amino acidic sequences present a signal peptide and eight or nine cysteines in a conserved array (Fig. 3.1). The predicted hydrophobin domain has been identified only in four proteins, with the FgHyd2 showing a *Dictyostelium* repeat as putative Pfam domain (Fig. 3.1). In particular, the FgHyd3, FgHyd4 and FgHyd5 include a higher number of hydrophobic residues (Fig. 3.2).

Phylogenetic analysis of known Ascomycetes hydrophobin proteins, including the five predicted *F. graminearum* hydrophobins, revealed an expected distribution of the proteins into two clades, corresponding to the two Classes of hydrophobins. Four of them (FgHyd1, FgHyd2, FgHyd3 and FgHyd4) belong to the Class I clade, while only the FgHyd5 is included in the Class II clade (Fig. 3.3).

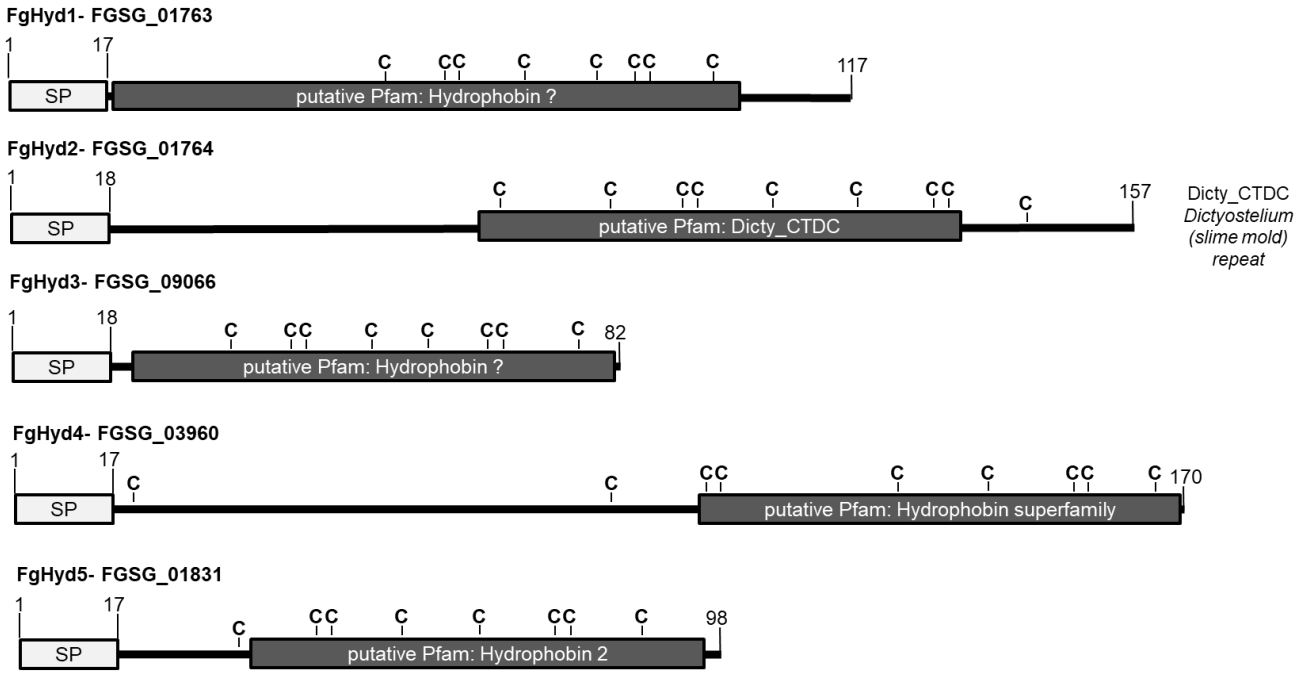

Fig. 3.1. Domain structure of the *Fusarium graminearum* putative hydrophobin proteins. Prediction of signal peptides (SP) was performed by "SignalP" analysis tool. The conserved cysteine residues are reported on the

protein sequences and are indicated with the “C” letter. Prediction of hydrophobin domains was performed using “Motif Scan” (MyHits, SIB, Switzerland).

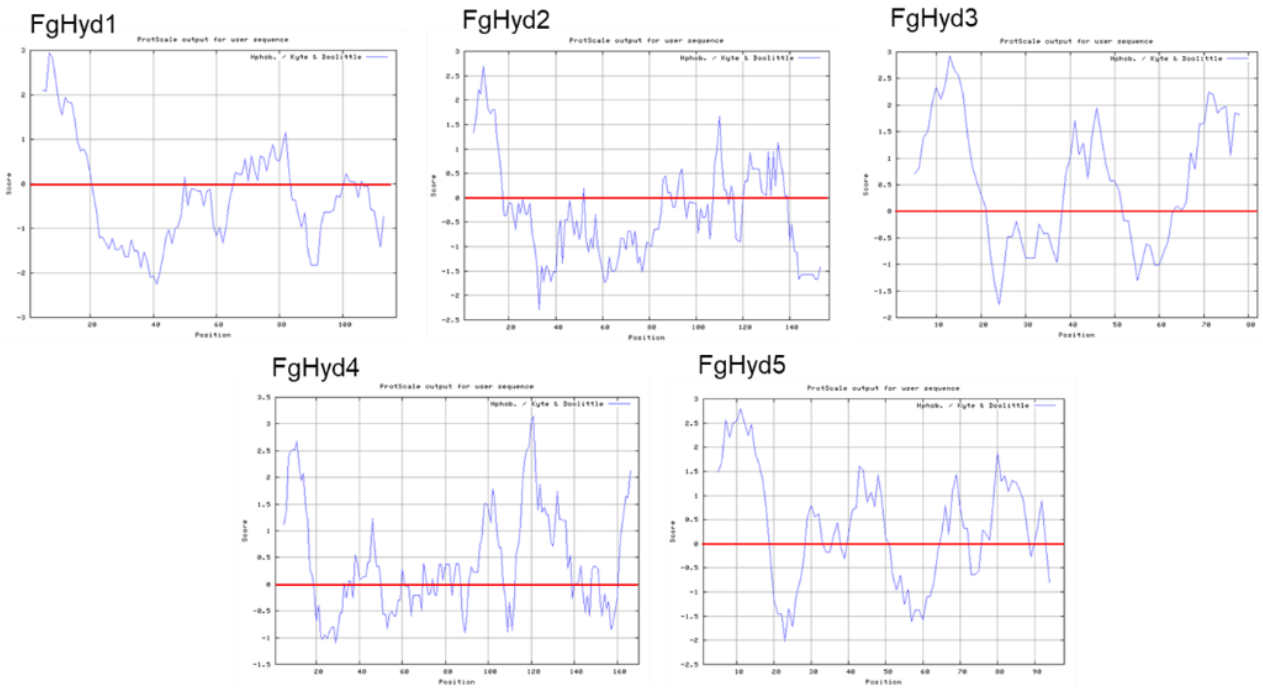

Fig. 3.2. Hydropathy plots of the *Fusarium graminearum* Hyd amino acid (aa) sequences. The hydropathy score was calculated with ProtScale software (http://expasy.org/tools/) by using the Kyle & Doolittle aa scale. Hydrophobic aa show positive peaks with values above 0 whereas hydrophilic aa show negative peaks.

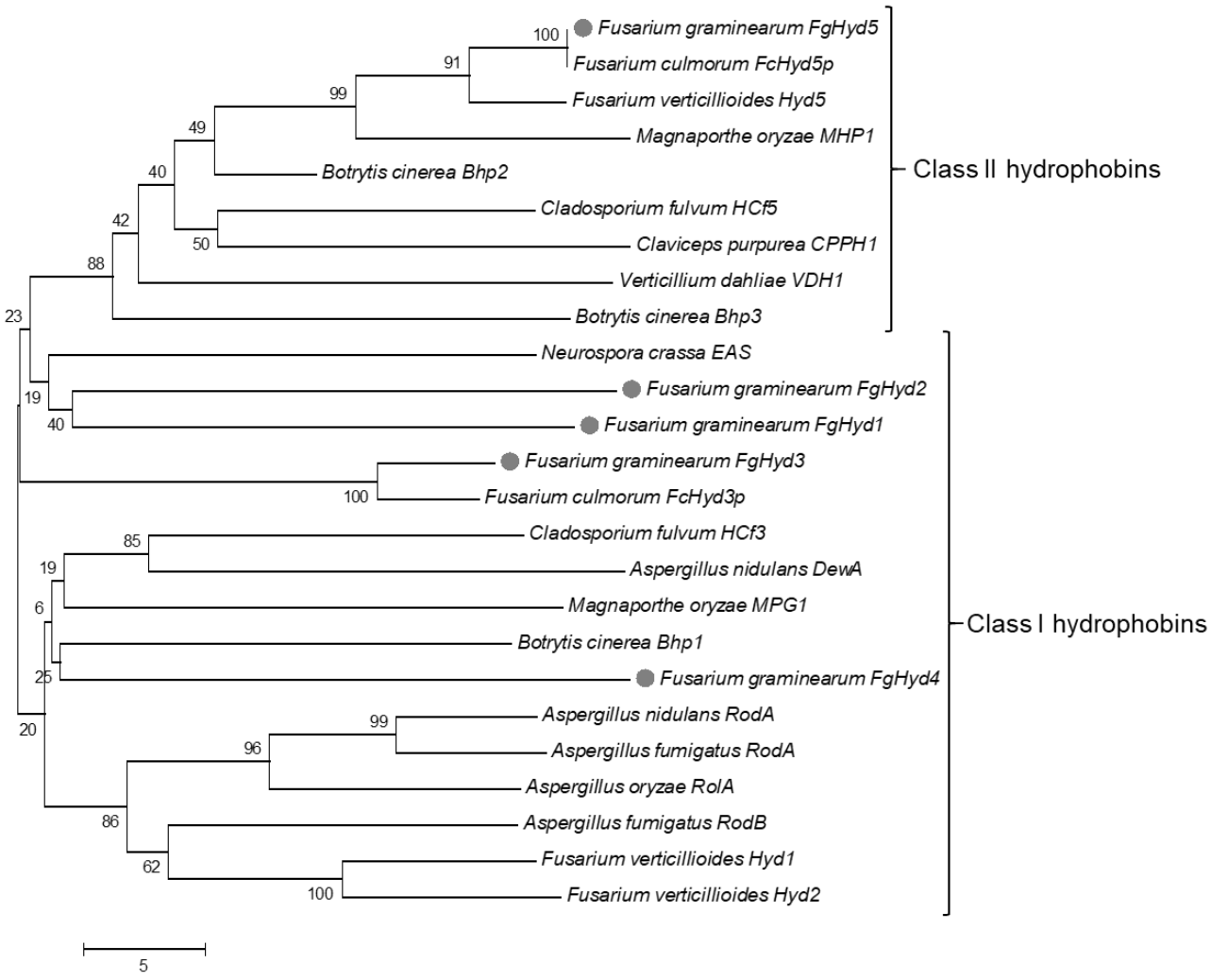

Fig. 3.3. Phylogenetic tree of the *Fusarium graminearum* hydrophobin proteins and the hydrophobins of different Ascomycetes plant pathogens. The Neighbour Joining model was built using MEGA 5 software. Robustness of the generated tree was determined using 1000 bootstrap replicates. Bootstrap values are provided at the beginning of each branch and are given as a percentage. The fungal proteins used are: *Cladosporium fulvum* HCf3 (CAD92803); *C. fulvum* HCf5 (CAC27408); *Fusarium graminearum* FgHyd1 (FGSG_01763); *F. graminearum* FgHyd2 (FGSG_01764); *F. graminearum* FgHyd3 (FGSG_09066); *F. graminearum* FgHyd4 (FGSG_03960); *F. graminearum* FgHyd5 (FGSG_01831); *F. verticillioides* Hyd1 (Q6YF32); *F. verticillioides* Hyd2 (Q6YF31); *F. verticillioides* Hyd5 (Q6YD93); *Botrytis cinerea* Bhp1 (BC1G_15273); *B. cinerea* Bhp2 (BC1G_03994); *B. cinerea* Bhp3 (BC1G_01012); *Aspergillus oryzae* RolA (BAC65230.1); *Verticillium dahliae* VDH1 (AAY89101.1); *Magnaporthe oryzae* MPG1 (P52751); *M. oryzae* MHP1 (AAD18059); *F. culmorum* FcHyd3p (ABE27987.1); *F. culmorum* FcHyd5p (ABE27986.1); *Neurospora crassa* EAS (EAA34064.1); *Claviceps purpurea* CPPH1 (CAD10781.1); *Aspergillus nidulans* RodA (AAA33321.1); *A. nidulans* DewA (AAC13762.1); *A. fumigatus* RodA (AAB60712.1) and *A. fumigatus* RodB (EAL91055.1). The corresponding accession numbers were obtained from the NCBI database (http://www.ncbi.nlm.nih.gov/).

3.3.2. Expression of the F. graminearum *hydrophobins during fungal growth and wheat infection*

The expression of the five *F. graminearum* hydrophobin genes was analysed on the mycelium grown up to 3 days on CM medium and on infection cushions and runner hyphae during infection of wheat palea and glume tissues. The FgHyd3 encoding gene resulted dramatically upregulated during fungal growth and during the initial epiphytical growth on wheat flower leaves. Furthermore, also FgHyd2 and FgHyd4 were clearly expressed in both mycelium and wheat tissues, although at lower level compared to FgHyd3 (Table 3.2); differently, the other two hydrophobin genes showed a low transcript level in both conditions (Table 3.2).

		CM 3 dpi	**Palea**		**Glume**	
Gene name	**Gene code**	**MY**	**IC**	**RH**	**IC**	**RH**
FgHyd1	FGSG_01763	0.0	0.6	0.0	0.1	14.7
FgHyd2	FGSG_01764	14.9	42.1	44.6	39.6	229.3
FgHyd3	FGSG_09066	957.9	51037.7	61273.1	88334.1	459929.0
FgHyd4	FGSG_03960	80.7	43.8	111.1	13.1	49.8
FgHyd5	FGSG_01831	11.936	0.5	0.0	0.2	6.9

Table 3.2. Transcriptomic data of the five *Fusarium graminearum* hydrophobin genes. The analysis was performed during fungal growth (MY: mycelium) on Complete Medium (CM) at 3 days post inoculation (dpi) and during wheat spike infection on infection cushions (IC) and runner hyphae (RH) collected from palea and glume tissues (A.L. Martínez-Rocha, personal communication).

3.3.3. Production of single and triple disruption mutants of F. graminearum *hydrophobin genes*

The five *F. graminearum* hydrophobin genes were individually disrupted by targeted homologous recombination at the Laboratory of Molecular Phytopathology and Genetics, Biocenter Klein Flottbek, University of Hamburg, and the obtained single mutants were analysed by PCR (Fig. S3.1A-E) and Southern blot analysis (Fig. S3.3A-B and A.L. Martínez-Rocha, personal communication) to confirm the deletion of the genes of interest. By combining the constructs with different antibiotic resistance, the triple knock-out mutants Δ*hyd1,2,3* and Δ*hyd2,3,4* and Δ*hyd2,3,5* were also produced and confirmed as above reported (Fig. S3.2A-C, Fig. S3.3A-B and A.L. Martínez-Rocha, personal communication).

3.3.4. The deletion of FgHyd2 reduces mycelia growth

In order to investigate the effect of the deletion of the five hydrophobin genes on fungal growth, the *F. graminearum* WT and the deletion mutant strains were inoculated on CM and MM and incubated up to 10 days. No significant difference in the visual appearance of mycelia was observed in the early stages of growth; mutants retained the ability to form radial colonies and the mycelia appeared white with the production of aerial hyphae (Fig. 3.4). Interestingly, the Δ*hyd2* single mutant and all the three triple mutants including the deletion of FgHyd2 presented a reduced growth compared to the WT strain and the other single mutants (Fig. 3.4).

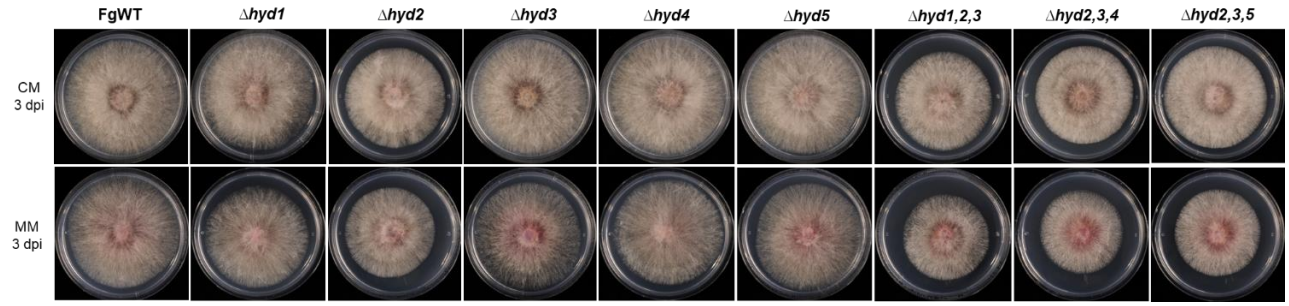

Fig. 3.4. *Fusarium graminearum* wild type (FgWT:8/1) and hydrophobin knock-out mutants grown on Complete (CM) and Minimal Medium (MM) for 3 days at 28 °C in the dark. The same result was observed at 10 days of growth. The assay was repeated 3 times with similar results.

Independently from the medium used (CMC or wheat medium), no significant differences were observed between the WT and all the mutant strains in the number and the germination capacity of conidia (data not shown).

3.3.5. Mutants without FgHyd2 recover their growth under osmotic and oxidative stress

The importance of the hydrophobins in stress responses was assessed by examining the ability of mutant strains to respond to different environmental conditions such as hydrogen peroxide (H_2O_2), KCl and the osmotic stabilizer sorbitol, which is able to reduce cellular turgor pressure.

Under ionic (KCl 750 mM) and non-ionic (sorbitol 1.5 M) osmotic stress conditions, the growth increase of the Δ*hyd2* single mutant and all the triple mutant strains was higher than the WT (Fig. 3.5

and Fig. S3.4). Under oxidative (H_2O_2 30 mM) stress condition, the growth of the Δ*hyd2* single mutant and all the triple mutant strains was less affected than the WT compared to their growth on CM (Fig. 3.6 and Fig. S3.5). Taken together, these results indicate that these mutants recover their growth under stress conditions. The same results were obtained on MM (data not shown).

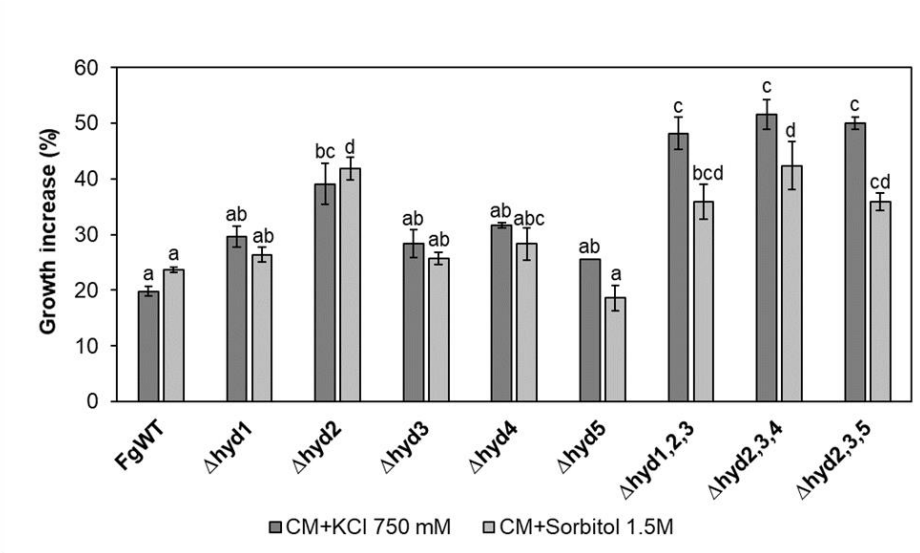

Fig. 3.5. Ionic and non-ionic osmotic stress-response phenotypes. Percentage of growth increase of the *Fusarium graminearum* wild type (FgWT:8/1), single and triple mutant strains in Complete Medium (CM) containing 750 mM KCl or 1.5 M Sorbitol. Data were analyzed by the ANOVA Tukey-Kramer test. Different letters (a, b, c, d) indicate significant differences at $P<0.05$. Data represent the mean of three independent experiments.

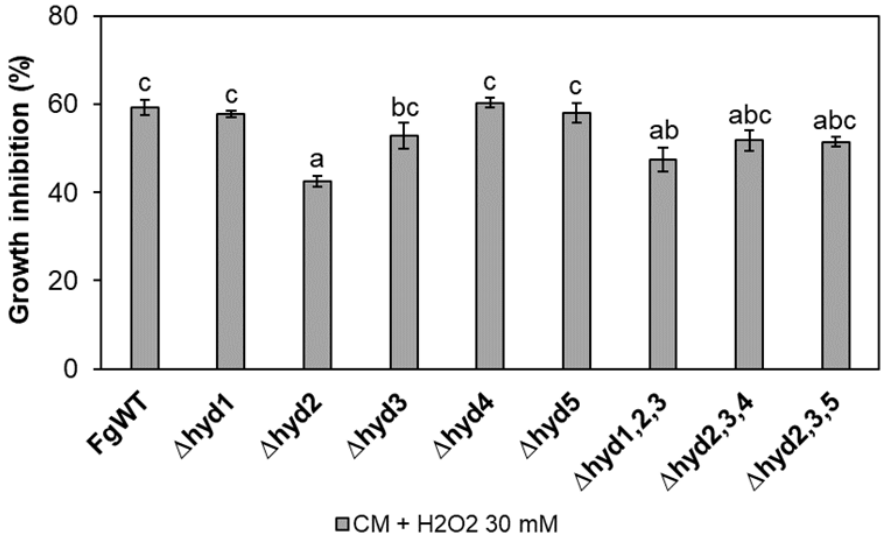

Fig. 3.6. Oxidative stress-response phenotype. Percentage of growth inhibition of the *Fusarium graminearum* wild type (FgWT:8/1), single and triple mutant strains in Complete medium (CM) containing 30 mM H_2O_2. Data were analyzed by the ANOVA Tukey-Kramer test. Different letters (a, b, c) indicate significant differences at $P<0.05$. Data represent the mean of three independent experiments.

3.3.6. The deletion of FgHyd2 and FgHyd3 affects hyphal ability to penetrate the water-air interface

A drop assay performed to evaluate the hydrophobicity of the hyphal surface showed a reduction of aerial hyphae production through the CM liquid medium for the Δ*hyd2*, Δ*hyd3* and the triple mutants (especially Δ*hyd1,2,3* and Δ*hyd2,3,4*), thus indicating a lower ability of the hyphae to penetrate the water-air interface and a possible contribution of these two proteins to the surface hydrophobicity of the *F. graminearum* aerial mycelia (Fig. 3.7).

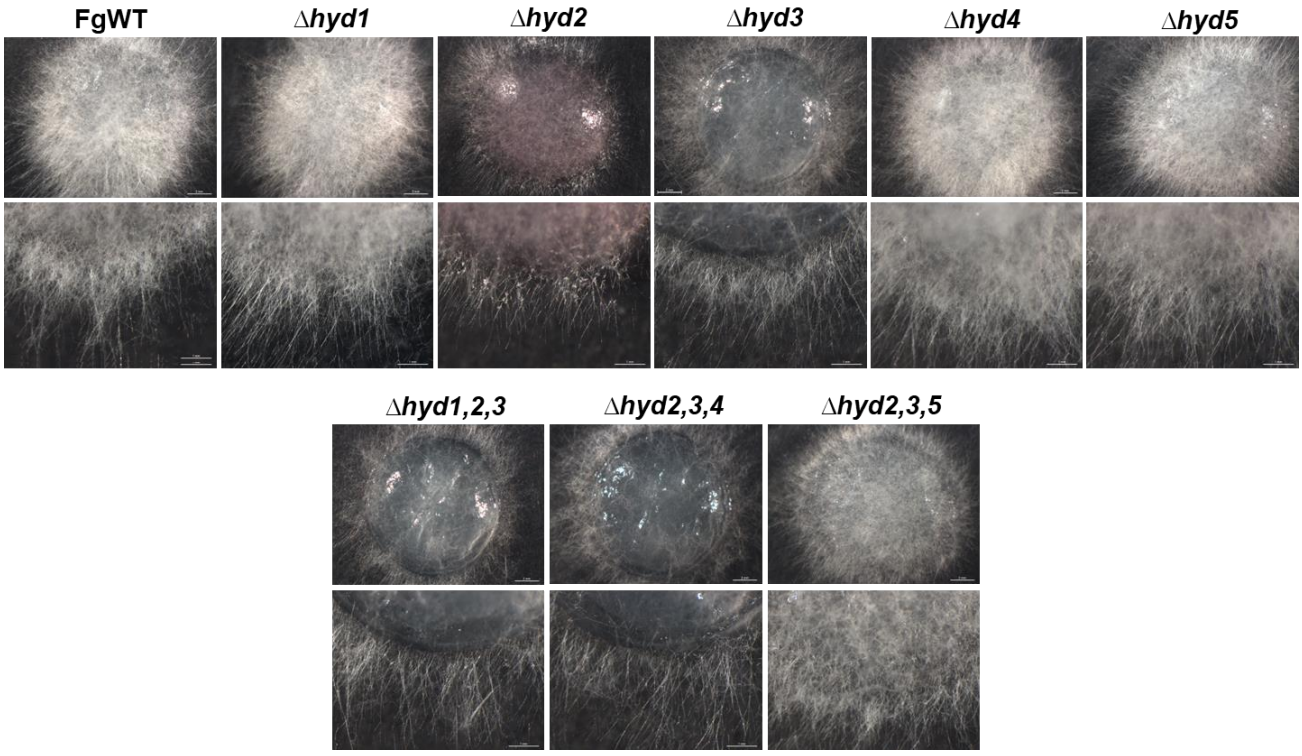

Fig. 3.7. Penetration of hyphae through the air-liquid interface. Drops of conidia (500 conidia/5 µL) of the *Fusarium graminearum* wild type (FgWT:8/1), single and triple hydrophobin mutants diluted in Complete liquid medium (CM) were put on plates and incubated at 28 °C in the dark up to 48 h. Pictures were taken with Leica stereo microscope at 36 h.

3.3.7. FgHyd2 and FgHyd3 are involved in adhesion of conidia to wheat spikes during the early stages of the infection process

To investigate whether the *F. graminearum* hydrophobins are involved in pathogenicity, point inoculations of wheat spikes (cv. Nandu) with the WT, single and triple mutant strains were

performed. At 21 dpi all the mutants showed full virulence as the WT strain (Fig. S3.6 and data not shown).

To further clarify the role of *F. graminearum* hydrophobins in the adhesion of conidia to wheat spikes tissues, spray inoculation with the Δ*hyd2* and Δ*hyd3* mutants, deleted of the genes shown to contribute to surface hydrophobicity and highly expressed during wheat infection, were performed. On cv. Nandu, the Δ*hyd2* and Δ*hyd3* mutants show, respectively, about 33% and 28% reduction of symptomatic spikelets at 21 dpi (Fig. 3.8A and Fig. S3.7). A similar result was obtained by spray inoculating cv. Amaretto wheat spikes, with about 25% reduction of symptomatic spikelets at 21 dpi (Fig. 3.8B). Taken together, these results indicate that Hyd2 and Hyd3 are involved in adhesion of conidia to the host surface.

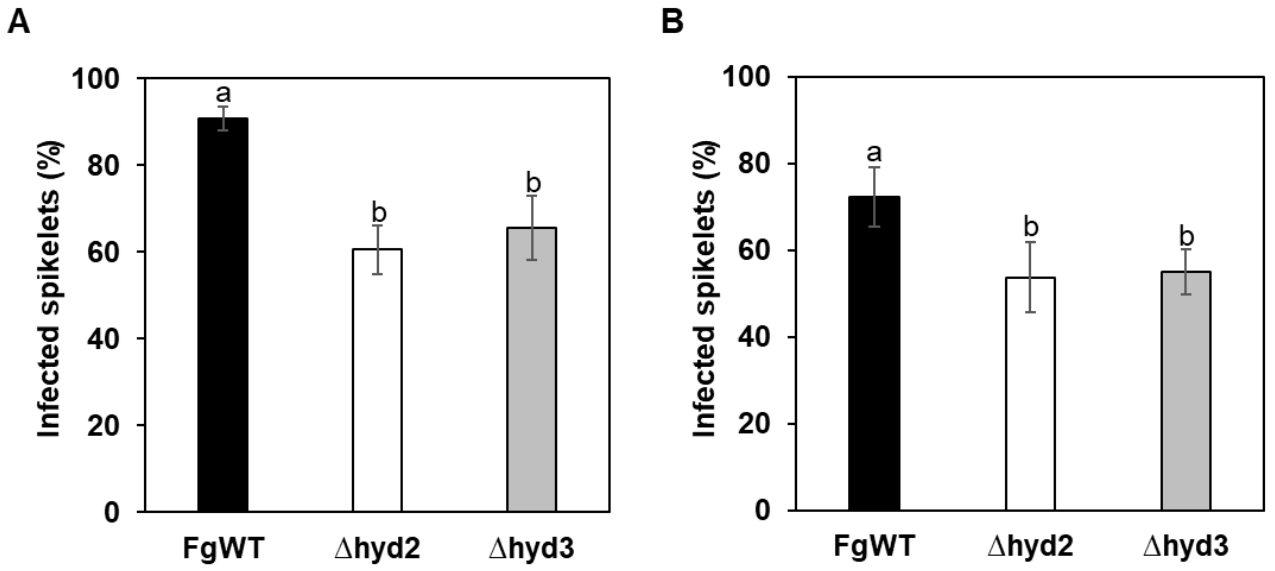

Fig. 3.8. Spray inoculation on cv. Nandu (A) and cv. Amaretto (B) wheat spikes were performed with the *Fusarium graminearum* wild type (FgWT:8/1), Δ*hyd2* and Δ*hyd3* single mutants. Two-100 µL sprays of a solution containing 500 conidia μL^{-1} were used. Disease symptoms were assessed at 21 days post inoculation (dpi) by counting the number of visually diseased spikelets. Infected spikelets are expressed as percentage of symptomatic spikelets on total number of spikelets of the respective head. Data represent the mean ± standard error (indicated by bars) of at least three independent infection experiments. Data were statistically analyzed by the ANOVA Tukey-Kramer test. Different letters (a, b) indicate significant differences at $P<0.05$.

A histological analysis was also performed by inoculating wheat paleas with a spore suspension of *F. graminearum* WT and single mutant strains constitutively expressing GFP. Fluorescence microscopy

performed at 6 days post infection showed that, compared to WT, mutants were able to produce normal infection structures such as infection cushions (Fig. 3.9 and data not shown).

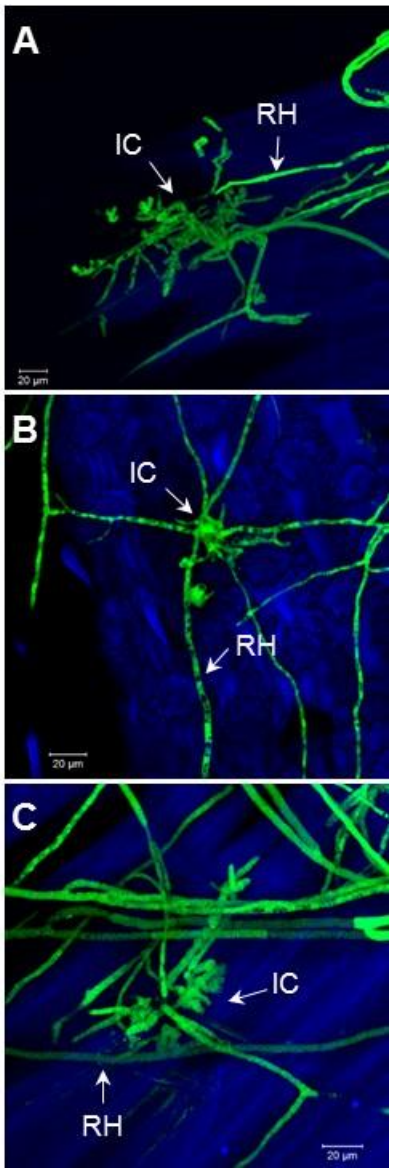

Fig. 3.9. Cellular morphology of infection cushions (IC) originating from runner hyphae (RH) produced by (A) *Fusarium graminearum* wild type (FgWT:8/1), (B) Δ*hyd2* and (C) Δ*hyd3* single mutants on the surface of paleas. Wheat paleas (cv. Nandu) were inoculated with 10 µL of a conidial suspension containing approximately 500 conidia and fluorescence microscopy was performed 6 days after inoculation. All pictures were taken using the same magnification and scale bars represent 20 µm. Detection of infection structures was performed using the Zeiss LSM 780 laser scanning microscope (CLSM). Images were taken with Zeiss AxioCam MRm CCD camera.

3.3.8. Deletion of the F. graminearum *hydrophobins do not cause chitin defects at the cell wall level*

To investigate possible effects of the deletion of the hydrophobin genes on cell wall integrity, *F. graminearum* WT, single and triples mutant strains were grown on CM and MM supplemented with

50 µg mL^{-1} of Calcofluor White (CFW), which acts by binding to nascent chitin chains. After two days of growth, all the mutant strains were not more inhibited than the WT by CFW treatment, thus suggesting that the hydrophobin genes deletion does not cause chitin defect at the cell wall level (Fig. 3.10 and Fig. S3.8).

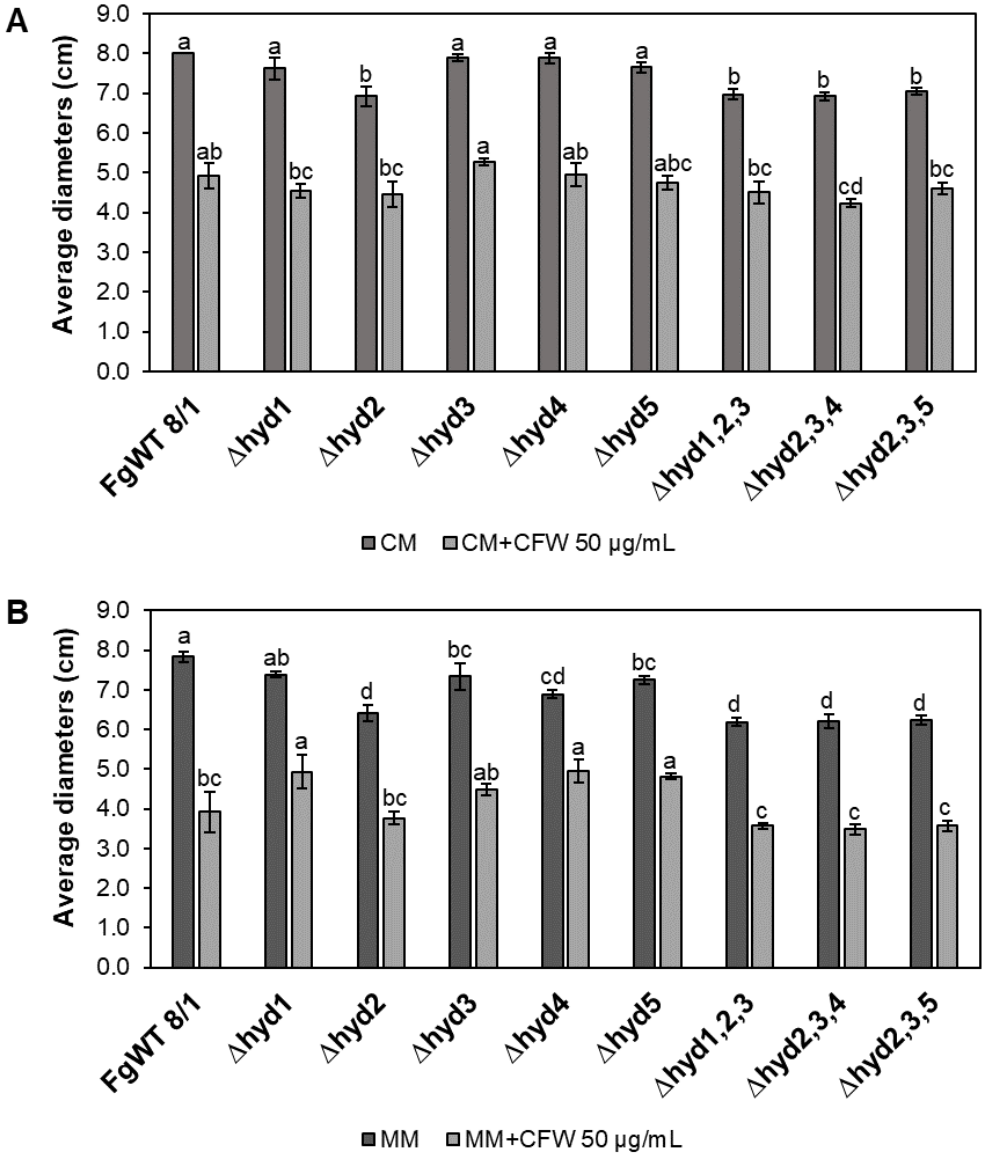

Fig. 3.10. Susceptibility of *Fusarium graminearum* hydrophobin mutants to Calcofluor white. (A) Complete (CM) or (B) Minimal medium (MM) plates supplemented with Calcofluor white (CFW, 50 µg mL^{-1}) and control plates were inoculated with 4-mm plugs of actively growing mycelia of the wild type (FgWT:8/1), single and triple mutant strains. Plates were incubated at 28 °C in the dark. The susceptibility to CFW was estimated by measuring mycelia diameters after 2 days. The experiment was repeated twice with similar results. Data were statistically analyzed by the ANOVA Tukey-Kramer test. Different letters (a, b, c, d) indicate significant differences at $P<0.05$.

3.3.9. F. graminearum *triple hydrophobin mutants are more sensitive to β-1,3-glucanase treatment*

To test possible cell wall defects, single and triple hydrophobin mutants were grown in the presence of the fungal cell wall degrading enzymes β-1,3-glucanase.

In a plate assay performed with 8 U of β-1,3-glucanase, among the single mutants only the Δ*hyd3* strain appeared slightly inhibited (Fig. 3.11), while Δ*hyd2,* Δ*hyd4* and Δ*hyd5* and WT were not affected by the treatment. Differently, all the triple mutant strains, particularly the Δ*hyd2,3,4* and Δ*hyd2,3,5*, resulted clearly inhibited (Fig. 3.11).

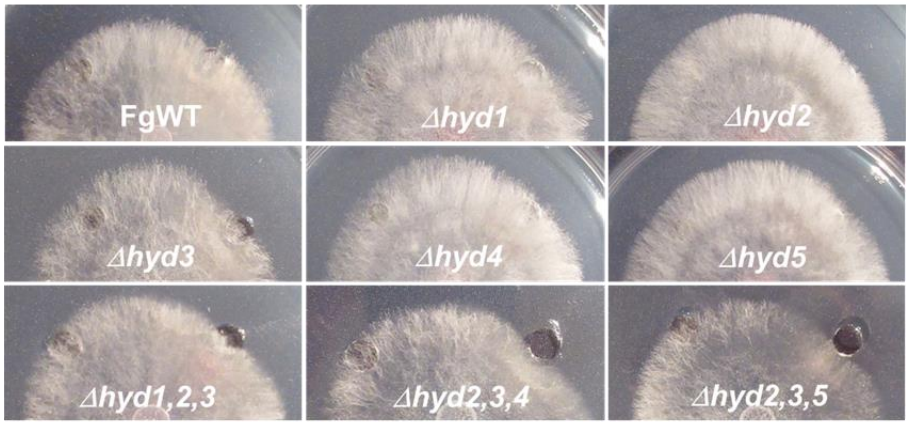

Fig. 3.11. Fungal growth inhibition assay in the presence of glucanase. *Fusarium graminearum* wild-type (FgWT:8/1), single and triple mutant strains were inoculated in the middle of Minimal medium (MM) plates and 8 U of β-1,3-glucanase enzymatic solution from *Trichoderma longibrachiatum* were loaded on wells produced in the agar plates at 1 cm from 2-days old actively growing mycelia. The inhibition effects were observed up to 48 hours after treatment.

3.3.10. F. graminearum *hydrophobin mutants exhibit higher susceptibility to tebuconazole fungicide*

F. graminearum hydrophobin mutants were grown in the presence of Folicur, a systemic triazole fungicide containing tebuconazole, an ergosterol biosynthesis inhibitor, as active substance. The inhibition effect was determined by measuring the radial growth after 4 days. Compared to WT, all the single mutants, in particular Δ*hyd2* and Δ*hyd3*, appeared slightly but not significantly more inhibited (Fig. 3.12). Among the triple mutants, Δ*hyd1,2,3* and Δ*hyd2,3,5* showed a higher inhibition

percentage compared to the other strains, although only the Δ*hyd2,3,5* mutant was significantly more inhibited by about 50% compared to the WT strain (Fig. 3.12).

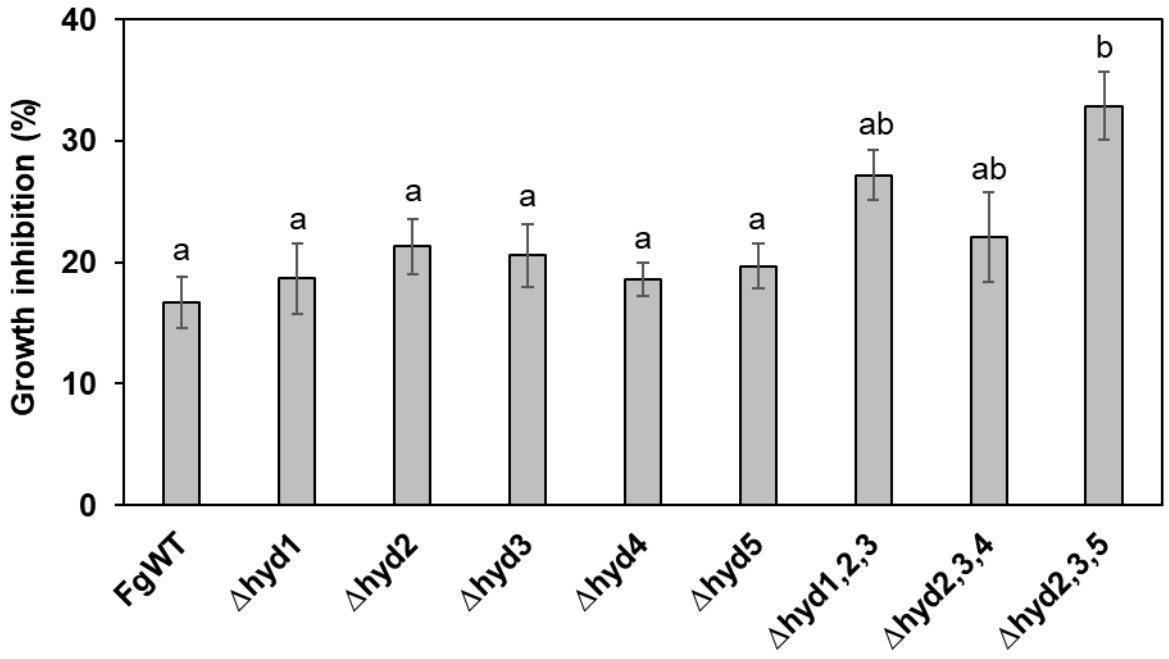

Fig. 3.12. Fungicide inhibition assay. Percentage of growth inhibition of the *Fusarium graminearum* wild type (FgWT:8/1), single and triple mutant strains grown on Minimal medium (MM) supplemented with 0.01 µg mL^{-1} of Folicur fungicide. Plates were incubated in the dark at 28 °C and the inhibition was determined by measuring the radial growth after 4 days of growth. Data represent the mean ± standard error (indicated by bars) of five independent experiments. Data were analyzed by the ANOVA Tukey-Kramer test. Different letters (a, b) indicate significant differences at $P<0.05$.

3.3.11. The deletion of F. graminearum *hydrophobins affects perithecia maturation*

The *F. graminearum* WT, single and triple mutant strains were tested for perithecia production. All the mutant strains confirmed the ability to develop normal perithecia (Fig. 3.13), thus indicating that the *F. graminearum* hydrophobins are not essential for the sexual reproduction of the fungus. However, all the triple mutants produced a reduced number of mature perithecia (Fig. 3.13), suggesting that the FgHyds could be involved in maturation timing or normal development of the fungal sexual fruiting body.

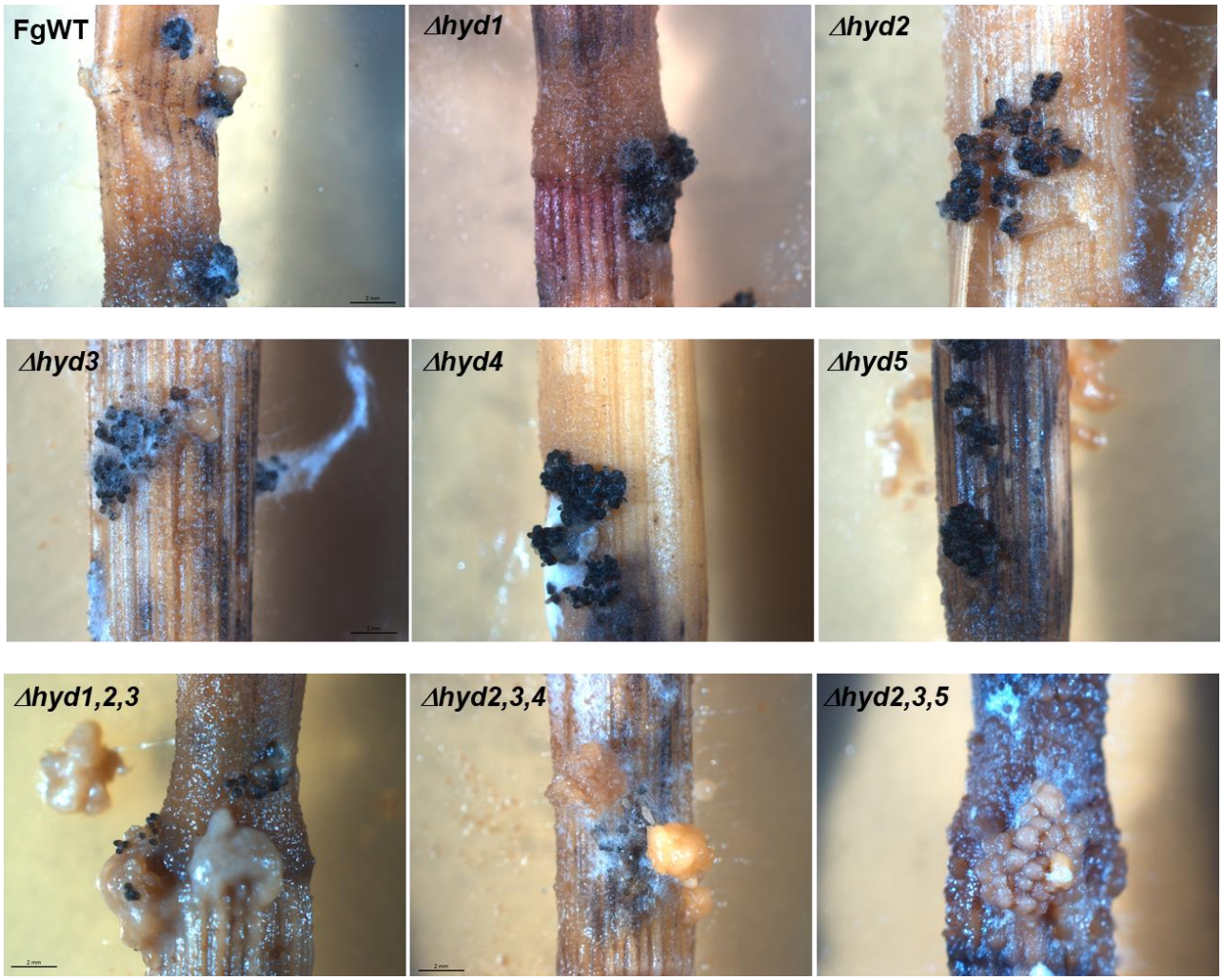

Figure 3.13. Perithecia viability assay. Five wheat stems per strain were inoculated on the nodes with a 10 µL drop containing 1000 conidia of the *Fusarium graminearum* wild type (FgWT:8/1), single and triple mutant strains and were incubated for 3 months in water agar plates under UV light. Pictures were taken with Leica stereo microscope and are representative of two independent experiments.

3.4. Discussion

Hydrophobins (HPs) are small cysteine-rich surface-active proteins (Wessels, 2000; Wösten, 2001) that are secreted only by fungi and may play several roles. Aim of the present study was to investigate the importance of the five hydrophobin encoding genes contained in the genome of the fungal pathogen *F. graminearum*, the causal agent of FHB disease of wheat. A preliminary transcriptomic analysis has shown that the expression of the FgHyd3 gene is dramatically upregulated during fungal growth and initial epiphytical growth on wheat paleas and glumes. Besides, also the FgHyd2 and FgHyd4 genes are clearly expressed in both conditions, although at lower level compared to FgHyd3. Single and triple FgHyd knock-out mutants have been therefore produced by targeted homologous recombination and characterized both in vitro and in vivo. Single and multiple deletion of all the encoding genes did not affect the ability of the fungus to form radial colonies, but a slightly reduced growth was observed for the Δ*hyd2* and all the three triple mutants including the deletion of FgHyd2. Interestingly, these mutants were then able to recover their growth under osmotic and oxidative stress. However, the biological function of this mechanism remains to be elucidated. Interestingly, the aerial hyphae of Δ*hyd2* and Δ*hyd3* single mutants, as well as the triple mutants including the deletion of the FgHyd2 and FgHyd3 genes, showed a reduced ability to penetrate through the water-air interface, thus suggesting a reduction of the cell surface hydrophobicity. Indeed, by self-assembling at the water-air interphases and forming a hydrophobic layer, HPs are known to play a crucial role at the surface of fungal hyphae conferring water-repellent properties to escape the aqueous environment (Wösten et al., 1999). Our drop assay confirmed previous data on the FgHyd5, which was shown to be not involved in the penetration of hyphae through the water-air interface (Minenko et al., 2014), although this protein is thought to affect the hydrophobicity of aerial mycelia (Minenko et al., 2014). To investigate whether the FgHyd are involved in fungal pathogenicity, wheat spike infections on *T. aestivum* (cv. Nandu and Amaretto) were performed. Although point inoculations did not highlight any reduction in virulence of the mutants compared to wild type, wheat infections carried out by spray inoculation showed in both cultivars a reduction of symptomatic spikelets with the Δ*hyd2* and Δ*hyd3*

mutants, deleted of two of the genes more expressed during wheat spike infection and previously shown to be affected in hyphal surface hydrophobicity and ability to penetrate through the water-air interface. Taken together, these results indicate that *F. graminearum* FgHyd2 and FgHyd3 are involved in adhesion of conidia to the host surface during the early stages of the infection process and thus can be considered virulence factors of the fungus. This hypothesis is strengthened by a histological analysis, performed by fluorescence microscopy, that showed no differences in the morphology of infection structures produced during wheat spikelets infection by wild type and single mutant strains constitutively expressing GFP. Our result is in agreement with previous data obtained with the Class I and Class II hydrophobins of *M. oryzae*, which have been shown to be involved in interaction with hydrophobic surfaces (Talbot et al., 1996), attachment to leaf surface (Whiteford and Spanu, 2001) and fungal pathogenicity (Talbot et al., 1993; Kim et al., 2005).

Whereas the deletion of all the FgHyd does not cause cell wall chitin defects, the triple mutants resulted significantly more sensitive than wild type to the fungal cell wall degrading enzyme β-1,3-glucanase. Interestingly, a similar protective role against this enzyme was also observed for the *F. graminearum* cerato-platanins (FgCPPs), another class of small secreted non-catalytic cysteine-rich proteins (Quarantin et al., 2016). Since FgCPPs and FgHyds show this common feature, the simultaneous deletion of *F. graminearum* cerato-platanins and hydrophobins could further affect fungal growth in the presence of fungal cell wall degrading enzymes and/or fungal virulence.

Possible defect at the cell wall was also investigated growing the mutants in the presence of Folicur, a systemic triazole fungicide containing an ergosterol biosynthesis inhibitor. In this case, only one of the triple mutants showed a significantly higher susceptibility compared to the wild type. These results suggest that the simultaneous presence of different HPs on the hyphal surface could form a hydrophobic coating with a protecting role for aerial hyphae. Interestingly, a protecting role of HPs for aerial conidia and hyphae has been suggested to date only against desiccation and wetting (Wösten, 2001; Whiteford and Spanu, 2002; Klimes and Dobinson 2006).

Finally, all the mutant strains confirmed the ability to develop perithecia, thus indicating that the FgHyd proteins are not essential for sexual reproduction of the fungus. However, all the triple mutants showed a reduced number of mature perithecia and this suggests that the FgHyd are involved in the normal development of sexual structures, as previously shown for the HPs of *Schizophyllum commune* and *B. cinerea* (Wessel et al., 1991a; Terhem and van Kan, 2014).

In conclusion, the *F. graminearum* Hyds play several roles during fungal growth and plant infection: FgHyd2 is involved in fungal growth; FgHyd2 and FgHyd3 are involved in hyphal ability to penetrate through the water-air interface, hydrophobicity and adhesion of conidia to the wheat spike surface; the presence of multiple HPs on the hyphal surface protects the fungus from β-1,3-glucanase and a systemic triazole fungicide and allow a normal development of perithecia.

Acknowledgments

This contribution has been presented at the XXIII National Congress of the Italian Society of Plant Pathology, Piacenza 4-6th October 2017, with the title "*Fusarium graminearum* hydrophobins: role in fungal growth and plant infection" by Alessandra Quarantin[1,2], Birgit Hadeler[2], Ellis B. Monaghan[2], Luca Sella[1], Wilhelm Schäfer[2] and Ana Lilia Martínez-Rocha[2], and will be submitted to an International Journal with IF with the title "*Fusarium graminearum* hydrophobins are involved in water-air interface penetration, maturation of perithecia and plant infection" by Alessandra Quarantin[1,2], Birgit Hadeler[2], Ellis B. Monaghan[2], Luca Sella[1], Wilhelm Schäfer[2] and Ana Lilia Martínez-Rocha[2].

[1]Dipartimento del Territorio e Sistemi Agro-Forestali (TESAF), research group in Plant Pathology, Università degli Studi di Padova, Viale dell'Università 16, 35020, Legnaro, Italy; [2]Biocenter Klein Flottbek, Molecular Phytopathology and Genetics, University of Hamburg, Hamburg (Germany).

References

Beckerman, J.L., Ebbole, D.J., 1996. MPG1, a gene encoding a fungal hydrophobin of *Magnaporthe grisea*, is involved in surface recognition. Mol. Plant-Microbe Interact. 9, 450-456.

Cuomo, C.A., Güldener, U., Xu, J.R., Trail, F., Turgeon, B.G., Di Pietro, A., Walton, J.D., Ma, L.J., Baker, S.E., Rep, M., et al., 2007. The *Fusarium graminearum* genome reveals a link between localized polymorphism and pathogen specialization. Science. 317, 1400-1402.

de Vries, O.M.H., Fekkes, M.P., Wösten, H.A.B., Wessels, J.G.H., 1993. Insoluble hydrophobin complexes in the walls of *Schizophyllum commune* and other filamentous fungi. Arch. Microbiol. 159, 330-335.

Fuchs, U., Czymmek, K.J., Sweigard, J.A., 2004. Five hydrophobin genes in *Fusarium verticillioides* include two required for microconidial chain formation. Fungal Genet. Biol. 41, 852-864.

Grünbacher, A., Throm, T., Seidel, C., Gutt, B., Röhrig, J., Strunk, T., Vincze, P., Walheim, S., Schimmel, T., Wenzel, W., Fischer1, R., 2014. Six Hydrophobins Are Involved in Hydrophobin Rodlet Formation in *Aspergillus nidulans* and Contribute to Hydrophobicity of the Spore Surface. PLoS ONE. 9, e94546.

Izumitsu, K., Kimura, S., Kobayashi, H., Morita, A., Saitoh, Y., Tanaka, C., 2010. Class I hydrophobin BcHpb1 is important for adhesion but not for later infection of *Botrytis cinerea*. J. Gen. Plant Pathol. 76, 254-260.

Kershaw, M.J., Talbot, N.J., 1998. Hydrophobins and repellents: proteins with fundamental roles in fungal morphogenesis. Fungal Genet. Biol. 23, 18-33.

Kim, S., Ahn, I.P., Rho, H.S., Lee, Y.H., 2005. MHP1, a *Magnaporthe grisea* hydrophobin gene, is required for fungal development and plant colonization. Mol. Microbiol. 57, 1224-1237.

Klimes, A., Dobinson, K.F., 2006. A hydrophobin gene, VDH1, is involved in microsclerotial development and spore viability in the plant pathogen *Verticillium dahliae*. Fungal Genet. Biol. 43, 283-294.

Lauter, F.R., Russo, V.E., Yanofsky, C., 1992. Developmental and light regulation of *eas*, the structural gene for the rodlet protein of *Neurospora*. Genes Dev. 6, 2373-2381.

Martínez-Rocha, A.L., Woriedh, M., Chemnitz, J., Willingmann, P., Kröger, C., Hadeler, B., Hauber, J., Schäfer, W., 2016. Posttranslational hypusination of the eukaryotic translation initiation factor-5A regulates *Fusarium graminearum* virulence. Sci. Rep. 6, 24698.

Mey, G., Correia, T., Oeser, B., Kershaw M.J., Garre, V., Arntz, C., Talbot, N.J., Tudzynski, P., 2003. Structural and functional analysis of an oligomeric hydrophobin gene from *Claviceps purpurea*. Mol. Plant Pathol. 4, 31-41.

Minenko, E., Rudi, F., Vogel, R.F., Niessen, L., 2014. Significance of the class II hydrophobin FgHyd5p for the life cycle of *Fusarium graminearum*. Fungal Biol. 118, 385-393.

Mosbach, A., Leroch, M., Mendgen, K.W., Hahn, M., 2011. Lack of evidence for a role of hydrophobins in conferring surface hydrophobicity to conidia and hyphae of *Botrytis cinerea.* BMC Microbiol. 11, 10.

Nguyen, T.V., Schäfer, W., Bormann, J., 2012. The stress-activated protein kinase FgOS-2 is a key regulator in the life cycle of the cereal pathogen *Fusarium graminearum*. Mol. Plant-Microbe Interact. 25, 1142-1156.

Paananen, A., Vuorimaa, E., Torkkeli, M., Penttila, M., Kauranen, M., Ikkala, O., Lemmetyinen, H., Serimaa, R., Linder M.B., 2003. Structural Hierarchy in Molecular Films of Two Class II Hydrophobins. Biochem. 42, 5253-5258.

Paccanaro, M.C., Sella, L., Castiglioni, C., Giacomello, F., Martínez-Rocha, A.L., D'Ovidio, R., Schäfer, W., Favaron, F., 2017. Synergistic Effect of Different Plant Cell Wall–Degrading Enzymes Is Important for Virulence of *Fusarium graminearum*. Mol. Plant-Microbe Interact. 30, 886-895.

Quarantin, A., Glasenapp, A., Schäfer, W., Favaron, F., Sella, L., 2016. Involvement of the *Fusarium graminearum* cerato-platanin proteins in fungal growth and plant infection. Plant Physiol. Biochem. 109, 220-229.

Sarlin, T., Kivioja, T., Kalkkinen, N., Linder, M.B., Nakari-Setälä, T., 2012. Identification and characterization of gushing-active hydrophobins from *Fusarium graminearum* and related species. J. Basic Microbiol. 52, 184-194.

Segers, G.C., Hamada, W., Oliver, R.P., Spanu, P.D., 1999. Isolation and characterisation of five different hydrophobin-encoding cDNAs from the fungal tomato pathogen *Cladosporium fulvum*. Mol. Genet. Genomics. 26, 644-652.

Sella, L., Gazzetti, K., Castiglioni, C., Schäfer, W., D'Ovidio, R., Favaron, F., 2016. The *Fusarium graminearum* Xyr1 transcription factor regulates xylanase expression but is not essential for fungal virulence. Plant Pathol. 65, 713-722.

Talbot, N.J., Ebbole, D.J., Hamer, J.E., 1993. Identification and characterization of *MPG1*, a gene involved in pathogenicity from the rice blast fungus *Magnaporthe grisea*. Plant Cell. 5, 1575-1590.

Talbot, N.J., Kershaw, M.J., Wakley, G.E., De Vries, O., Wessels, J., Hamer, J.E., 1996. MPG1 encodes a fungal hydrophobin involved in surface interactions during infection-related development of *Magnaporthe grisea*. Plant Cell. 8, 985-999.

Terhem, R.B., van Kan, J.A., 2014. Functional analysis of hydrophobin genes in sexual development of *Botrytis cinerea*. Fungal Genet. Biol. 71, 42-51.

Wessels, J.G.H., de Vries, O.M.H., Asgeirsdóttir, S.A., Schuren, F.H.J., 1991a. Hydrophobin genes involved in formation of aerial hyphae and fruit bodies in *Schizophyllum commune.* Plant Cell. 3, 793-799.

Wessels, J.G.H., de Vries, O.M.H., Asgeirsdóttir, S.A., Springer, J., 1991b. The *thn* mutation of *Schizophyllum commune*, which suppresses formation of aerial hyphae, affects expression of the Sc3 hydrophobin gene. J. Gen. Microbiol. 137, 2439-2445.

Wessels, J.G.H., 1994. Developmental regulation of fungal cell wall formation. Annu. Rev. Phytopathol. 32, 413-437.

Wessels, J.G.H., 1997. Hydrophobins, proteins that change the nature of the fungal surface. Adv. Microbial Physiol. 38, 1-45.

Wessels, J.G.H., 2000. Hydrophobins, unique fungal proteins. Mycol. 14, 153-159.

Whiteford, J.R., Spanu, P.D., 2001. The hydrophobin HCf-1 of *Cladosporium fulvum* is required for efficient water-mediated dispersal of conidia. Fungal Genet. Biol. 32, 159-168.

Whiteford, J.R., Spanu, P.D., 2002. Hydrophobins and the interactions between fungi and plants. Mol. Plant Pathol. 3, 391-400.

Wösten, H.A., Schuren, F.H., Wessels, J.G., 1994. Interfacial self-assembly of a hydrophobin into an amphipathic protein membrane mediates fungal attachment to hydrophobic surfaces. EMBO J. 13, 5848-5854.

Wösten, H.A., van Wetter, M.A., Lugones, L.G., van der Mei, H.C., Busscher, H.J., Wessels, J.G., 1999. How a fungus escapes the water to grow into the air. Curr. Biol. 9, 85-88.

Wösten, H.A.B., de Vocht, M.L., 2000. Hydrophobins, the fungal coat unravelled. Biochim Biophys Acta. 1469, 79-86.

Wösten, B., 2001. Hydrophobins: multipurpose proteins. Annu. Rev. Microbiol. 55, 625-646.

Zadoks, J.C., Chang, T.T., Konzak, C.F., 1974. A decimal code for the growth stages of cereals. Weed Res. 14, 415-421.

Supplementary figure captions

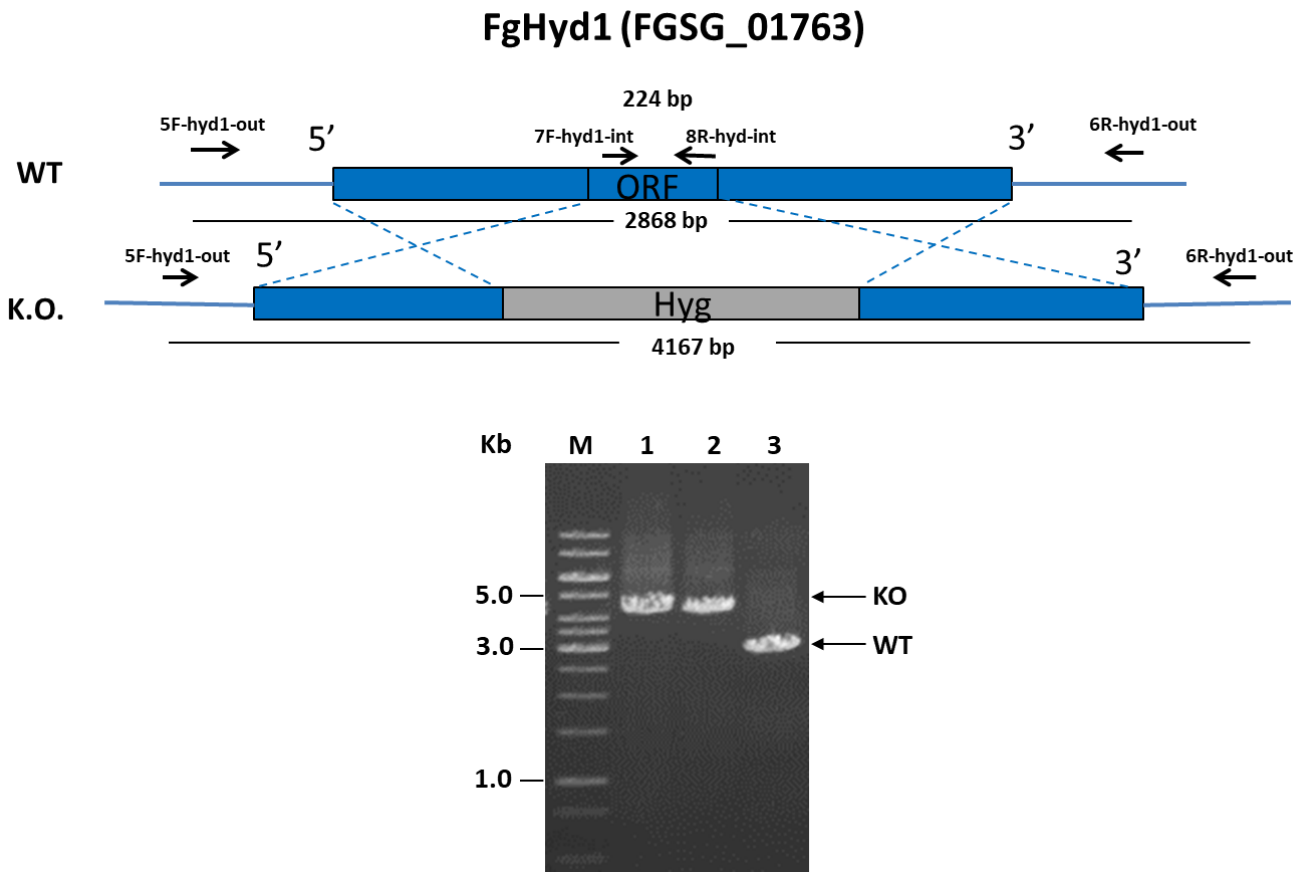

Fig. S3.1. (A) Scheme of the construct produced and used in this work to obtain the mutant and PCR selection of the Δ*hyd1* knock-out mutant strains by using the Fghyd1-out primers pair (Table S3.1). M: molecular size markers (GeneRuler™ DNA ladder, Fermentas); lane 1: #1801.14. mutant strain; lanes 2: #1801.22. mutant strain; lanes 3: *Fusarium graminearum* wild type (WT:8/1) strain.

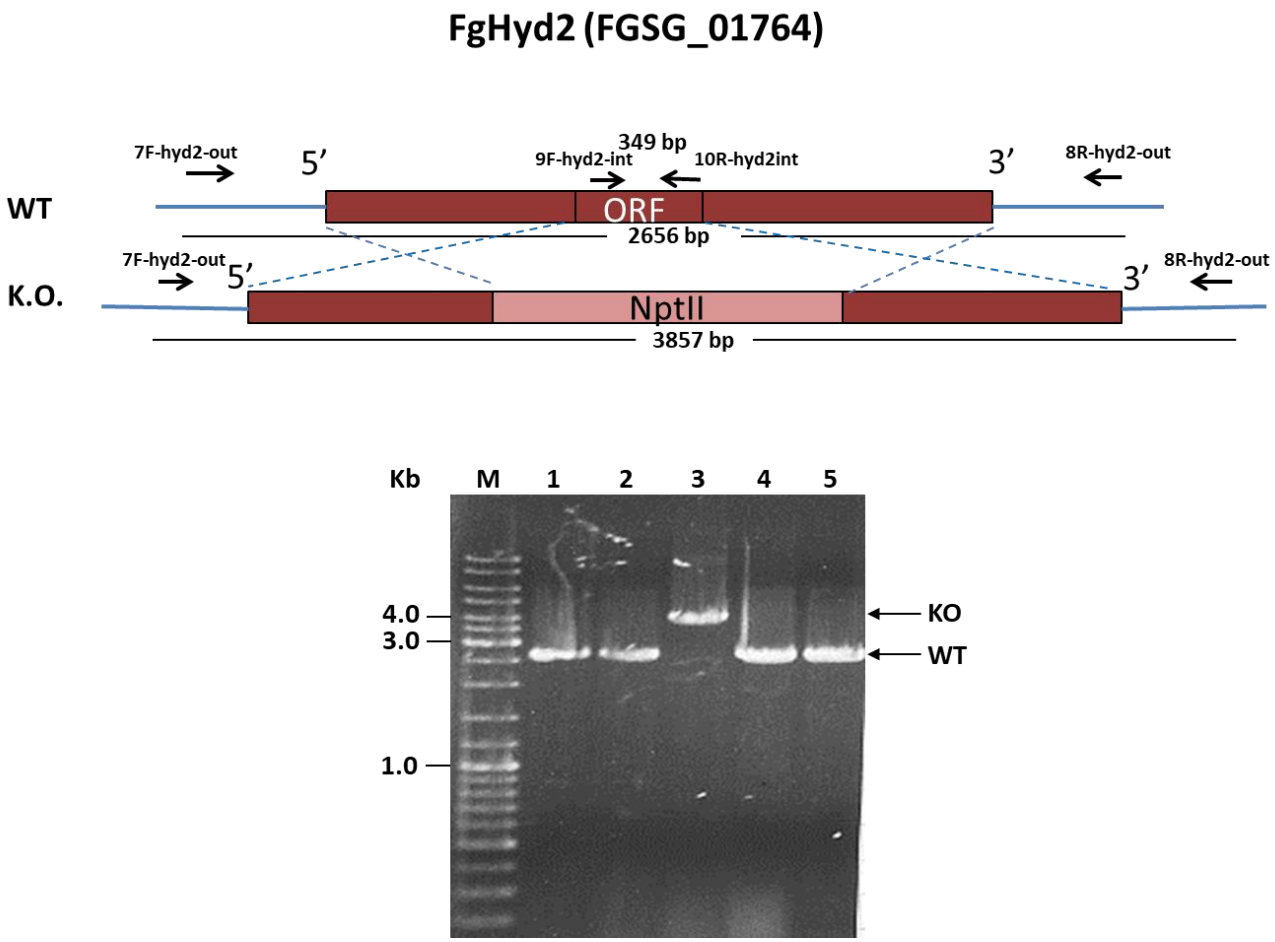

Fig. S3.1. (B) Scheme of the construct produced and used in this work to obtain the mutant and PCR selection of the Δ*hyd2* knock-out mutant strains by using the Fghyd2-out primers pair (Table S3.1). M: molecular size markers (GeneRuler™ DNA ladder, Fermentas); lane 1: #1661.1. mutant strain; lanes 2: #1661.2. mutant strain; lanes 3: #1661.3. mutant strain; lanes 4: #1661.4. mutant strain; lanes 5: *Fusarium graminearum* wild type (WT:8/1) strain.

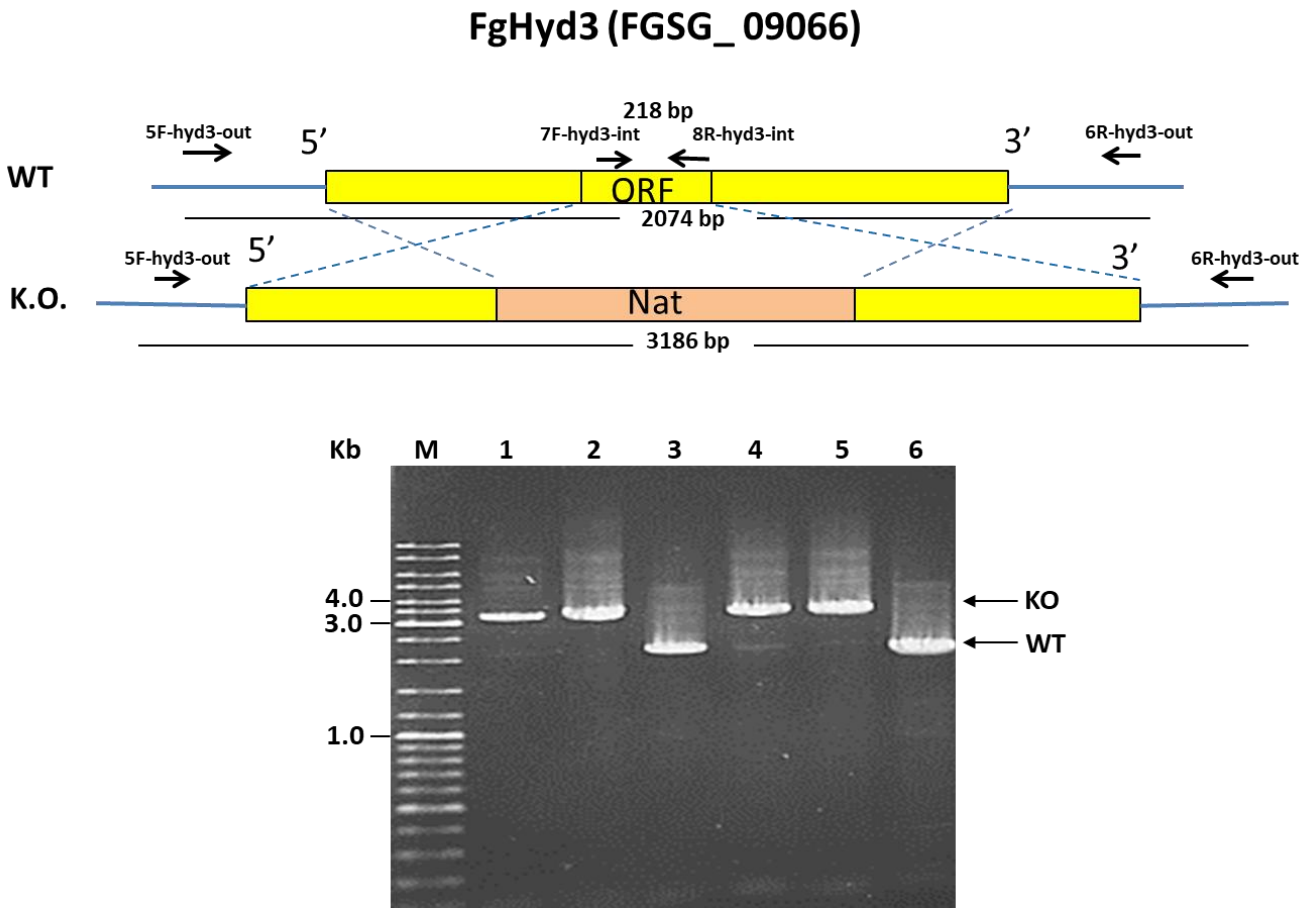

Fig. S3.1. (C) Scheme of the construct produced and used in this work to obtain the mutant and PCR selection of the Δ*hyd3* knock-out mutant strains by using the Fghyd3-out primers pair (Table S3.1). M: molecular size markers (GeneRuler™ DNA ladder, Fermentas); lane 1: #1640.2. mutant strain; lanes 2: #1640.3. mutant strain; lanes 3: #1640.6. mutant strain; lanes 4: #1640.8. mutant strain; lanes 5: #1640.12. mutant strain; lanes 6: *Fusarium graminearum* wild type (WT:8/1) strain.

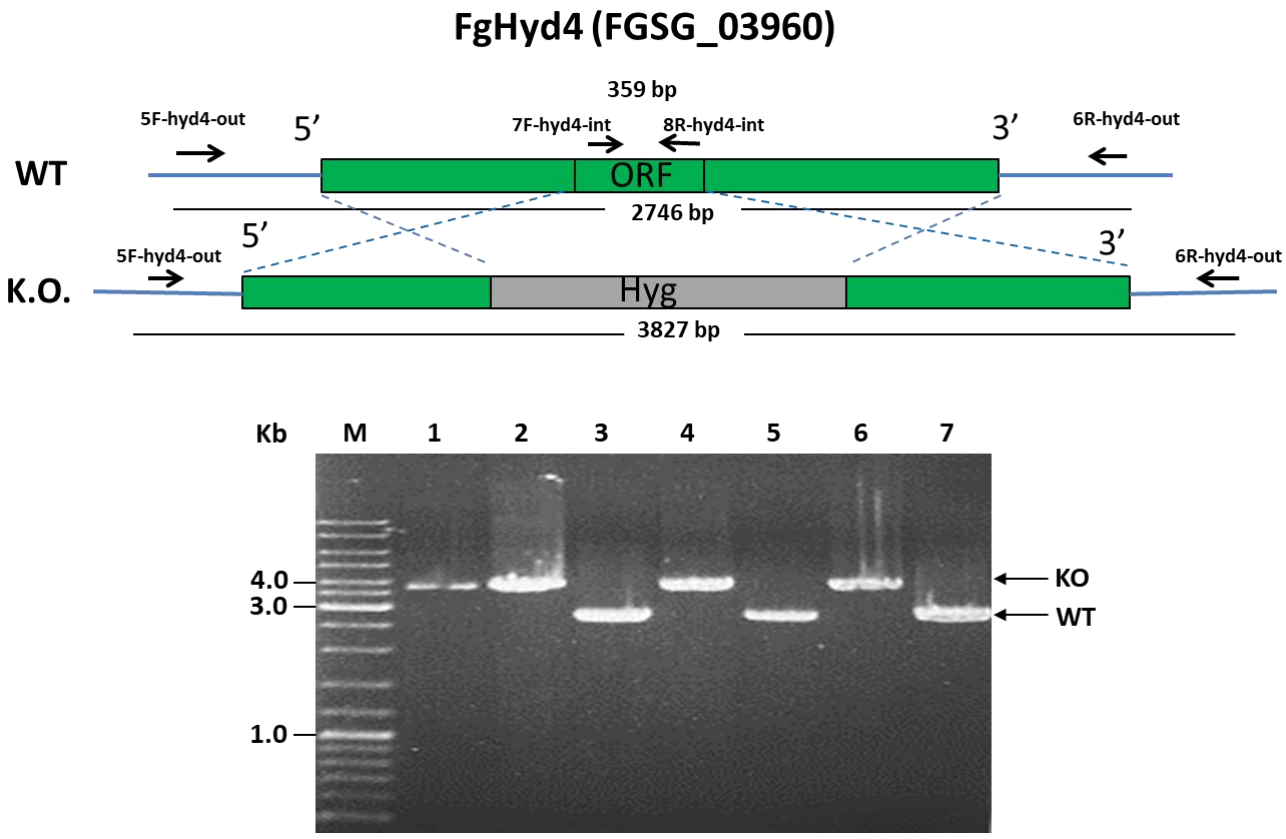

Fig. S3.1. (D) Scheme of the construct produced and used in this work to obtain the mutant and PCR selection of the Δ*hyd4* knock-out mutant strains by using the Fghyd4-out primers pair (Table S3.1). M: molecular size markers (GeneRuler™ DNA ladder, Fermentas); lane 1: #1653.6. mutant strain; lanes 2: #1653.7. mutant strain; lanes 3: #1653.8. mutant strain; lanes 4: #1653.24. mutant strain; lanes 5: #1653.26. mutant strain; lanes 6: #1653.34. mutant strain; lanes 7: *Fusarium graminearum* wild type (WT:8/1) strain.

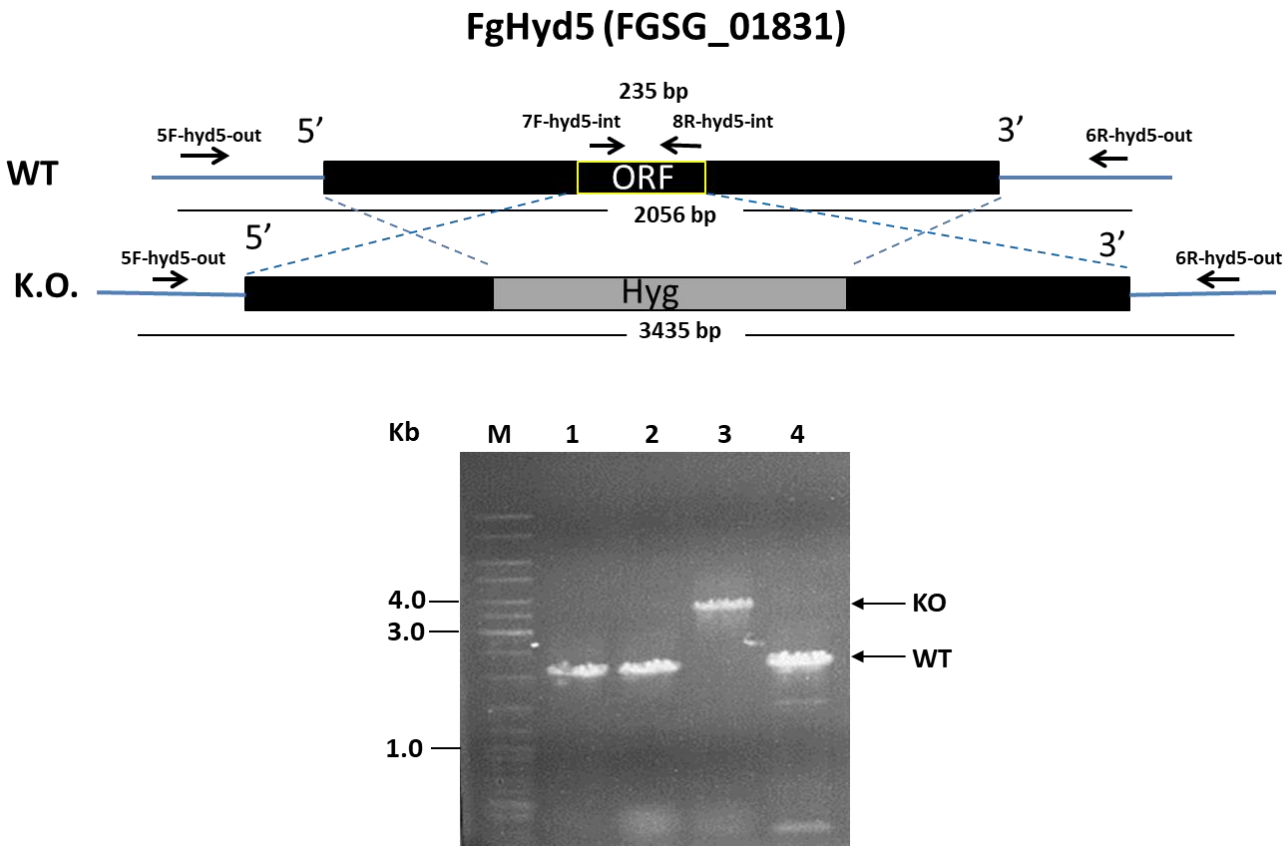

Fig. S3.1. (E) Scheme of the construct produced and used in this work to obtain the mutant and PCR selection of the Δ*hyd5* knock-out mutant strains by using the Fghyd5-out primers pair (Table S3.1). M: molecular size markers (GeneRuler™ DNA ladder, Fermentas); lane 1: #1652.26. mutant strain; lanes 2: #1652.27. mutant strain; lanes 3: #1652.28. mutant strain; lanes 4: *Fusarium graminearum* wild type (WT:8/1) strain.

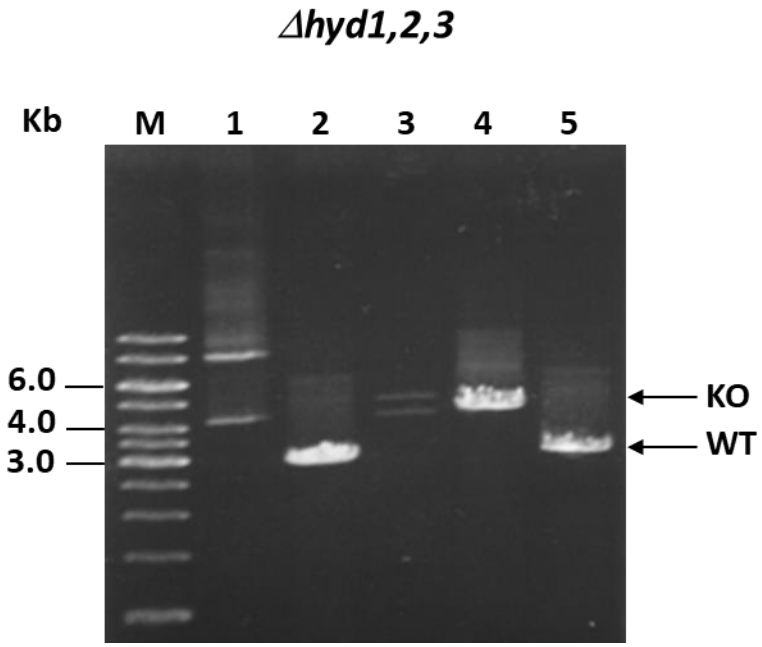

Fig. S3.2. (A) PCR selection of the Δ*hyd1,2,3* knock-out mutant strains using primers 5F-Fghyd1-out and 6R-Fghyd1-out (Table S3.1) specific for the FgHyd1 gene. M: molecular size markers (GeneRuler™ DNA ladder, Fermentas); lane 1: #1802.1. mutant strain; lanes 2: #1802.2. mutant strain; lanes 3: #1802.3. mutant strain; lanes 4: #1802.4. mutant strain; lanes 5: *Fusarium graminearum* wild type (WT:8/1) strain.

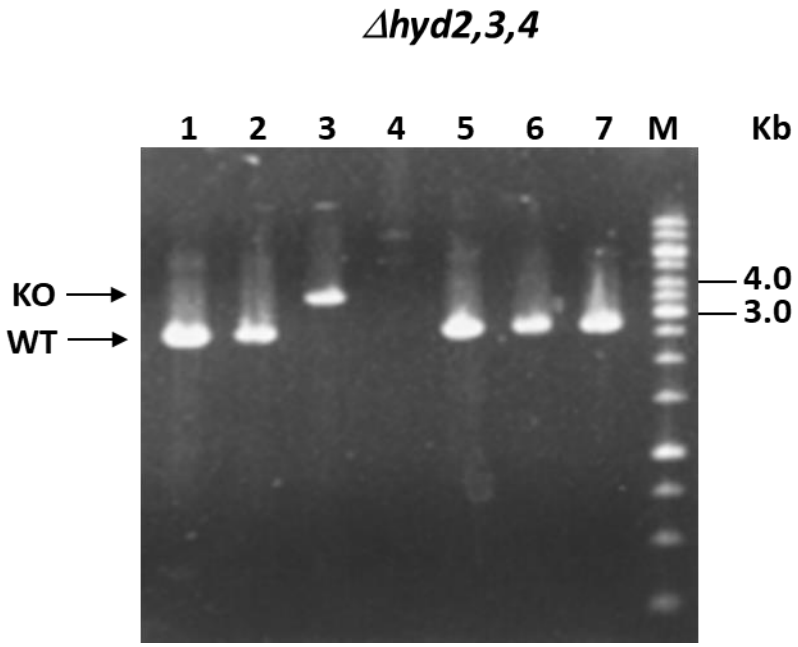

Fig. S3.2. (B) PCR selection of the Δ*hyd2,3,4* knock-out mutant strains using primers 5F-Fdhyd4-out and 6R-Fdhyd4-out (Table S3.1) specific for the FgHyd4 gene. Lane 1: *Fusarium graminearum* wild type (WT:8/1) strain; lane 2: #1745.1. mutant strain; lanes 3: #1745.4. mutant strain; lanes 4: #1745.6. mutant strain; lanes 5: #1745.8. mutant strain; lanes 6: #1745.19. mutant strain; lanes 7: #1745.20. mutant strain; lanes 8: M: molecular size markers (GeneRuler™ DNA ladder, Fermentas).

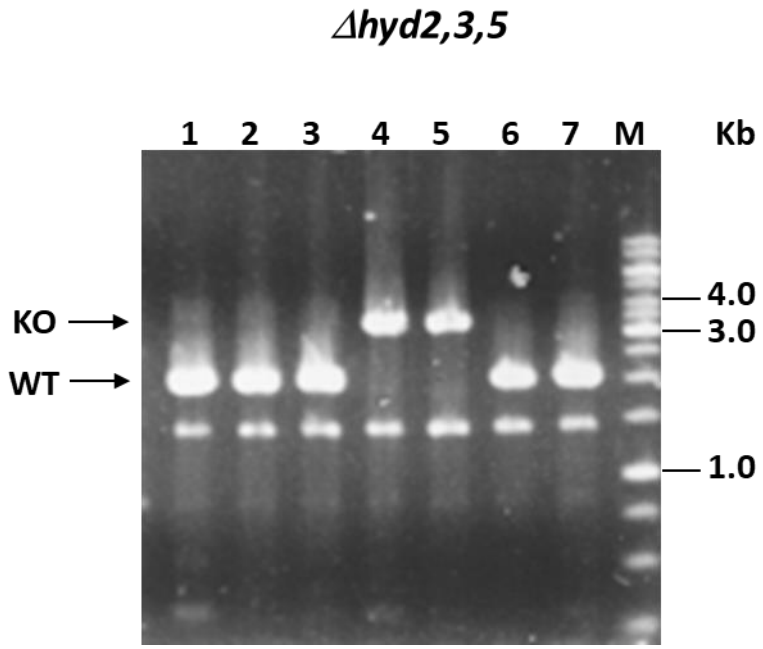

Fig. S3.2. (C) PCR selection of the Δ*hyd2,3,5* knock-out mutant strains using primers 5F-Fdhyd5-out and 6R-Fdhyd5-out (Table S3.1) specific for the FgHyd5 gene. Lane 1: *Fusarium graminearum* wild type (WT:8/1) strain; lane 2: #1748.1. mutant strain; lanes 3: #1748.2. mutant strain; lanes 4: #1748.3. mutant strain; lanes 5: #1748.22. mutant strain; lanes 6: #1748.23. mutant strain; lanes 7: #1748.30. mutant strain; lanes 8: M: molecular size markers (GeneRuler™ DNA ladder, Fermentas).

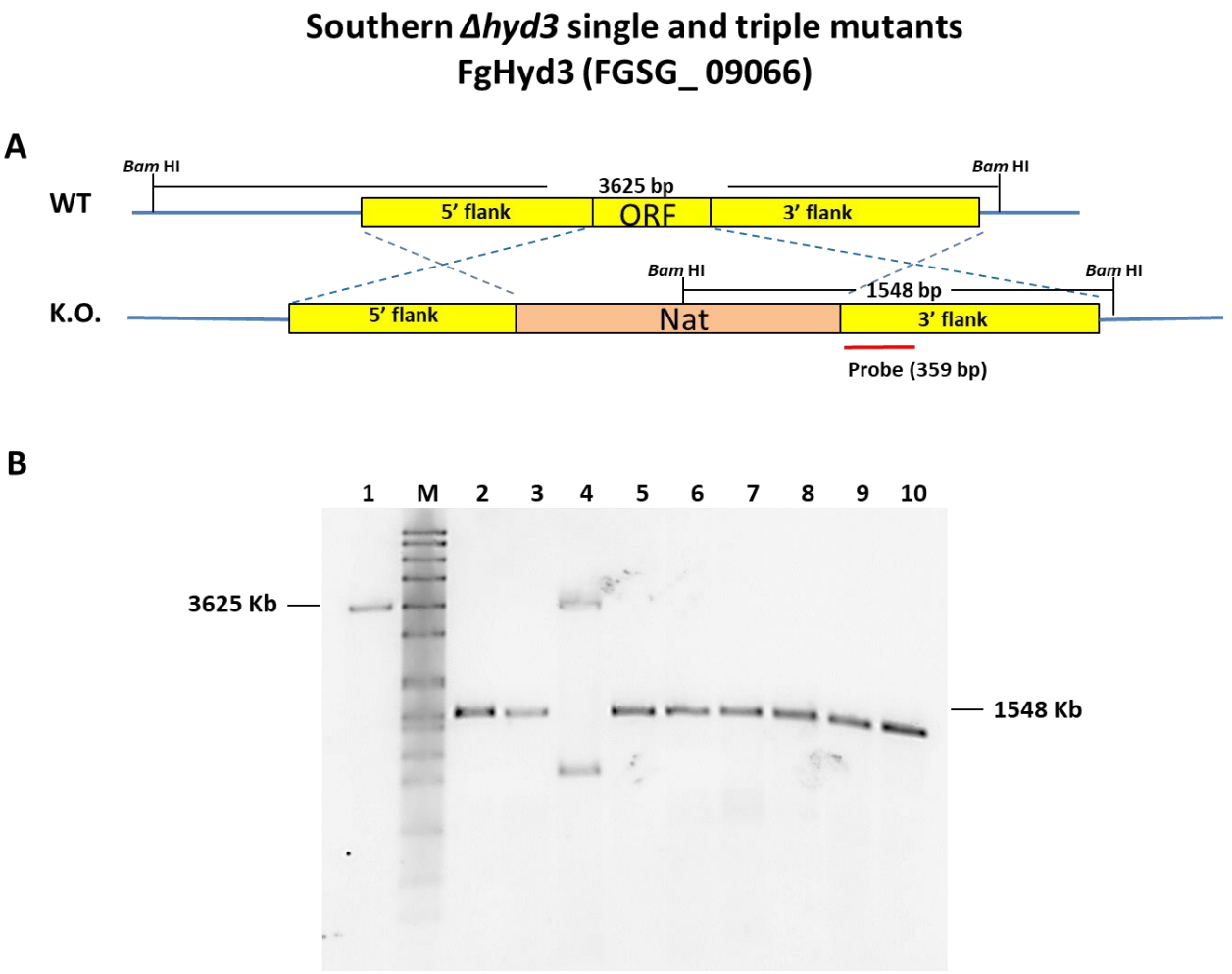

Fig. S3.3. Southern blot analysis of the single Δ*hyd3* and the triple mutants Δ*hyd1,2,3*, Δ*hyd2,3,4* and Δ*hyd2,3,5*. (A). Scheme of the construct produced and used in this work to obtain the mutants, indicating the sites recognized by the restriction enzyme used for the Southern blot analysis (*BamH*I) and the position of the right flanking probe specific for the FgHyd3 locus used for hybridization and obtained by PCR using the primers pair Fghyd3-pro. (B) Southern blot hybridization of *Fusarium graminearum* wild type (WT:8/1) (lane 1), single knock-out mutants #1640.3. (lane 2) and #1640.12. (lane 3), ectopic mutant #1640.5. (lane 4) and triple knock-out mutants #1745.4. (lane 5), #1745.6. (lane 6), #1748.3. (lane 7), #1748.22. (lane 8), #1802.1. (lane 9), #1802.4. (lane 10). M: marker VII (Fermentas). The size of the hybridizing bands is reported.

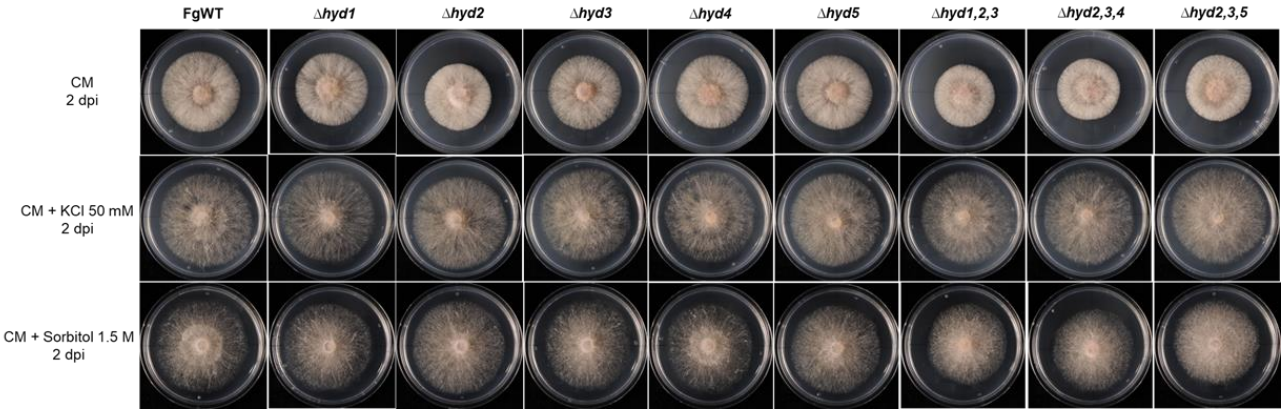

Fig. S3.4. Ionic and non-ionic osmotic stress-response phenotypes. Complete medium (CM) plates containing 750 mM KCl or 1.5 M Sorbitol were inoculated with 4-mm mycelial plugs of the *Fusarium graminearum* wild type (FgWT:8/1), single and triple mutant strains, incubated in the dark at 28 °C and the growth was determined by measuring the radial growth every 24 h up to 2 days.

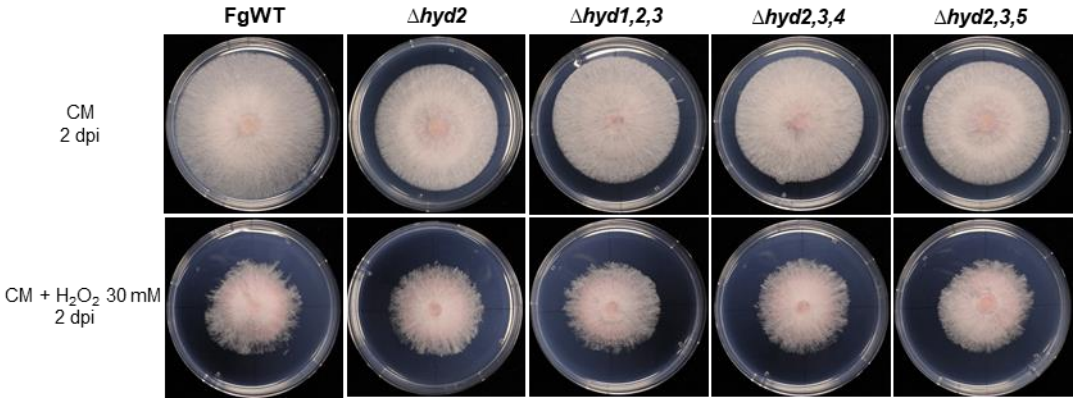

Fig. S3.5. Oxidative stress-response phenotype. Complete medium (CM) plates containing 30 mM hydrogen peroxide (H_2O_2) were inoculated with 4-mm mycelial plugs of the *Fusarium graminearum* wild type (FgWT:8/1), single and triple mutant strains, incubated in the dark at 28 °C and the growth was determined by measuring the radial growth every 24 h up to 2 days.

Fig. S3.6. Point inoculation (200 conidia per flower) on wheat spikes (cv. Nandu) with the *Fusarium graminearum* wild type (FgWT:8/1) and the single and triple mutant strains.

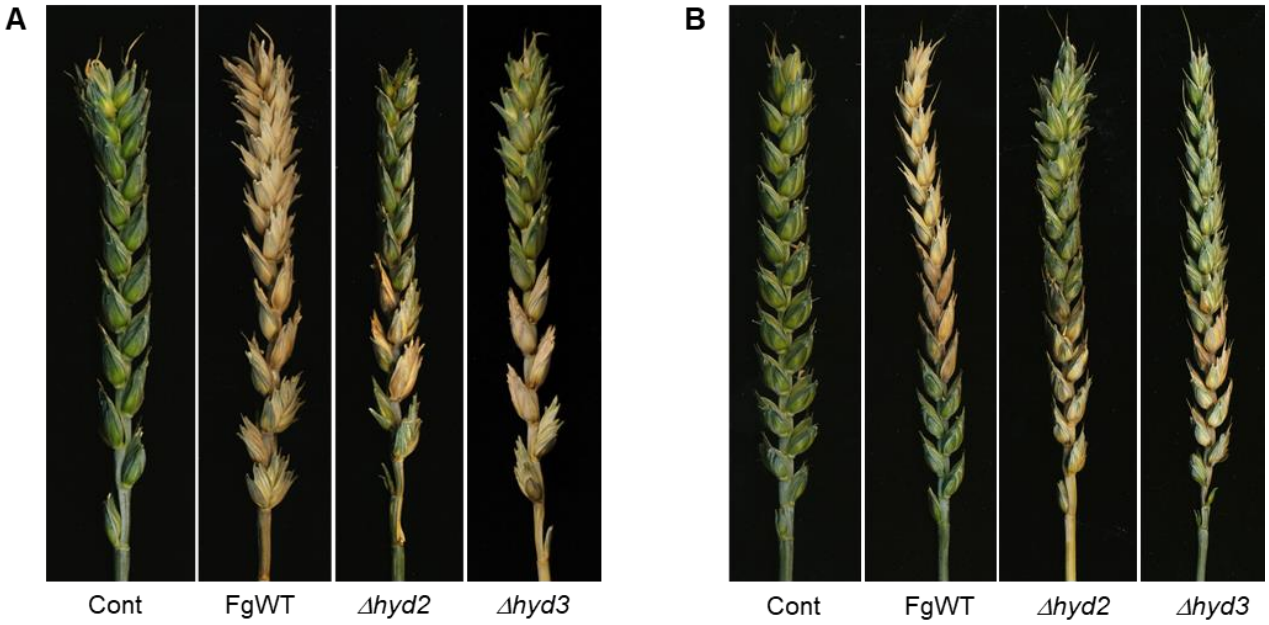

Fig. S3.7. Spray inoculation performed on (A) cv. Nandu and (B) cv. Amaretto wheat spikes with the *Fusarium graminearum* wild type (FgWT:8/1), Δ*hyd2* and Δ*hyd3* single mutants. Two-100 µL sprays of a solution containing 500 conidia μL^{-1} were used and disease symptoms were assessed at 21 dpi.

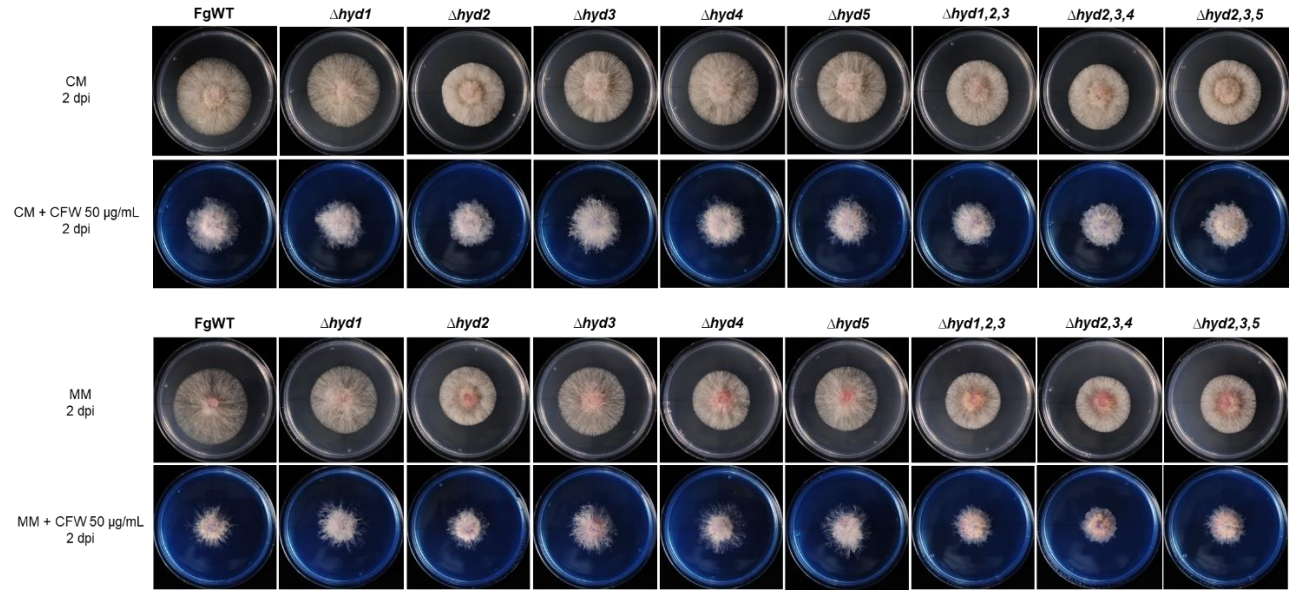

Fig. S3.8. Susceptibility of *Fusarium graminearum* hydrophobin mutants to Calcofluor white. Complete (CM) or Minimal medium (MM) plates supplemented with Calcofluor white (CFW, 50 µg mL^{-1}) and control plates were inoculated with 4-mm plugs of actively growing mycelia of the wild type (FgWT:8/1), single and triple mutant strains. Plates were incubated at 28 °C in the dark and pictures were taken after 2 days of growth.

Table S3.1. Oligonucleotide primers used in this study.

Primer	Sequence (5´-> 3´)	Application
1F-Fghyd1-Vect	tgtaaaacgacggccagtgagcgcgcgtACATGCACAGCAGTTGAACAAC	FgHyd1 deletion construct (FGSG_ 01763)
2R-Fghyd1-Hyg	aaaggaatagagtagatgccgaccgaacGAGGGTTGGAAAAGTGTTTGTC	
3F-Fghyd1-Hyg	agtcaatgctacatcacccacctcgctcCACATCAACCTTTTTACTGGGA	
4R-Fghyd1-vect	ctctagaactagtggatcccccgggctgGAATGGAGTAGGGAATGAATGG	
5F-Fghyd1-out	GTCAAGTCGATTAAGGGCTAG	Primers outside of the construct for knock-out checking
6R-Fghyd1-out	GGTGCGATTGGCGTTTTTATG	
7F-Fdhyd1-int	CTCTACTGCTGCACCAACGAA	Internal primers for knock-out checking
8R-Fghyd1-int	CTGGGTGAAGGTGATGGAGC	
9F-Fghyd1-pro	CATGGATCGACACTTACTCAC	Probe
10R-Fghyd1-pro	GGTAGAACAGATAGCTCAAGG	
1F-Fghyd2-Vect	tgtaaaacgacggccagtgagcgcgcgtTGCATGTAACAGTCAGGCCAC	FgHyd2 deletion construct (FGSG_ 01764)
2R-Fghyd2-Gen	ctatcgccttcttgacgagttcttctgaGATGATGATGGTTGATAGTAGC	
5F-Fghyd2-Gen	caggtaggccgaataacttgcacaaattggGTCGAGACACCGCGTTGCTT	
6R-Fghyd2-vect	cacacaggaaacagctatgaccatgattaTGATGCTCTAGCCGTCTTTGG	
7F-Fdhyd2-out	GCATGGCCTGTCTGTCTCAA	Primers outside of the construct for knock-out checking
8R-Fghyd2-out	TCAGAGAAGTGGCTATTGGG	
9F- Fdhyd2-int	CAAGAAGACTGCCAAAGGTAG	Internal primers for knock-out checking
10R- Fdhyd2-int	CCACCCTTGTAGATGTTGATG	
11F-Fghyd2-pro	GCCGAAGTACAAAGACCAACC	Left flanking probe
12R-Fghyd2-pro	GACCAACATGCATGCTACCG	
1F-Fghyd3-Vect	ggccccccctcgaggtcgacggtatcgatCAGACGTCGAATGAGAGCCGC	FgHyd3 deletion construct (FGSG_09066)
2R-Fghyd3-Nat	acatgagcatgccctgcccctgagcggccGTGTTGAAAGTGTTGGAGGAT	
3F-Fghyd3-Nat	cccgaatcgggaatgcggctctagagtagTGTTGTAAGTTTCACTCACAC	
4R-Fghyd3-vect	gctctagaactagtggatcccccgggctgACCAGAAATGTTGGTCGCTTG	
5F-Fdhyd3-out	CGATCCCTTCTACAAATAAACGTC	Primers outside of the construct for knock-out checking
6R-Fghyd3-out	GATAAAGGTTCCTCAAGGCCC	
7F- Fdhyd3-int	ATGCAGTTCTCTACTCTCACC	Internal primers for knock-out checking
8R- Fdhyd3-int	GTGTGAGTGAAACTTACAACA	

9F-Fghyd3-pro 10R-Fghyd3-pro	CACTCACACACTCTACAAACG GGAAATGTGTGCAGATGTCAG	Right flanking probe
1F-Fghyd4-Vect	tgtaaaacgacggccagtgagcgcgcgtGAATATGAAGGTTTTGCTGGTG	FgHyd4 deletion construct (FGSG_03960)
2R-Fghyd4-Hyg	caaaggaatagagtagatgccgaccgaacTTGGTGGATCAGGTGGCTTTC	
3F-Fghyd4-Hyg	agtcaatgctacatcacccacctcgctcAGATAAAGCCACTACTGAACTG	
4R-Fghyd4-vect	ctctagaactagtggatcccccgggctgTAGCAGTTTGTCTTATTGGTGG	
5F-Fdhyd4-out	TGGACGATGGGAAGATATGGG	Primers outside of the construct for knock-out checking
6R-Fghyd4-out	GGGGATAACATGATTGACGTGA	
7F- Fdhyd4-int	CTTCCACGACTGCTGCTTCT	Internal primers for knock-out checking
8R- Fdhyd4-int	GTACAGCCAATAGCAACAAGG	
9F-Fghyd4-pro	TACTGAACTGGTTGGCTGCAT	Probe
10R-Fghyd4-pro	CTACAATCTTCCCTCACTTCC	
1F-Fghyd5-Vect	tgtaaaacgacggccagtgagcgcgcgtGGTCAACGTTTACGATCCCAG	FgHyd5 deletion construct (FGSG_01831)
2R-Fghyd5-Hyg	aaaggaatagagtagatgccgaccgaacAGAGTGATTGGTTTAGGAGAGT	
3F-Fghyd5-Hyg	agtcaatgctacatcacccacctcgctcTCCTCTGCAATACCCCTACTG	
4R-Fghyd5-vect	ctctagaactagtggatcccccgggctgGTATCATAGCGTACAACTGTGT	
5F-Fdhyd5-out	GTGTTAGGGGAGATTCAAGGA	Primers outside of the construct for knock-out checking
6R-Fghyd5-out	TGGGGACGACAAGGATGCTG	
7F- Fdhyd5-int	AACGAGAAGCGACAGGCCTA	Internal primers for knock-out checking
8R- Fdhyd5-int	GATGGGGAGGACACAGCAG	
9F-Fghyd5-pro	CCGCACTTTAAGACAGCCACT	Probe
10R-Fghyd5-pro	CGAAATCGCCACAGCAAGTTA	
1F-Hyg 2R-Hyg	GAGCGAGGTGGGTGATGTAG CGGTCGGCATCTACTCTATTC	Hygromicin (Hyg) resistance cassette
1F-NptII 3R-NptII	GCCAGTTGTTCCCAGTGATCT GCGAGGTCCAATGCATTAATG	Geneticin (NptII) resistance cassette
1F- Nat 5R-Nat	CTAAAGGGAACAAAAGCTGGAG ACGATATCGAATTCCTGCAGG	Nourseothricin (Nat) resistance cassette
F: forward primer; R: reverse primer. Lowercase: overhangs for fusion.		

Table S3.2. Plasmids used or generated in this work.

Name	Use	References
pRS426	Yeast cloning method	Christianson et al., 1992
pNRI	Nourseothricine (Nat) selectable marker	Malonek et al. 2004
pGEM-Hyg	Hygromicin (Hyg) selectable marker	Maier et al., 2005
pII99	Geneticin (NptII) selectable marker	Beck et al., 1982
pIGPAPA	GFP constitutive with Hyg selectable marker (PgpdA:GFP:hyg)	Leach et al., 2003
pBH-GFP	GFP constitutive with NptII selectable marker (PgpdA:GFP:NptII)	This study
pALM-Fghyd1::Hyg	Fghyd1 deletion construct	This study
pALM-Fghyd2::NptII	Fghyd2 deletion construct	This study
pJB-Fghyd3::Nat	Fghyd3 deletion construct	This study
pALM-Fghyd4::Hyg	Fghyd4 deletion construct	This study
pALM-Fghyd5::Hyg	Fghyd5 deletion construct	This study

Beck, E., Ludwig, G., Auerswald, E.A., Reiss, B., Schaller, H., 1982. Nucleotide sequence and exact localization of the neomycin phosphotransferase gene from transposon Tn5. Gene. 19, 327-336.

Christianson, T.W., Sikorski, R.S., Dante, M., Shero, J.H., Heiter, P., 1992. Multifunctional yeast high-copy-number shuttle vectors. Gene. 110, 119-122.

Leach, J., Lang, B.R., Yoder, O.C., 1982. Methods for selection of mutants and in vitro culture of *Cochliobolus heterostrophus*. Microbiol. 128, 1719-1729.

Malonek, S., Rojas, M.C., Hedden, P., Gaskin, P., Hopkins, P., Tudzynski, B., 2004. The NADPH-cytochrome P450 reductase gene from Gibberella fujikuroi is essential for gibberellin biosynthesis. J. Biol. Chem. 279, 25075-25084.

Maier, F.J., Malz, S., Lösch, A.P., Lacour, T., Schäfer, W., 2005. Development of a highly efficient gene targeting system for *Fusarium graminearum* using the disruption of a polyketide synthase gene as a visible marker. FEMS Yeast Res. 5, 653-662. Doi: 10.1016/j.femsyr.2004.12.008.

Conclusions

Cerato-platanins (CPPs) and hydrophobins (HPs) are small secreted cysteine-rich non-catalytic proteins typical of filamentous fungi. It was previously suggested that CPPs are hydrophobin-like proteins, but structural analysis revealed that there are different biochemical and structural properties between CPPs and HPs (Seidl et al., 2006).

CPPs seem more similar to expansins for many aspects (Sampedro and Cosgrove, 2005; Baccelli, 2015), such as carbohydrate-binding/loosening properties with a non-enzymatic mechanism (de Oliveira et al., 2011; Baccelli et al., 2014), but also the ability to self-assemble and change the polarity of surfaces and solutions, which are properties that are reminiscent of HPs (Frischmann et al., 2013). CPPs and HPs could play a broad spectrum of functions in fungi; being localized at the cell wall, they could be involved in fungal growth, and might also play a more elusive role in pathogenicity due to their secretion and possible interaction with plants. In particular, because of their hydrophobicity, HPs could be involved in the attachment to host-hydrophobic surfaces (Wösten, 2001). In order to characterize their role in the hemi-biotrophic fungus *Fusarium graminearum*, single and multiple knock-out mutants of the corresponding encoding genes were produced.

The two *F. graminearum* cerato-platanins (FgCPPs) contribute to protect fungal cell wall polysaccharides from enzymatic degradation by β-glucanase and chitinase, and their heterologous expression has demonstrated their ability to loosen cellulose, mainly with a non-enzymatic activity, and to favor the enzymatic activity of cellulases. Although this result seems to suggest that the FgCPPs could contribute to the infection process by favoring the degradation of plant cellulose, the double knock-out mutant Δ*Δfgcpp*$_{1,2}$ resulted as virulent as the wild type on both wheat and soybean. However, a role of these proteins during plant infection cannot be conclusively ruled out since the Δ*Δfgcpp*$_{1,2}$ mutant grown on carboxymethyl cellulose substrate produces more cellulase activity than the wild type, probably to compensate for the absence of the FgCPPs.

Two of the five *F. graminearum* hydrophobins (FgHyds) are mainly responsible of the hydrophobicity of aerial hyphae, and protect the fungal cell wall from β-glucanase treatment and the

plasma membrane from toxicity of a triazole fungicide. Most of all, these hydrophobins are involved in the adhesion to the wheat spike surface during the first phases of the infection process. Indeed, their deletion shows a reduced virulence of mutants on wheat spikes only by spray inoculation experiments.

Having observed common features among FgCPPs and FgHyds, a triple knock-out mutant could be produced by using the double cerato-platanin mutant as background (Quarantin et al., 2016) and disrupting one of the two hydrophobin encoding genes (FgHyd3) showing a noteworthy phenotype. The characterization of this triple mutant will allow to verify the effect of the simultaneous deletion of these different classes of proteins on fungal growth and virulence.

In the last few years, different applications for these two protein families have been studied and hypothesized (Cox and Hooley, 2009; Gaderer et al., 2014; Wösten and Scholtmeijer, 2015; Kulkarni et al., 2017; Politi et al., 2018). Considering our results, it could be interesting in the future to develop innovative field disease management strategies for wheat protection based on the identification or synthesis of new molecules targeting the FgCPPs and the FgHyds in order to increase fungal susceptibility to plant defense proteins, such as glucanase or chitinase enzymes, or to reduce fungal ability to adhere to host plant tissues and thus their virulence. Furthermore, the FgCPPs could also be exploited for industrial applications such as the production of biofuel. In particular, by increasing the activity of cellulolytic enzymes, the FgCPPs could facilitate cellulose degradation in cereal straw, a potential biofuel resource abundantly produced worldwide.

References

Baccelli, I., Luti, S., Bernardi, R., Scala, A., Pazzagli, L., 2014. Cerato-platanin shows expansin-like activity on cellulosic materials. Appl. Microbiol. Biotechnol. 98, 175-184.

Baccelli, I., 2015. Cerato-platanin family proteins: one function for multiple biological roles? Front. Plant Sci. 5, 769.

Bai, G.H., Desjardins, A.E., Plattner, R.D., 2002. Deoxynivalenol-nonproducing *Fusarium graminearum* causes initial infection, but does not cause disease spread in wheat spikes. Mycopathol. 153, 91-98.

Boenisch, J.M., Schäfer, W., 2011. *Fusarium graminearum* forms mycotoxin producing infection structures on wheat. BMC Plant Biol. 11, 110.

Brown, N.A., Antoniw, J., Hammond-Kosack, K.E., 2012. The predicted secretome of the plant pathogenic fungus *Fusarium graminearum*: A refined comparative analysis. PLoS One. **7**, e33731.

Cox, P.W., Hooley, P., 2009. Hydrophobins: New prospects for biotechnology. Fungal Biol. Rev. 23, 40-47.

de Oliveira, A.L., Gallo, M., Pazzagli, L., Benedetti, C.E., Cappugi, G., Scala, A., Pantera, B., Spisni, A., Pertinhez, T.A., Cicero, D.O., 2011. The structure of the elicitor Cerato-platanin (CP), the first member of the CP fungal protein family, reveals a double ψβ-barrel fold and carbohydrate binding. J. Biol. Chem. 286, 17560-17568.

Frischmann, A., Neudl, S., Gaderer, R., Bonazza, K., Zach, S., Gruber, S., et al., 2013. Self-assembly at air/water interfaces and carbohydrate binding properties of the small secreted protein EPL1 from the fungus *Trichoderma atroviride*. J. Biol. Chem. 288, 4278-4287.

Gaderer, R., Bonazza, K., Seidl-Seiboth, V., 2014. Cerato-platanins: a fungal protein family with intriguing properties and application potential. Appl. Microbiol. Biotechnol. 98, 4795-4803.

Goswami, R.S., Kistler, H.C., 2004. Heading for disaster: *Fusarium graminearum* on cereal crops. Mol. Plant Pathol. 5, 515-525.

Kulkarni, S., Nene, S., Joshi, K., 2017. Production of Hydrophobins from fungi. Process Biochem. 61, 1-11.

McMullen, M., Jones, R., Gallemberg, D., 1997. Scab of wheat and barley: a remerging disease of devastating impact. Plant Dis. 81, 1340-1348.

Nicholson, P., Turner, J.A., Jenkinson, P., Jennings, P., Stonehouse, J., Nuttall, M., Dring, D., Weston, G., Thomsett, M., 2003. Maximising control with fungicides of *Fusarium* ear blight in order to reduce toxin contamination of wheat. HGCA Project Report No. 297.

Pioli, R.N., Mozzoni, L., Morandi, E.N., 2004. First report of pathogenic association between *Fusarium graminearum* and soybean. Plant Dis. 88, 220.

Politi, J., De Stefano, L., Giardina, P., Casale, S., Rea, I., 2018. Hybrid hydrophobin/gold nanoparticles: Synthesis and characterization of new synthetic probes for biological applications. 3rd National Conference on Sensors. 431, 169-176.

Quarantin, A., Glasenapp, A., Schäfer, W., Favaron, F., Sella, L., 2016. Involvement of the *Fusarium graminearum* cerato-platanin proteins in fungal growth and plant infection. Plant Physiol. Biochem. 109, 220-229.

Sampedro, J., Cosgrove, D.J., 2005. The expansin superfamily. Genome Biol. 6, 242.

Schäfer, W., 1994. Molecular mechanisms of fungal pathogenicity to plants. Annu. Rev. Phytopathol. 32, 461-477.

Seidl, V., Marchetti, M., Schandl, R., Allmaier, G., Kubicek, C.P., 2006. Epl1, the major secreted protein of *Hypocrea atroviridis* on glucose, is a member of a strongly conserved protein family comprising plant defense response elicitors. FEBS J. 273, 4346-4359.

Sella, L., Gazzetti, K., Castiglioni, C., Schäfer, W., Favaron, F., 2014. *Fusarium graminearum* Possesses Virulence Factors Common to Fusarium Head Blight of Wheat and Seedling Rot of Soybean but Differing in Their Impact on Disease Severity. Phytopathol. 104, 1201-1207.

Voigt, C.A., Schäfer, W., Salomon, S., 2005. A secreted lipase of *Fusarium graminearum* is a virulence factor required for infection of cereals. Plant J. 42, 364-375.

Wösten, B., 2001. Hydrophobins: multipurpose proteins. Annu. Rev. Microbiol. 55, 625-646.

Wösten, H.A.B., Scholtmeijer, K., 2015. Applications of hydrophobins: current state and perspectives. Appl. Microbiol. Biotechnol. 99, 1587-1597.